The Dissertation Committee for Dong Gyu Cho Certifies that this is the approved version of the following dissertation:

Syntheses and Studies of Sapphyrins and Anion Receptors

Committee:

Jonathan L. Sessler, Supervisor

Hung-wen (Ben) Liu

Michael J. Krische

Bradley J. Holliday

Christine E. Schmidt

Syntheses and Studies of Sapphyrins and Anion Receptors

by

Dong Gyu Cho, B.S.; M.S.

Dissertation

Presented to the Faculty of the Graduate School of

The University of Texas at Austin

in Partial Fulfillment

of the Requirements

for the Degree of

Doctor of Philosophy

The University of Texas at Austin

May 2008

Dedication

To my wife Ok-Shin Moon, my son Jung-Hyung Cho, and my parents.

Acknowledgements

First of all, I would like to give special thanks to the following three people: My wife Ok-shin who gives me endless support and the courage to confront all difficulties, my son Jung-Hyung who provided endless joyful moments in my life, and my advisor, Prof. Jonathan L. Sessler who taught me how to survive in the scientific jungle and helped me to see the forest beyond the trees.

Early on, Janan, Dustin and Jongrock helped me to settle down in Austin and I will never forget their kindness and good friendship. I am also grateful to all the past and present coworkers of the Sessler group for sharing not only nice science but also jokes and good times. Special thanks to Peter, Marcin, Patrick, Joao, Jong-Hoon and Sung-Kuk for collaborative efforts to advance my research, and Mandy, Candace and other friends in the Sessler group for proofreading this dissertation. Thanks to all of my brilliant coworkers outside of the Sessler group and two visiting scholars from South Korea, Prof. Dongho Kim, Zin-Seok Yoon, Prof. Jaeck Waluk, Prof. Jongmin Kang and Prof. Chang-Hee Lee.

I also really appreciate two other mentors. The first is Prof. Suk-Ku Kang who taught me that hard work pays off during my master study. Unfortunately, he has passed away and I hope he enjoys his home in Heaven. The secod mentor, Prof. Chan-Mo Yu is my role model and he continues to help me to become the person who I have always dreamed of being.

Finally, I like to thank to my parents, sisters and my wife's family who have supported my studies in the United States.

Syntheses and Studies of Sapphyrins and Anion Receptors

Publication No._____

Dong Gyu Cho Ph. D.

The University of Texas at Austin, 2008

Supervisor: Jonathan L. Sessler

Polypyrrolic (or aromatic) macrocycles have attracted considerable recent interest due to their potential utility in various applications, including as novel materials, anion receptors, and therapeutic leads. In order to explore further the range and utility of this generalized class of molecules, various sapphyrin and sapphyrin analogues were synthesized. Among the new compounds prepared is an inverted sapphyrin, a species that displayed weak, but noticeable aromaticity. Another new system, benzoxasapphyrin was found to display a reduced anion binding affinity compared to other analogous macrocycles. Finally, several derivatized sapphyrins were prepared as potential anti-cancer leads.

Separate from the above, efforts were made to develop anion receptors based on the indole motif. This substructure plays a key role is stabilizing a range of non-covalent interactions in complex biological structures. However, prior to the present study, indole-

type hydrogen bonding donors had not been widely used to prepare synthetic anion receptors. Accordingly, a diindolyl quinoxaline system was prepared; it served to demonstrate that small molecule indole receptors can effectively bind phosphate anions in organic media.

Finally, a set of cyanide anion indicators were prepared; these were predicated on the use of a cyanide-specific reaction, namely the benzil rearrangement reaction. The benzil reaction-based indicators produced in this way were found to be quite selective for the cyanide anion in organic solvents. Further, their study helped provide insights into the mechanism of this as-yet not fully studied reaction. In the context of developing this specific anion indicator, a review of other reaction-based indicators was reviewed. This is provided in Chapter 3.

TABLE OF CONTENTS

List of Tables

List of Figures

xiii

List of Schemes

Chapter 1 Sapphyrins

1.1 INTRODUCTION

Expanded porphyrins are synthetic analogues of porphyrins that have a larger central core, typically with a minimum 17 atoms, which maintain an extended conjugation pathway.[1] These extended conjugation pathways endow expanded porphyrins with unique characteristics that have made them of interest in a variety of potential applications. These include nonlinear optical materials in the case of the core modified octaphyrins **1.1**[2] and proto-liquid crystals in the case of compound **1.2**.[3] In addition, Photofrin® **1.3** is the first FDA approved PDT (photodynamic therapy) drug.[4] Likewise, other expanded porphyrins have been developed as potential PDT drugs.[5]

R =

X= S, Se

1.1

R = (CH$_2$)$_{13}$CH$_3$

1.2

n = 1-7

1.3
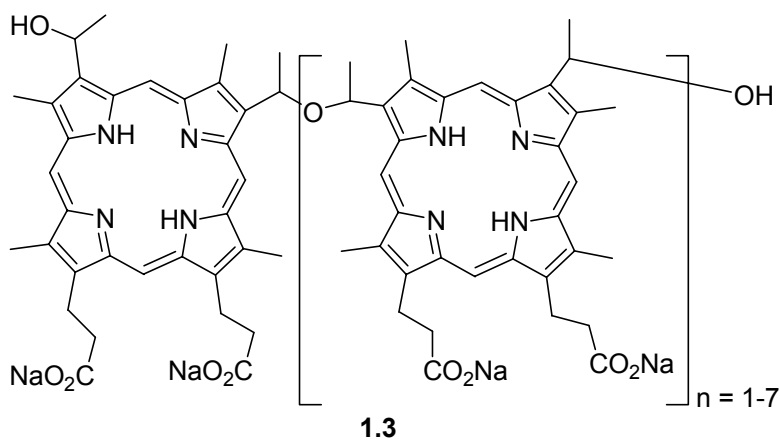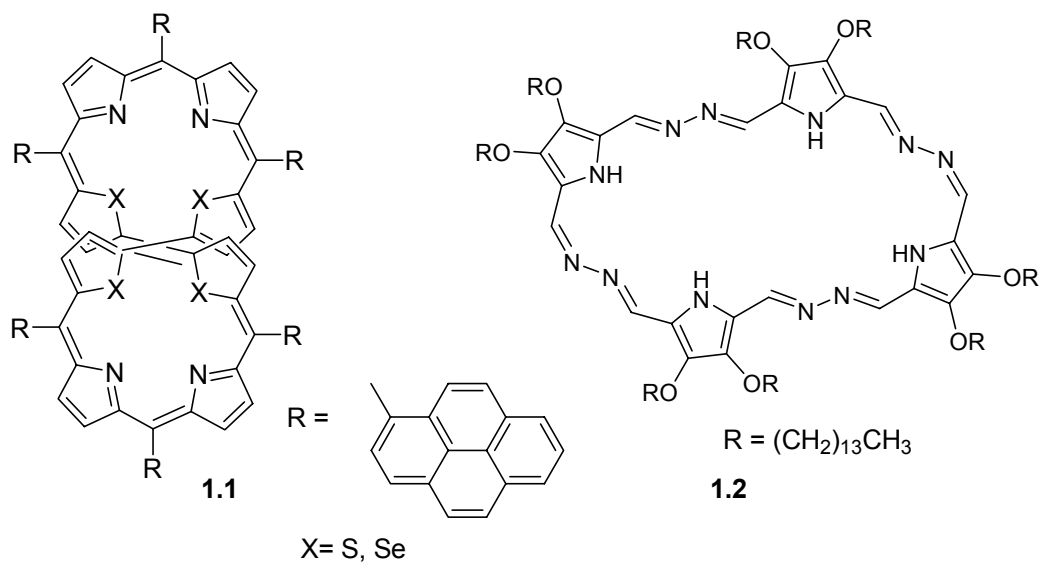
To synthesize new expanded porphyrins, two general strategies have been relied on, namely i) the use of different combinations of pyrrole units and bridging carbons and ii) new building blocks, which can replace pyrroles. Most of the classic expanded porphyrins, including sapphyrin **1.4**, were synthesized using a combination of these approaches. Sapphyrin **1.4**, for instance, has three pyrroles, four bridging carbons, and contains one bipyrrole unit that can be thought of as a pyrrole replacement. Historically, sapphyrin **1.4** was discovered serendipitously by the Woodward group during efforts

2

devoted to the synthesis of vitamin B$_{12}$.[6] They named the compound "sapphyrin" due to its blue-green metallic color in the solid state. The first rational syntheses of sapphyrin and its oxygen version, oxasapphyrin, (two bipyrrolic nitrogen atoms are replaced by two oxygen atoms) were accomplished by Broadhurst, Grigg and Johnson.[7] Later, an independent synthesis of sapphyrin was reported by Woodward and coworkers.[8] Sapphyrin, a species with no known conterpart in Nature, acts as an aromatic compound (22 π-electrons). The crystal structure and initial anion-binding properties were disclosed by the Sessler group in 1990.[9]

1.4a *meso*-tetraaryl sapphyrin
1.4b decaalkyl sapphyrin

1.5

1.6, (X = S, Se)

1.7

1.8
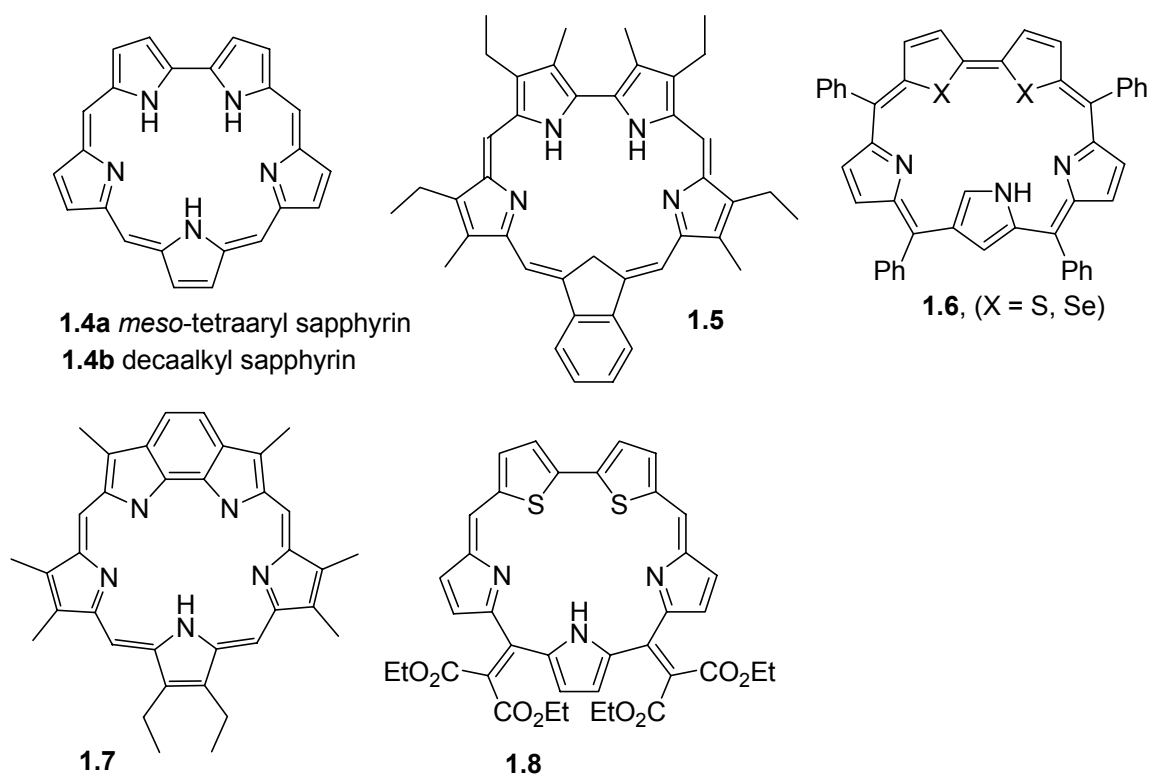
Over the last two decades, the representation of new sapphyrin analogues has profited from the availability of new building blocks including many that do not contain simple pyrroles. Sapphyrins produced using non-pyrrolic precursors include Lash's carbasapphyrin **1.5**,[10] Furuta and Chandrashekar's N-confused core modified sapphyrin **1.6**,[11] Lee's benzosapphyrin **1.7**,[12] and dithiabenzisapphyrin **1.8**.[13] In the case of Lash's carbasapphyrin **1.5**, the fully protonated form was characterized by a strong Soret band and a weak Q-band at 476 nm and 788 nm in chloroform, respectively. This system also displays features consistent with aromaticity. For instance, the signals for meso protons in the ^{1}H-NMR spectrum are found to resonate at 10.4 and 11.0 ppm, respectively, while the inner NH chemical shifts appear at 0.67, -0.56 and -3.75 ppm, respectively.

The inner NH chemical shifts of the N-confused core modified sapphyrin **1.6** are also diagnostic. They appear at -1.8 ppm, but only as a very broad band. The characteristic N-confused pyrrole shows two distinct chemical shifts at 2.73 and 9.79 ppm at 228 K. More importantly, the ^{1}H-NMR spectrum of sapphyrin **1.6** shows little change after warming in toluene at 313 K. On this basis, it was concluded that inversion of the pyrrole unit was not occuring. In the UV-vis spectrum, the protonated form of this sapphyrin (**1.6**) is characterized by two Soret bands at 410 nm ($\varepsilon = 1.0 \times 10^5$) and 531 nm ($\varepsilon = 2.6 \times 10^5$), respectively (CH$_2Cl_2$, 2.5 equiv. of TFA).

In 2005, the Lee group published benzosapphyrin **1.7**. The synthesis of the diformylbenzodipyrrole precursor, the key intermediate upon which its preparation is based, had been reported by Vogel.[14] The free base form of Lee's benzosapphyrin displays ring current features consistent with aromaticity. For instance, three sets of NH chemical shifts at, -0.87, -1.30 and -2.46 ppm, respectively, are seen for the NH protons

in the ^{1}H-NMR spectrum. This system also displays red-shifted absorption bands at 466 nm ($\varepsilon = 8.3 \times 10^4$) and 727 nm ($\varepsilon = 1.6 \times 10^4$) in its UV-vis spectrum.

More recently, the core and *meso*-modified sapphyrin **1.8** were reported by Lee and Sessler. This system displays no evidence of aromaticity. For instance, the β-pyrrolic protons resonated at 6.74 and 6.80 ppm in the ^{1}H-NMR spectrum, and an X-ray structure of sapphyrin **1.8** revealed a system that was not planar. The observed absorption band intensities in the UV-vis spectrum were also relatively low (465 nm ($\varepsilon = 4.4 \times 10^4$) and 630 nm ($\varepsilon = 1.3 \times 10^4$)). The absence of aromaticity was reasonably explained by the steric congestion between the *meso*-(α)-substituents and the benzene moiety.

Apart from their structural and electronic diversity, sapphyrins can be protonated, with the resulting cationic forms often interacting with anions. The anion binding ability was recognized by Sessler and coworkers in 1990 as implied above.[15] It was extensively studied in the case of sapphyrin **1.4b** via UV-vis titrations carried out in MeOH. It was found on this basis that sapphyrin **1.4b** is very selective for fluoride anions over chloride anions ($K_a = 2.8 \times 10^5$ M^{-1}) *vs.* ($K_a = 10^2$ M^{-1}).

Another interesting feature of sapphyrin is that it contains two prodigiosin-like subunits (Figure 1.1). Prodigiosins[16] are naturally occurring tripyrroles that have been studied as anticancer agents. Intuitively, the Sessler group posed the question whether this structural similarity would endow the sapphyrins with anticancer activity. The cytotoxic effects of prodigiosin are believed to arise from its ability to affect the transport of H$^+$ and Cl$^-$ ions across membranes. Specifically, prodigiosin is rather basic and readily protonated. Binding of chloride allows for charge neutralization and produces a species,

prodigiosin·HCl, that is readily transported across membranes. Resulting ion transport events give rise to the reduction of intracellular pH, an effect that is known to trigger apoptosis.[17] This is shown schematically in Figure 1.1.
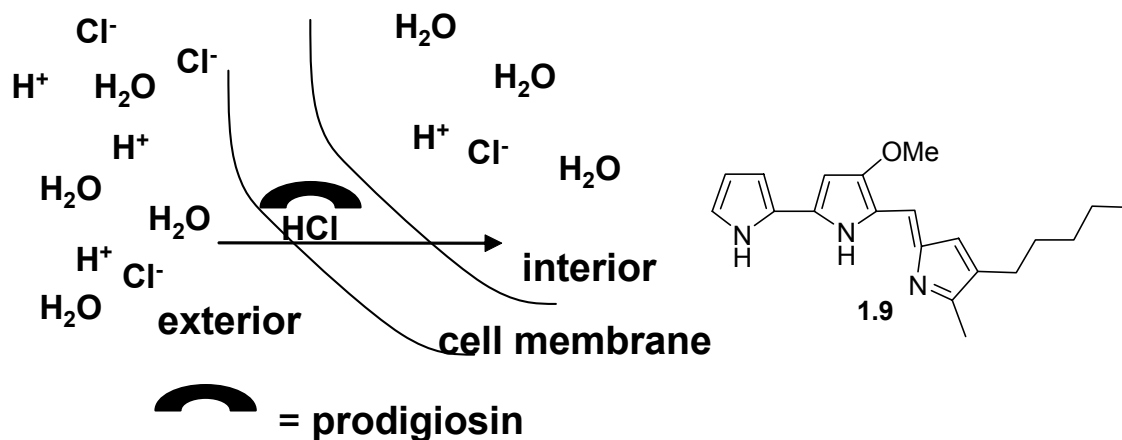
Figure 1.1 Proposed H^+Cl^- symport mechanism of actiom for prodigiosin **1.9**

Prodigiosin has been extensively studied.[16, 17] Sessler et al. have reported that the anticancer activity of polypyrrolic molecules can be closely related to their chloride anion transport efficiency.[18] In this study, the chloride anion transport efficiency of polypyrrolic molecules was compared with the initial rate of each compound. The order of transport efficiency was found to be **1.10 >> 1.11 ≈ 1.13 > 1.14 >> 1.12**. In addition, anticancer activity was evaluated *in vitro* in cell lines (A549, human lung cancer cells, and PC3, human prostate cancer cells). The order of anti-cancer efficacy was **1.10 > 1.11 > 1.13 > 1.14 ≥ 1.12**. Unfortunately, a direct comparison of binding constants to the kinetic terms

6

such as transport efficiency and anti-cancer efficacy could not be made because of inconsistencies in the kinetic and thermodynamic data. Nonetheless, these experiments did provide support for the proposal that symport of ions is an important component of the mode of action for prodigiosin.
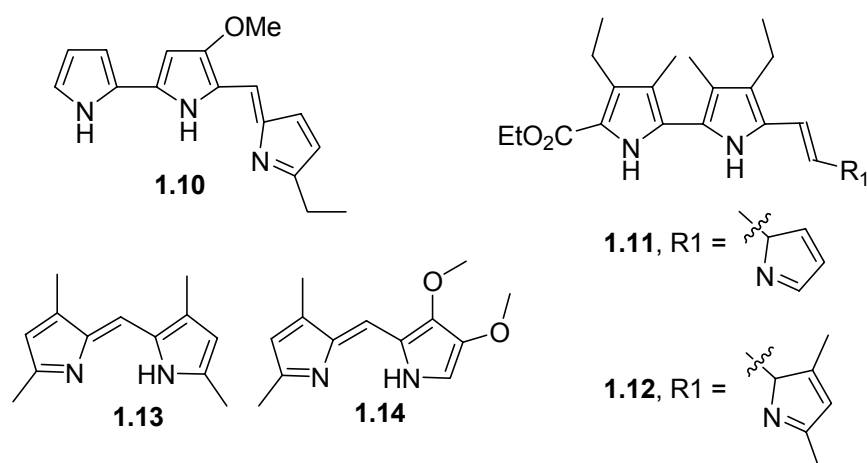
As briefly discussed here, sapphyrins have been one of the more extensively studied molecules in the Sessler group. Given its central role in assessing aromacity effects in expanded porphyrins[19] and its potential utility in drug development, efforts were devoted to preparing new analogues of this venerable system.

In this chapter, two new sapphyrins (inverted sapphyrin and benzoxasapphyrin) and our efforts to develop new anti-cancer drug candidates are described.

1.2 INVERTED SAPPHYRIN

1.2.1 BACKGROUND

As noted above, several new sapphyrin analogues have been synthesized recently from new building blocks. One such building block is the N-confused pyrrole and related subunits introduced by the Furuta group. First noted in the context of porphyrins by Latos-Grażyński[20] and Furuta,[21] N-confused building blocks have led to important developments in the area of expanded porphyrin chemistry.[22] The N-confused core modified sapphyrins **1.6**, synthesized by Furuta and Chandrashekar, are noteworthy examples. In this system, the N-confused pyrrolic NH is located within the cavity instead of pointing outward as is the case for the corresponding sapphyrin **1.4**. While the structure of **1.6** resembles that of sapphyrin **1.4**, the presence of N-confused pyrroles can induce unexpected intramolecular reactions. Therefore, rational syntheses of N-confused systems might not be expected or possible. For instance, it proved impossible to introduce a double N-confused building block without disturbing the parent sapphyrin structure.[22] These led us to consider whether it might be possible to prepare a sapphyrin where inversion of one or more of the pyrrolic nitrogen atoms is configurationally enforced. In this respect, the use of a 3,3'-bipyrrolic subunit was considered as being potentially enabling. Indeed, using such a building block, which has not hitherto been incorporated in a macrocycle, it proved possible to prepare the inverted sapphyrin **1.15**.
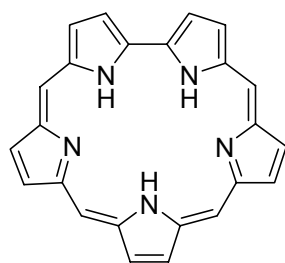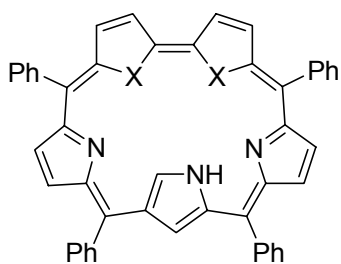
1.4a meso-tetraaryl sapphyrin
1.4b decaalkyl sapphyrin
1.6 (X = S, Se)
1.15
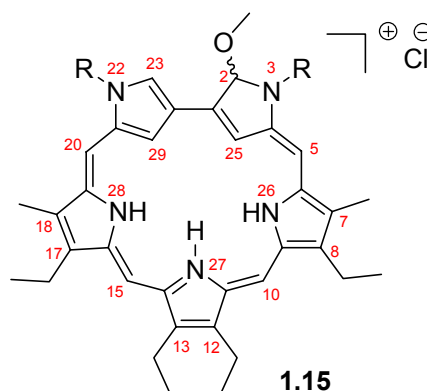
1.2.2 SYNTHESIS, CHARACTERIZATION AND AROMATICITY

The synthesis of 3,3'-bipyrrole began with commercially available pyrrole-2-carboxaldehyde. Pyrrole-2-carboxaldehyde was protected with pyrrolidine and the electron-withdrawing nature of the product **1.16** facilitated subsequent selective iodination on the pyrrole ring. The product obtained, **1.17**, was N-Boc protected in quantitative yield to give **1.18**. Unfortunately, the next proposed step, a modified Stille coupling, was not successful and the desired product **1.19**, was obtained only in impure form and in low yield. It was considered that unprotected pyrroles can poison the palladium catalyst. To avoid this potential problem, the pyrrole was protected with *p*-TsCl. In this case, Stille coupling afforded the target compound **1.21**[23] in 53% yield.

9
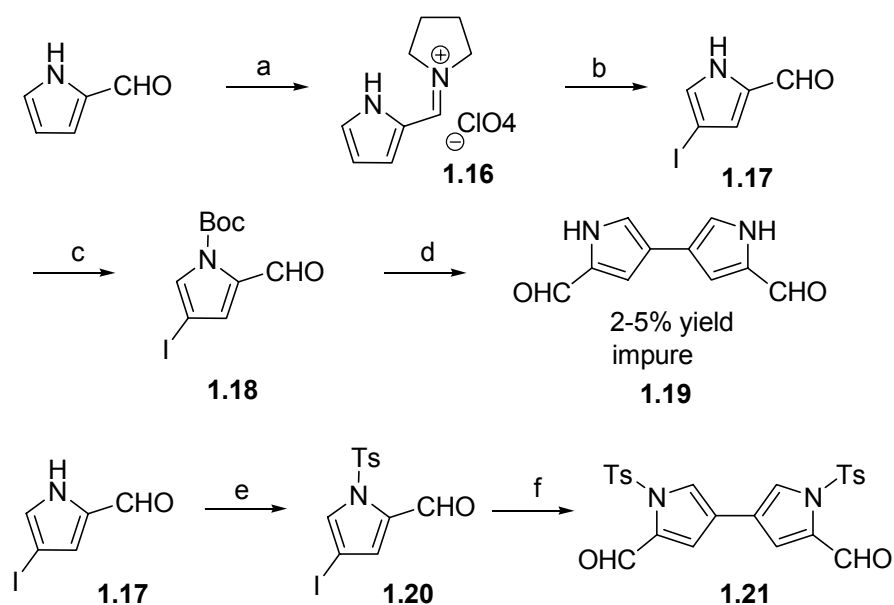
Conditions: (a) $HClO_4$, pyrrolidine, benzene, quantitative; (b) (i) NIS, Acetone, -78 $^{\circ}$C → r.t; (ii) $NaHCO_3$, 52%; (c) $(BOC)_2O$, DMAP, TEA, THF, quantitative; (d) $Pd(PPh_3)_4$, DMF, 2-5%; (e) TsCl, DIEA, DMAP, 81%; (f) Hexa-n-butylditin, $Pd(PPh_3)_4$, DMF, 53%.

Scheme 1.1 Synthetic scheme of **1.21**

The synthesis of inverted sapphyrin **1.15** was accomplished *via* the acid-catalyzed 3+2 condensation between the 3,3'-bipyrrole dialdehyde **1.21** and the tripyrrane diacid **1.22**.[24] The expected compound, **1.23**, if it was formed, proved difficult to isolate, although its presence was noted by HRMS in the crude mixture. In any event, the dominant product isolated from this reaction was a blue metallic solid. On the basis of an HRMS analysis, it was considered likely that it corresponded to **1.15**. Subsequent single crystal X-ray diffraction analysis and ^{1}H-NMR spectroscopic studies of **1.15** (Figures 1.2 and 1.3) confirmed this suggestion. All our efforts to isolate the putative intermediate **1.23** failed and what was obtained in all cases was the methanol adduct **1.15**. We proposed that **1.23** is formed as an intermediate but is not stable under the reaction

10

conditions or during workup. The final product, **1.15**, can be formed by the nucleophilic attack of MeOH to one of the tautomers of intermediate **1.23** during the reaction or during chromatography.[25] After chromatography on silica gel and treatment with aqueous NH$_4$Cl, the inverted sapphyrin **1.15** was obtained in 8-9% yield (Scheme 1.2).
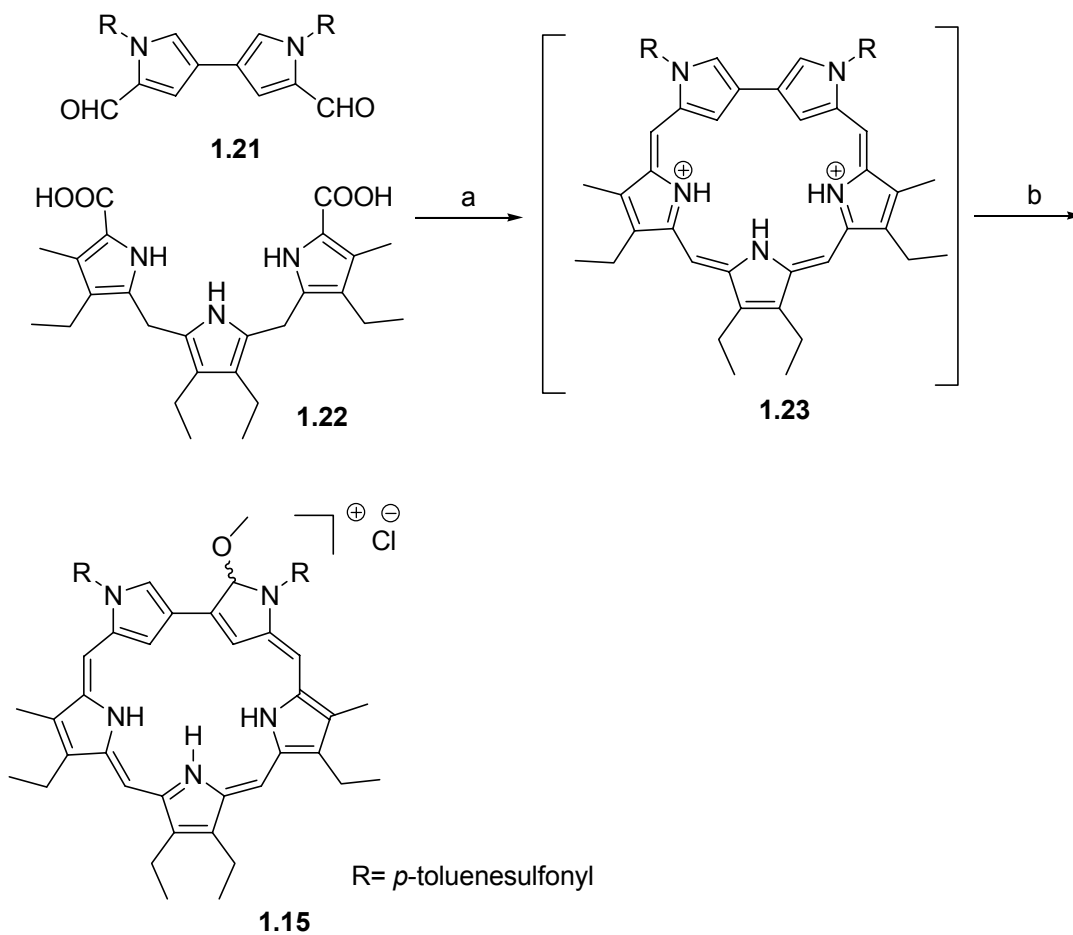
Conditions: (a) (i) TFA, CH$_2$Cl$_2$, N$_2$, 12 h; (ii) DDQ, 30 min; (b) (i) silica gel, MeOH; (ii) NH$_4$Cl (aq.).

Scheme 1.2 Condensation between 1.21 and 1.22 and formation of **1.15**

The question we first posed was whether the new sapphyrin **1.15** is aromatic or not. Usually, aromatic compounds can be easily distinguished by the presence of ring current effects, which can be easily detected by ^{1}H NMR spectroscopy features. In the case of inverted sapphyrin, the ^{1}H NMR spectral features correspond to weak aromaticity. For example, the internal *β*-pyrrolic CH protons are observed as two broad peaks at 3.77 and 4.04 ppm in DMSO-d_6, while the external pyrrolic CH resonance is observed at 8.56 ppm in the same solvent. The chemical shift differences between the internal protons and external protons ($\Delta\delta$ = 4.79 and 4.52 ppm), generally considered a benchmark of aromaticity, is thus consistent with the presence of a ring current. However, the $\Delta\delta$ values of inverted sapphyrin **1.15** are considerably less than those seen for typical all-aza *meso*-tetraaryl sapphyrins (e.g., **1.4a**, average $\Delta\delta$ of 10.97 ppm).[26] Other observed chemical shifts also support the proposed weak aromatic ring current, including the four *meso* proton resonances (7.89, 7.75, 7.63 and 6.93 ppm) and the three pyrrolic NH signals (8.10, 7.36, and 5.99 ppm).

Figure1.2 ^{1}H-NMR spectrum of inverted sapphyrin recorded in DMSO-d_6
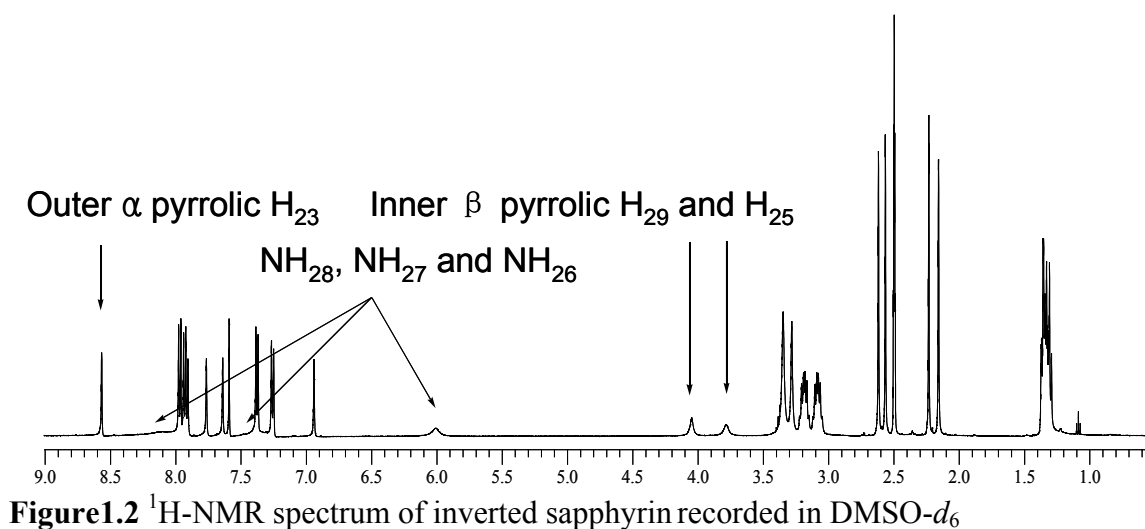
(a)
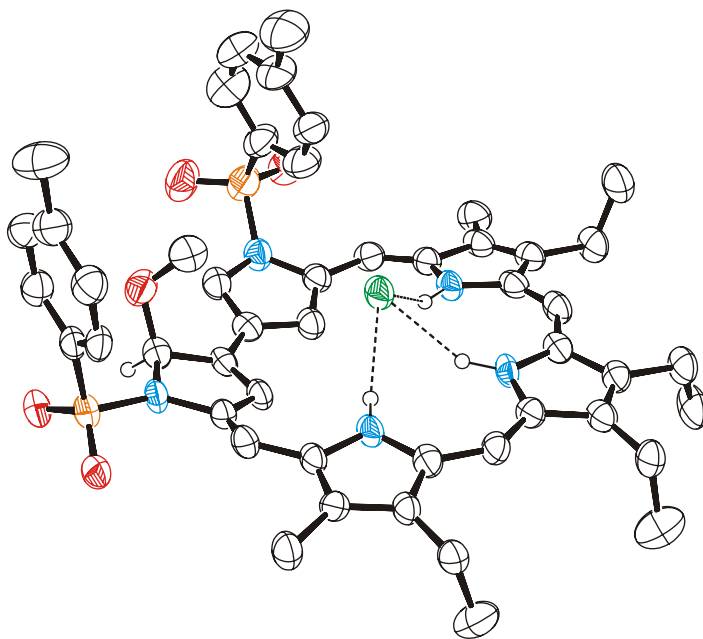
(b)
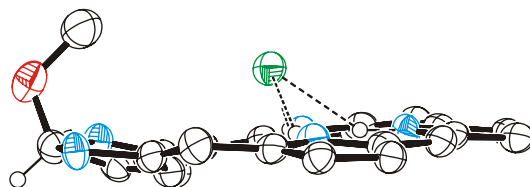
Figure 1.3 X-ray crystal structure of **1.15**·Cl$^-$. (a) Top view; (b) Side view. Thermal ellipsoids are scaled to the 50% probability level. Most hydrogen atoms and the disorder present in one of the *p*-tolyl substituents have been omitted for clarity.

The structure of sapphyrin **1.15** was confirmed by single crystal X-ray diffraction analysis. In this structure, **1.15** is seen to bind the chloride anion in a similar fashion to that displayed by regular sapphyrin **1.4**. The chloride is located 1.57 Å above the mean plane of the macrocycle and forms hydrogen bonds with the three pyrrolic hydrogens (NH···Cl = 2.24–2.36 Å). The CH···Cl distances in the macrocyclic cavity are markedly longer (2.84 Å and 2.95 Å). Both tosyl substituents, the methoxy group, and the chloride anion lie on the same side of the macrocyclic plane. The macrocycle is slightly ruffled, especially in its bipyrrolic part. The inverted pyrrole rings are tilted by 16.1–18.7° with respect to the mean macrocyclic plane. For the regular pyrroles of the tripyrane part, the tilt angles are in the range of 6.5–8.0°.
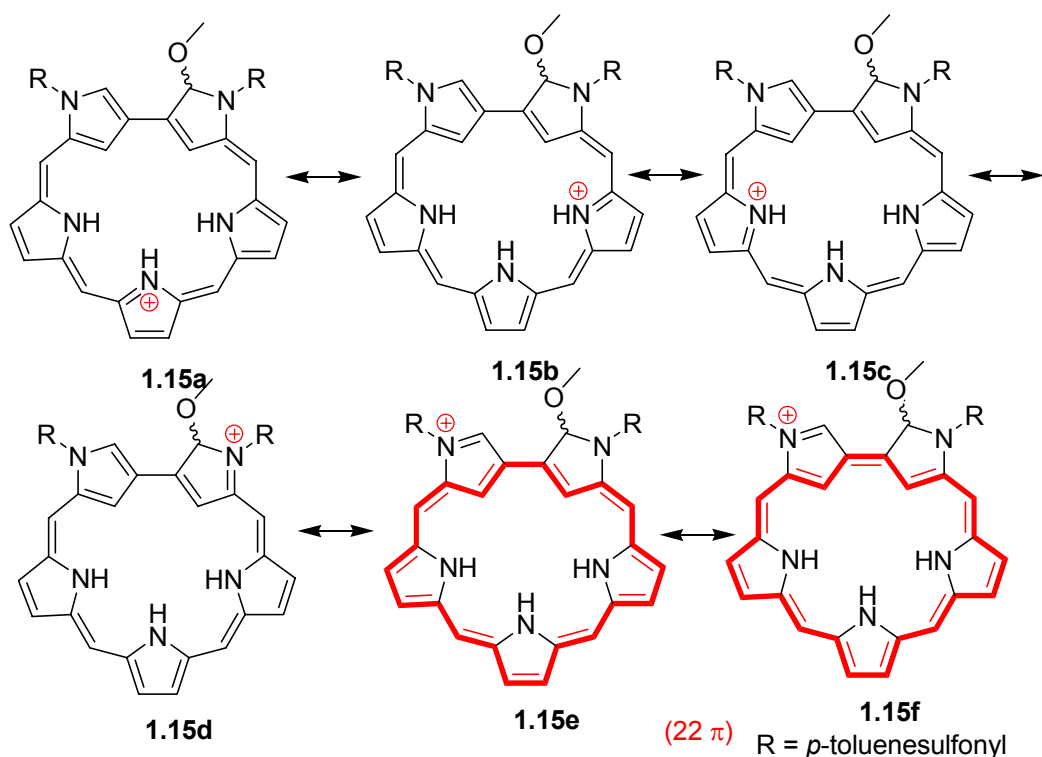
Figure 1.4. Resonance structures of inverted sapphyrin **1.15**. In structures 1.15e and 1.15f, the 22 π-electron configuration pathways are shown.

14

1.24a   **1.24b** $\longleftrightarrow$ **1.24c**
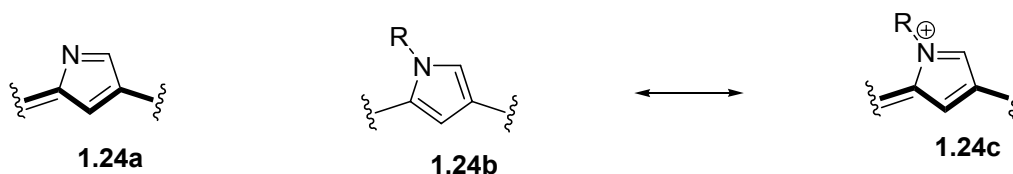
The smaller $\Delta\delta$ value observed for **1.15**, compared to the regular sapphyrin **1.4,** is attributed to the presence of the inverted, N-substituted bipyrrole unit within the macrocycle. Because of this substitution, resonance structures containing uninterrupted 22 π-electron aromatic peripheries can only be written when the charge is present on the inverted, pyrrolic nitrogen (cf. Figure 1.4). The net consequence of this limitation is that aromaticity is reduced, as it is in most N-substituted N-confused systems reported to date. In normal N-confused porphyrins resonance structures containing the imine-like state **1.24a** can dominate with the consequence that the observed ring current is usually comparable to that seen in the absence of N-confusion.[20, 21, 26] In the case of N-substituted systems containing fragments such as **1.24b**, aromatic delocalization is only available through charge separated resonance contributions (shown in part as structure **1.24c**). Consequently, the observed ring currents are significantly weaker. Examples of this effect include N-methyl N-confused porphyrin,[20, 21] doubly N-confused porphyrin,[27] and the N-confused sapphyrins **1.6** reported previously, as well as the inverted sapphyrin described in this chapter, **1.15**.[28]

The observed UV-vis spectral features are consistent with weak aromaticity. Whereas the decaalkyl sapphyrin **1.4b** displays Soret and Q-like bands at 448 and 673 nm when studied as its mono-protonated form in CH_2Cl_2 (Figure 1.5), the UV-Vis spectrum of inverted sapphyrin **1.15** is characterized by features that are shifted to longer wavelengths (λ_{max} (ε) = 464 nm ($4.45 \cdot 10^4$ $M^{-1}cm^{-1}$) and 827 nm ($2.45 \cdot 10^4$ $M^{-1}cm^{-1}$)) for

the Soret- and Q-like bands, respectively (Figures 1.5 and 1.6). Interestingly, the extinction coefficient of the Soret band of **1.15** is only 10% of the value observed for regular sapphyrin.[15] However, the intensity of Q-like bands is very similar in both compounds (cf. Figure 1.5 vs. Figure 1.6).
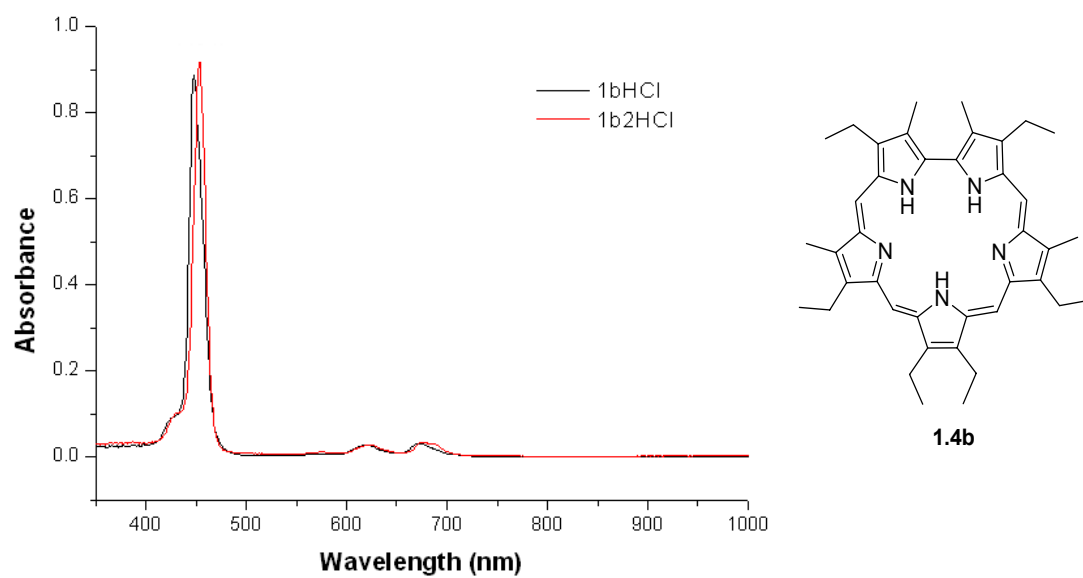
Figure 1.5 UV-Vis spectrum of sapphyrin **1.4b** recorded in CH$_2$Cl$_2$
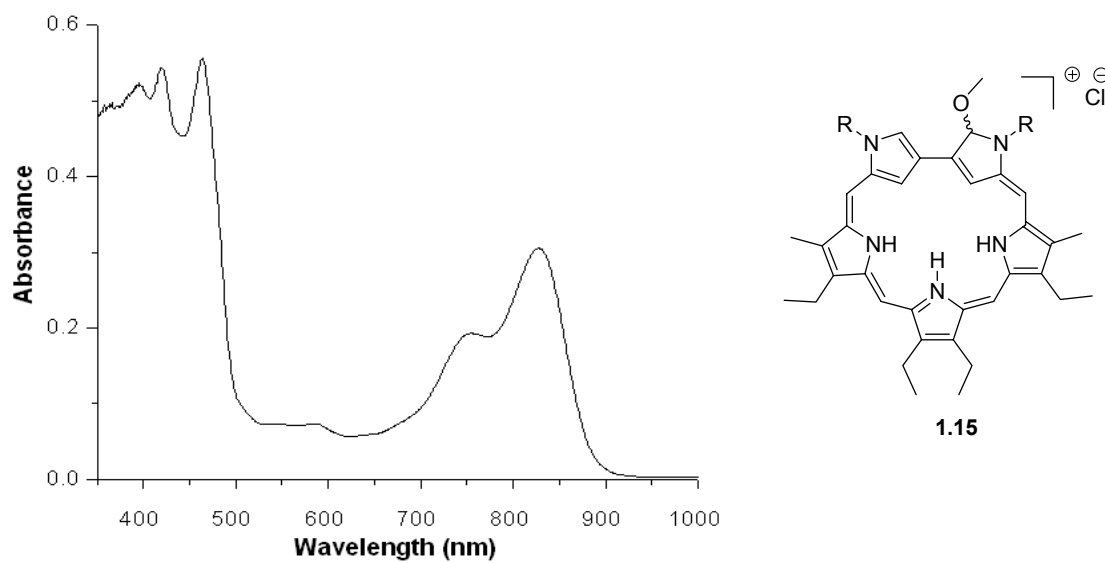
Figure 1.6 UV-Vis spectrum of sapphyrin **1.15** recorded in CH$_2$Cl$_2$

17

The electronic structure and proposed aromaticity of inverted sapphyrin **1.15** are consistent with what is predicted by AM1 using the X-ray data of inverted sapphyrin **1.15**. Based on the π molecular orbitals calculated in this way, the HOMO splitting is much smaller than that of the LUMO pair. Using perimeter model terminology, inverted sapphyrin **1.15** should thus behave as a "negative-hard" chromophore, which is similar to what is seen in the case of isosmaragdyrin, a contracted, aromatic analogue of sapphyrin.[29] For such a chromophore, a large ratio of Q versus Soret type band intensity is predicted, as well as a -, +, -, + sequence of MCD Faraday *B* terms for the lowest four π-π* electronic transitions. In fact, the Q/Soret intensity ratio of **1.15** in the absorption spectrum is similar to that of isosmaragdyrin, while the predicted sequence of B terms is clearly seen in the MCD spectrum of **1.15** (Figure 1.7) for the Soret bands. However, the Q region is somewhat more difficult to interpret, although the overall shape of the spectrum agrees with our expectations. ZINDO/S calculations also predict similar absorption patterns for isosmaragdyrin and inverted sapphyrin **1.15**. The Q_1 transitions are likewise predicted to be only about 4 times weaker than the Soret bands and the Q_2 band is predicted to lie closer to the Soret band than Q_1. The MCD spectrum of **1.15** and supporting theoretical analyses were kindly provided by our collaborator, Prof. Jacek Waluk of The Polish Academy of Sciences.
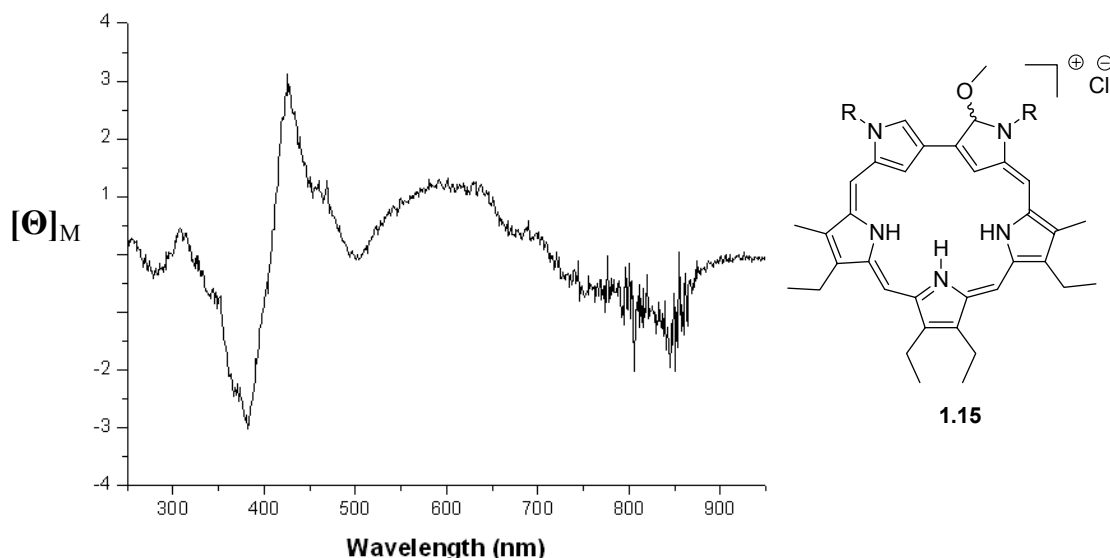
Figure 1.7 MCD spectrum of sapphyrin **1.15** recorded in CH_2Cl_2 at 293K at a concentration of ca. 3.8×10^{-5} M in a 1 cm cell. The units of molar ellipticity (Y axis) are deg L m^{-1} mol^{-1} Gauss^{-1}.

Interatomic distances within the macrocycle are also indicative of localization and delocalization of double bonds. While the observed bond alternation pattern follows approximately that expected for valence structure **1.15a** (Table 1), HOSE(harmonic oscillator stabilization energy) calculations [30] based on the X-ray data were used to estimate more precisely the relative importance of canonical structures **1.15a-f** within the overall resonance hybrid. In detail, harmonic oscillator stabilization energies were calculated using the method of Krygowski et al. using the original parameterization;[31] weights were calculated according to the formula:

$$C_i = [\text{HOSE}_i]^{-1}/(\Sigma_j\ [\text{HOSE}_j]^{-1})$$

where *j* runs over structures **1.15a** through **1.15f**. All C–C and C–N bonds of the macrocycle were included in the calculations except for C(1)–C(2) and C(2)–N(3). Error

19

estimates for HOSE and C_i were obtained from bond esd's using the method of total differentials. On this basis, it was estimated that the total input of structures **1.15a-d** is 78%, whereas the Kekulé-type structures **1.15e-f** each contribute 11%. This result is in qualitative agreement with the relatively weak aromatic ring current inferred from the ^{1}H NMR spectrum. In addition, the nucleus-independent chemical shifts (NICS(0)) values, an indicator of aromaticity,[32] were calculated by our collaboration group (Prof. Dongho Kim of Yonsei University). Particularly, NICS calculation is a powerful tool when ^{1}H NMR accessible protons are not available in the middle of the ring current. This calculation was found to be much less negative for inverted sapphyrin **1.15** (roughly -2.0 ppm), than for sapphyrin **1.4** (-12 ppm). Details of the calculations are provided in the experimental section.

Table 1.1 Harmonic oscillator stabilization energies (HOSE$_i$, kcal/mol) and estimated weights (C_i) for canonical structures **1.15a–f**

Structure	HOSE$_i$	C_i
1.15a	181(34)	0.26(5)
1.15b	266(42)	0.18(2)
1.15c	230(38)	0.20(3)
1.15d	341(48)	0.14(1)
1.15e	419(57)	0.11(1)
1.15f	412(56)	0.11(1)

1.1.3 CONCLUSION

In summary, inverted sapphyrin **1.15**, a new sapphyrin analogue, was successfully synthesized. It was found to be weakly aromatic on the bases of its spectroscopic properties, structural features, and NICS calculations. This system is interesting in that it lies along the continuum between typical highly aromatic expanded porphyrin species, such as sapphyrin, and others, not reviewed in this chapter, that are best considered as nonaromatic or antiaromatic.

1.3 BENZOXASAPPHYRIN: A NEW MACROCYCLE AND ITS ANION BINDING PROPERTIES

1.3.1 BACKGROUND

Over the last two or three decades, a range of modified sapphyrins have been sucessfuly synthesized. The structural differences they embody have often been reflected in changes in the fundemental properties of sapphyrin. One such potentially mutable property is anion binding. However, anion binding studies involving modified sapphyrins have not been carried out to an appreciable extent, even for simple heterosapphyrins, i.e. those where one or more pyrrolic nitrogen atoms is replaced by another atom. This could reflect the complex nature of the doubly protonated sapphyrins compared to easier-to-study neutral anion receptors. One exception is a report by Chandrashekar and coworkers involving *meso*-aryl functionalized heterosapphyrins of structure **1.24**.[33] Unfortunately, the results of this study could not be compared with those for decaallkysapphyrin reported by our group,[15] in part because the unsubstituted thiophene in their system was found to lie outside of the macrocycle in the solid state and was thought to undergo "flipping" or "inversion" in solution, with the net result that the S atom is not completely localized within the central macrocyclic core. Given our interest in sapphyrin anion binding studies, we sought to generate a system that would allow for such a comparison.[34]

To examine the effect of oxygen atoms, benzoxasapphyrin **1.25** was synthesized. This system represents an analogue of a more restricted sapphyrin prepared by the Lee

group. In this section, we describe the synthesis of benzoxasapphyrin **1.25**, its characterization, and its anion binding properties. A further motivation for this work was to understand in greater detail a series of earlier oxasapphyrins for which only the syntheses were reported.[7, 35]

1.4b

1.24 (X = S, Y = O) or
(X = S, Y = S)

1.25
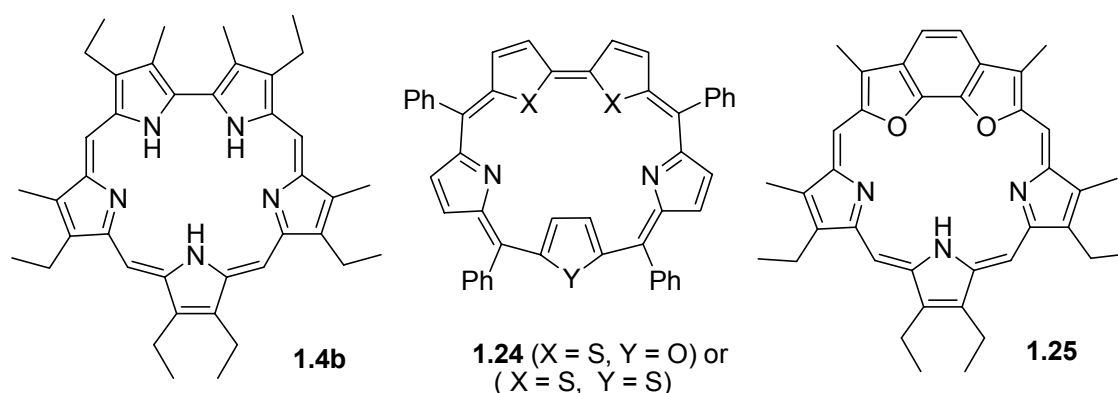
1.3.2 SYNTHESIS AND CHARACTERIZATION

The synthesis of benzoxasapphyrin was straightforward. It is shown in Scheme 1.3. Although a description of compound **1.26**[36] was first published by Nuth in 1887, this species has neither been fully characterized nor used as an intermediate in the construction of macrocyclic systems. Accordingly, compound **1.26** was resynthesized using the original procedure and fully characerized. LAH reduction of diester **1.26** afforded diol compound **1.27**. To obtain dialdehyde **1.28**, diol compound **1.27** was subjected to oxidation with manganese dioxide. The two important intermediates **1.28** and **1.22**[24] were condensed with TFA and the final compound, benzoxasapphyrin **1.25**, was synthesized in 40% yield.

23
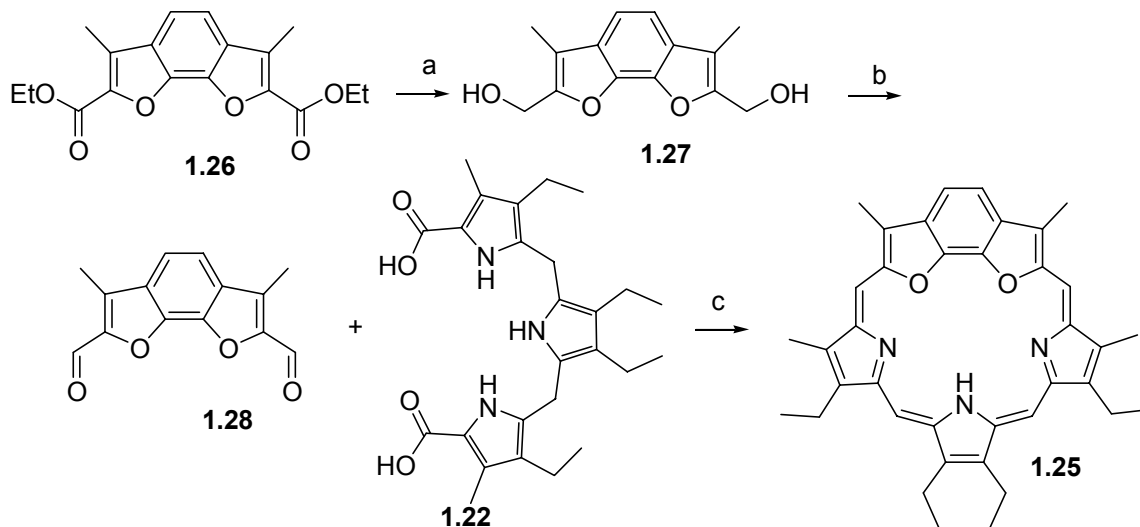
Conditions: (a) LAH, THF, 70% (b) MnO$_2$, CH$_2$Cl$_2$, 75% (c) TFA, CH$_2$Cl$_2$, 40%

Scheme 1.3. Synthesis of **1.25**

The structure of benzosapphyrin **1.25** was unambiguously proven by X-ray structure analysis. In the solid state, one tosylate is bound to the NHs of the macrocycles. Two tosylates are bound to a hydronium ion outside of the macrocycle. The tosylate in the macrocyle is located closer to the NH than to the two oxygen atoms. Presumably, there is an electrostatic repulsion between the oxygen atoms and the tosylate anion. The average NH···TsO and O···OTs bond distances are 2.107 and 2.839 Å, respectively.

(a)

(b)
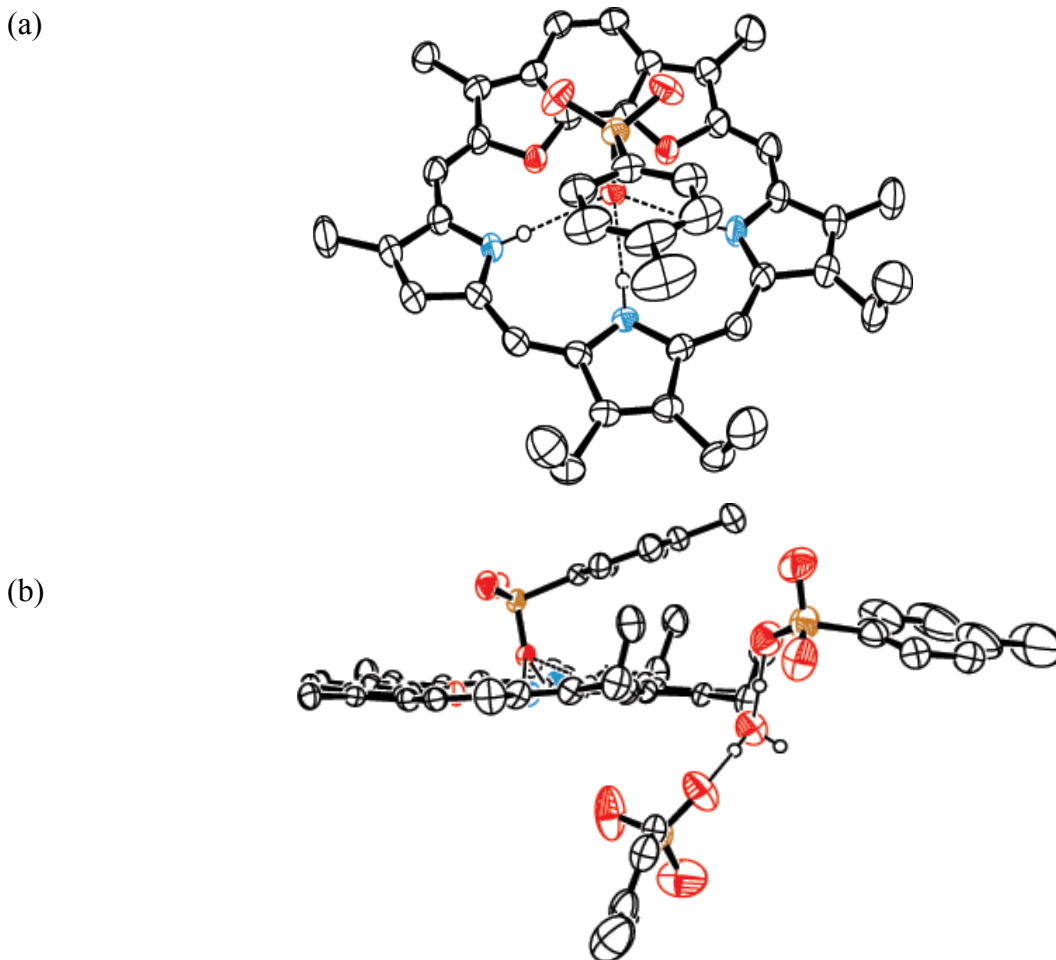
Figure 1.8. X-ray crystal structure of **1.25**·(*p*-TsOH)$_2$. (a) Top view; (b) Side view. Thermal ellipsoids are scaled to the 50% probability level. Most hydrogen atoms have been omitted for clarity.

The UV-vis spectrum of benzoxasapphyrin **1.25** is characterized by a Soret like band and two Q-bands appear at 458 nm (ε = 2.00 × 10^5 M^{-1}cm^{-1}), 673 nm (ε = 2.33 × 10^4 M^{-1} cm^{-1}), and 681 nm (ε = 1.61 × 10^4 M^{-1} cm^{-1}), respectively. The UV-vis spectrum of protonated benzoxasapphyrin is similar to decaalkylsapphyrins (Figure 1.5) with the observed red shift for benzoxasapphyrin being small relative to sapphyrin **1.4b**

(only 3nm). However, the neutral form of benzosapphyrin **1.25** displays a peak intensity that is substantially reduced over the full spectral range compared to the protonated form. While further study is warranted, this finding is tentatively ascribed to a reduced level of structural rigidity in the free-base form relative to the diprotonated salt.
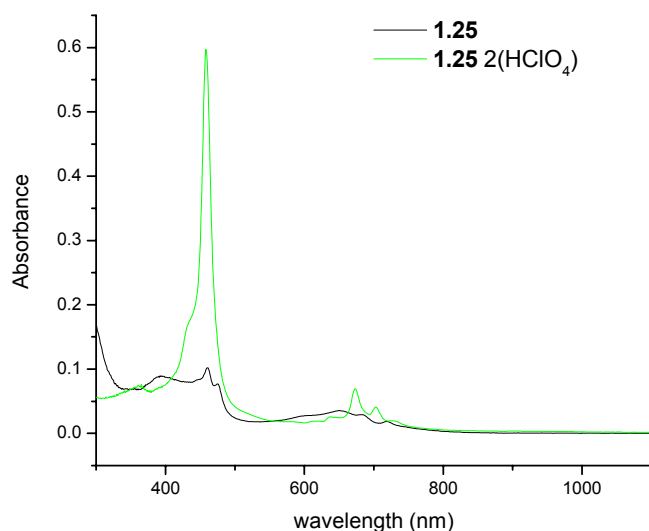
Figure 1.9 UV-vis spectrum of benzoxasapphyrin and **1.25**·(HClO$_4$)$_2$ in CH$_2$Cl$_2$

1.3.3 ANION AND NEUTRAL GUEST BINDING PROPERTIES

Tests of whether the diprotonated form of **1.25**·(HF)$_2$ would bind anions were made by carrying out standard UV-vis titrations in MeOH. Upon addition of tetrabutylammonium fluoride (TBAF) to solutions of diprotonated benzoxasapphyrin, an increase in the intensity of the band at 449 nm in the UV-vis spectrum was seen, along with a concommitant decrease in the intensity of the band at 469 nm (Figure 1.10). The normal binding stoichiometry for sapphyrin and most anionic guests is 1 : 1 in solution.[15] This was also expected to be true for [H$_2$·**1.25**]$^{2+}$, based on the crystal structure of

bezoxasapphyrin shown in Figure 1.8 as well as that of $[H_2 \cdot \textbf{4b} \cdot F^-]^+$.[9] Interestingly, the diprotonated form of benzoxasapphyrin was found to bind F^- roughly 170 times less effectively than the parent decasapphyrin **1.4b** in MeOH. Such a reduction in the K_a value can be explained by either lone pair electron repulsion between the two oxygen atoms in the core and the bound anion, the fact that the internal hydrogen bonding between the furan oxygen atoms and the pyrrolic NHs expected to be present in the macrocycle in the absence of guest has to be broken to interact with the anionic guests, or the fact that the total number of macrocycle-anion hydrogen bonds may be reduced. Surprisingly, the binding affinity of chloride could not be calculated due to the abnormal looking titration curve obtained, as shown in Figure 1.11. Similar abnormal-looking titration curves, observed in the case of other, non-expanded porphyrin-type anion receptors, have been explained by the formation of stable ion pairs upon the binding of one equivalent of an anion salt by a host.[37] However, this possibility is ruled out on the basis of two experiments. Two different benzoxasapphyrin salts such as perchlorate and chloride have similar titration curves in CH_3OH. We thus postulated that the binding ability of benzoxasapphyrin is affected by the solvent MeOH acting as a guest. Thus, we investigated the effect of MeOH in a less polar solvent, dichloroethane (DCE). Although a direct titration of MeOH in DCE leads to a change in the UV-vis spectrum, the resulting titration curve could not fit to any reasonable binding equation. However, similar experiments carried out using more acidic aromatic alcohols, such as phenol and 4-nitrophenol, which showed more normal changes in that they could be fit to 1 : 1 binding profiles. The resulting affinity constants were 15 and 25 M^{-1} for phenol and 4-nitrophenol in DCE, respectively. Based on this set of findings, it was inferred that i) MeOH is likely

binding to benzoxasapphyrin and that ii) this sapphyrin analogue might be considered as a very primitive alcohol receptor. While these solvent effects are likely important for weakly interacting guests, such as Cl⁻ and TsO⁻ anions, fluoride anion effectively competes with MeOH, at least to a first approximation. In the case of chloride and tosylate anion, a comparison of the floride anion constants for dacaalkylsapphyrin and benzoxasapphyin suggest that the affinity constant for Cl⁻ could be estimated to be less than 1 M^{-1} in MeOH.

Table1.2. Affinity constants (M^{-1}) for various anions for decaalkylsapphyrin (**1.4b**) and benzoxasapphyrin (**1.25**) determined at 23 °C.

	F	Cl	Phenol	4-nitrophenol
Decaalkylsapphyrin (**1.4b**)	96000±20000[a]	>100[a]	[f]	[f]
Benzoxasapphyrin (**1.25**)	552±70[b]	N/A [b, c, d]	15±0.3[e]	25±2.3[e]

[a] Literature K_a values determined by fluorescence titration.[15] [b] K_a values were determined from UV-vis titrations in MeOH. [c] Perchlorate salts were used. [d] K_a value of anion can not be calculated due to an abnormal looking titration curve. [e] K_a values were determined from fluorescence titrations carried out in DCE. [f] K^a values have not yet been determined.

(a)
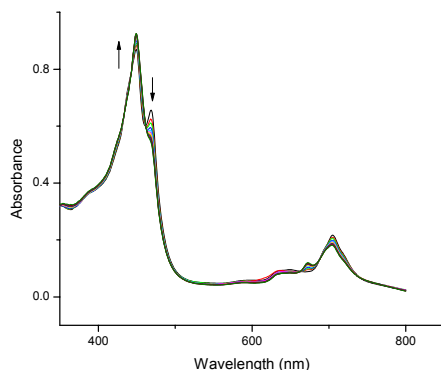
(b)
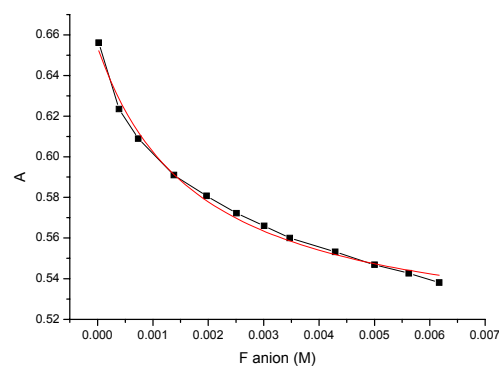
Figure 1.10 (a) Effect of the addition of TBAF on the absorption spectrum of benzoxasapphyrin·(HF)$_2$ in MeOH. The concentration of the benzoxasapphyrin used was 1.21×10^{-5} M and the concentration rage of anion was 2.43×10^{-5} to 6.17×10^{-3} M. (b) Plot of the absorption change of **1.25**·(HF)$_2$ at 469 nm vs the concentration of TBAF overlaid by the calculated 1 to 1 binding profile (derived for a UV-vis titration).

(a)
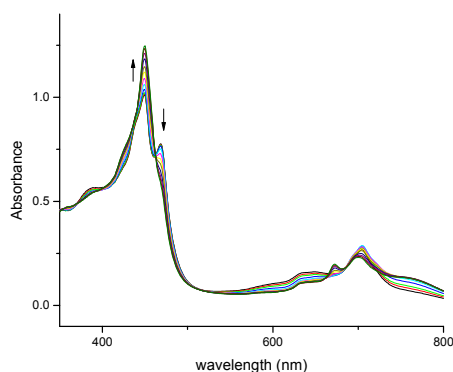
(b)
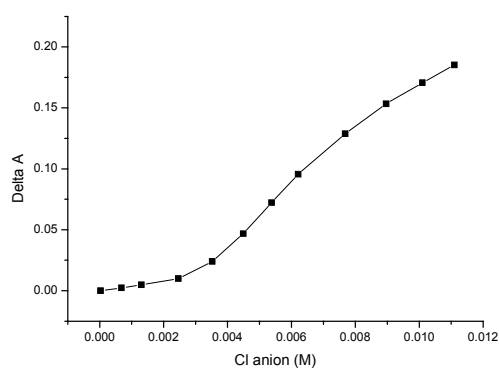
Figure 1.11 (a) Effect of Cl anion titration on absorption spectrum of benzoxasapphyrin 2HClO$_4$ in MeOH. The concentration of the benzoxasapphyrin used was 4.11×10^{-5} M and the concentration range of anion was 6.54×10^{-4} to 1.10×10^{-2}. (b) Abnormal looking Cl titration curve in MeOH. Plot of the absorption change of 1.25·(HClO$_4$)$_2$ at 469 nm vs the concentration of TBACl.

1.3.4 CONCLUSION

Benzoxasapphyrin **1.25** was successfully synthesized using intermediate **1.26**, a precursor that had not previously been used in macrocyclic synthesis. Additionally, binding studies of an oxasapphyrin derivative, benzooxasapphyrin **1.25**, were carried out. On this basis, it was determined that phenol and 4-nitrophenol are bound weakly. Further studies of this rigid sapphyrin analogue could contribute to our fundamental understanding of oxasapphyrin derivatives, a class of compounds first synthesized in 1971.

1.4 SAPPHYRINS AS POTENTIAL ANTI-CANCER AGENTS

1.4.1 BACKGROUND

For quite same time, sapphyrins have been studied as potential photodynamic therapy (PDT) agents.[5] However, prior to a preliminary report in 2002,[38] they had not been considered as direct anti-cancer agents. Subsequently, the Sessler group found that some sapphyrin derivatives act as better anti-cancer activity than prodigiosin (Figure 1.12). Among these compounds, sapphyrin **1.29** was chosen as a lead compound because it proved easier to functionalize than other sapphyrins. This success provided an incentive to make a better sapphyrin. Thus, sapphyrin **1.29** was subject to further derivatization. Described below are these new sapphyrins and a summary of their *in vitro* biological properties. The latter results were generated by Phamacyclics, Inc.

1.29. R = CH$_2$OH
1.30. R = CH$_2$NH$_2$
1.31. R = CO$_2$H

1.32. R = O(CH$_2$CH$_2$O)$_3$CH$_3$

1.33

1.10
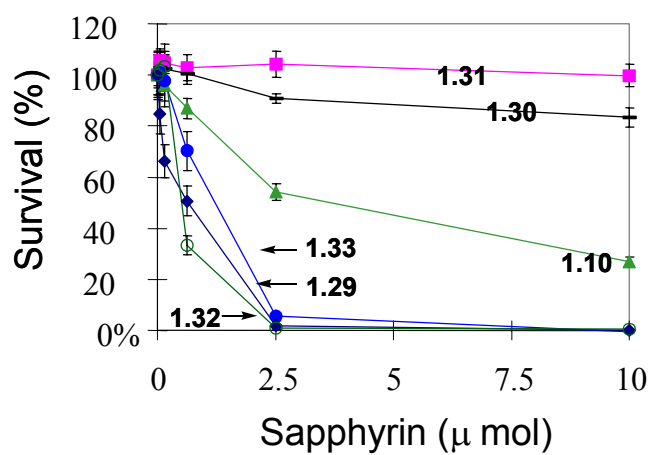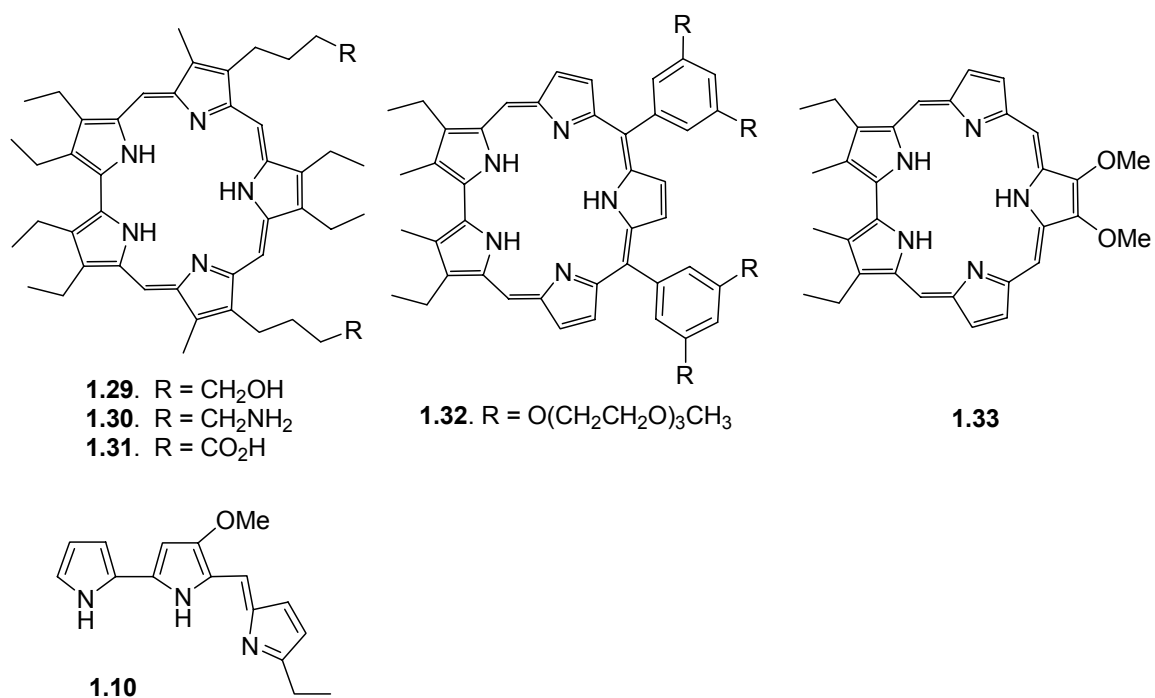
Figure 1.12 Summary of proliferation studies using the A549 human lung cancer cell line

1.4.2 SYNTHESIS AND EVALUATION

The retrosynthesis of β-pyrrole substituted bis-hydroxypropyl sapphyrins requires bipyrrole **1.34** and tripyrane **1.35**. To obtain new sapphyrins of this type, two general strategies were applied to the bipyrrole and diol units. The first derivatives were synthesized by replacing the bipyrrole units. The second set involved modifications of the amphiphilicity *via* introduction of, e.g., PEG-groups. This PEG-chemistry has proved very successful in the case of preparing biological active texaphyrins derivatives.[39]
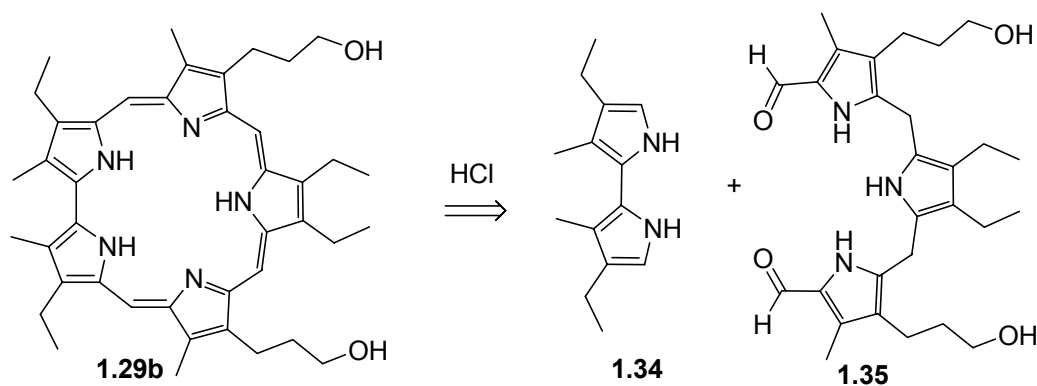
Scheme 1.4 Retrosynthesis of Sapphyrins

Tripyrrane **1.35** was provided by Pharmacyclics, Inc. The synthesis of bipyrrole **1.34** requires 8 steps (Scheme 1.5). Compound **1.36** was obtained *via* an aldol reaction and then acylated with acetic anhydride. The isocyanate **1.37** was condensed with the resulting acetoxy nitroalkane **1.36** in a base-catalyzed reaction that afforded ethyl 3-ethyl-4-methyl-pyrrole-2-carboxylate **1.38** in 68% yield. Pyrrole **1.38** was then iodinated with NaI/I$_2$ and N-protected using BOC anhydride. The N-protected pyrrole obtained in this

way, **1.40**, was then subject to an Ullmann coupling and the Boc-group was removed to produce the diethylester bipyrrole **1.41** in 74% yield. Removal of the ester followed by decarboxylation afforded bipyrrole **1.34** in a one-pot procedure. Parent sapphyrin **1.29b** was then synthesized in 47% yield *via* an acid catalyzed '3+2' condensation involving bipyrrole **1.34**[9] and tripyrrane **1.35**[24] with (Schemes 1.4 and 1.5).

With this key intermediate in hand, various sapphyrins were then synthesized according to the general procedure shown in Scheme 1.4 and summarized in Table 3. Generally, the use of a more electron rich bipyrrole afforded a higher isolated yield. Consistent with this thinking, sapphyrin **1.29d** was synthesized in particularly low yield because of the lower nucleophilicity of the unsubstituted bipyrrole.
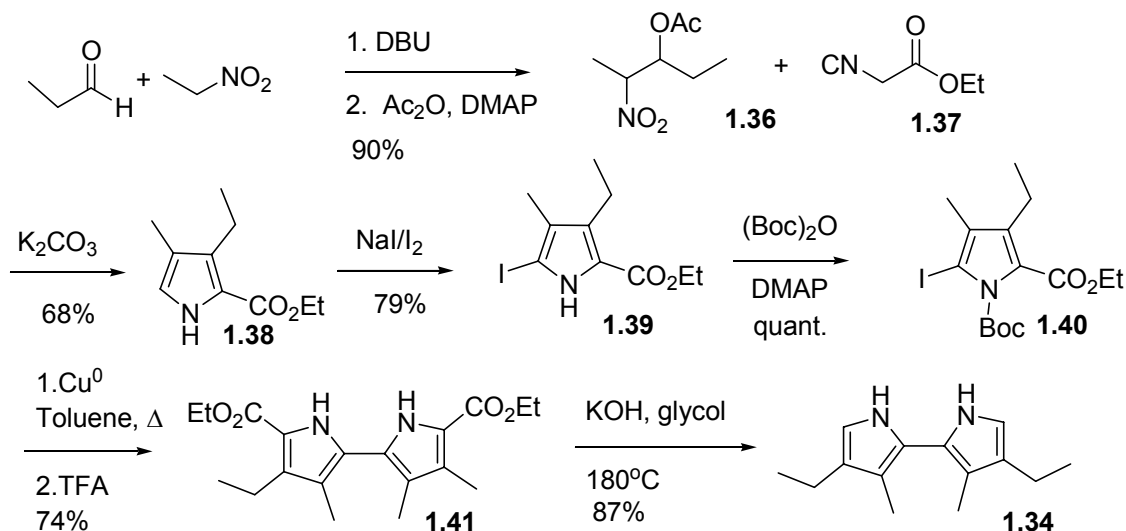
Scheme 1.5 Synthesis of bipyrrole **1.34**

Table 1.3 Yields of hydroxypropyl substituted sapphyrins produced according to the general procedure shown in Scheme 1.4

compound	R_1	R_2	Yield%
1.29a	Et	Et	48
1.29b	Me	Et	47
1.29c	H	Me	20
1.29d	H	H	<2
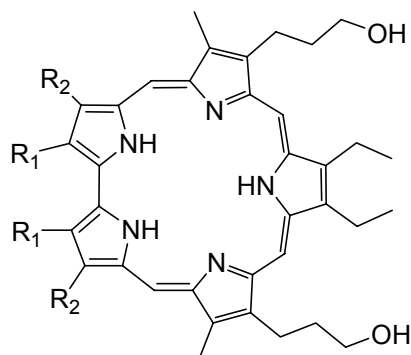
To increase the water solubility of the parent sapphyrin **1**.**29**, various ethylene glycol (PEG) groups were introduced *via* carbamate linkers. The target sapphyrins **1.42b** and **1.43** were synthesized in one step by coupling reactions involving sapphyrin **1.29** and the water solubilizing **1.44**[40] and mono-PEG amine **1.45**[41] group using carbamate linkers. The final compounds **1.42b** and **1.43** were obtained in 50 and 58% yield, respectively. Further sapphyrin derivatives for use in biological SAR (sructure-activity relation) studies were carried out by the changing alkyl substituents on the bipyrroles subunits of the sapphyrins under consideration (see Table 1.4).

Once prepared, samples were transmitted to Pharmacyclics for *in vitro* analyses. The resulting IC_{50} of **1.42b** is 0.5 μM and the order of anti-cancer activity for all compounds is **1.42b** >**1.42a** = **1.43** > **1.42c** = **1.42d** in Ramos cell lines. It is interesting to note that a one carbon difference on the bipyrrole subunit can affect the anti-cancer activity significantly. Additionally, the use of the more water soluble bis-PEG amine (leading to sapphyrin **1.42b**) afforded a compound with 0.5 μM better activity than **1.43**

(**1.42a**, 0.5 µM *vs*. **1.43,** 1 µM) in Ramos cell line. All biological activities were evaluated by Pharmacyclics, Inc.
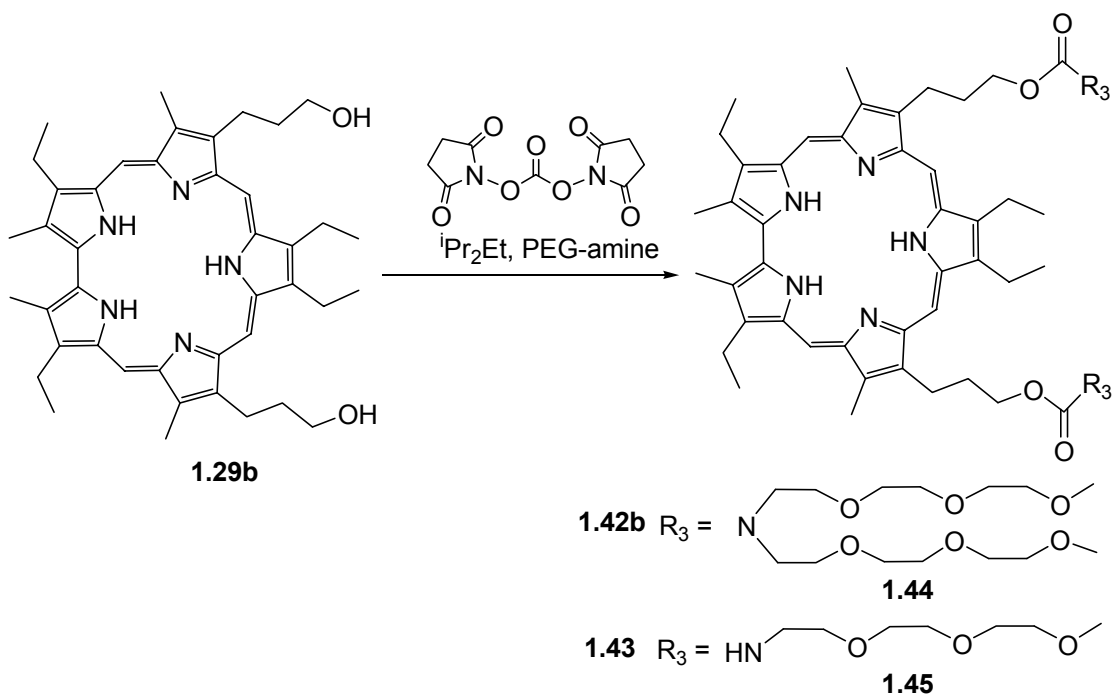
Scheme 1.6 Synthesis of target compounds **1.44** and **1.45**

Table 1.4 Anti-cancer activity of various sapphyrins in Ramos cell line

compounds	R_1	R_2	R_3	IC_{50} (µM)
1.42a	Et	Et	Bis-PEG (**1.44**)	1
1.43	Me	Et	Mono-PEG (**1.45**)	1
1.42b	Me	Et	Bis-PEG (**1.44**)	0.5
1.42c	H	Me	Bis-PEG (**1.44**)	5
1.42d	H	H	Bis-PEG (**1.44**)	5
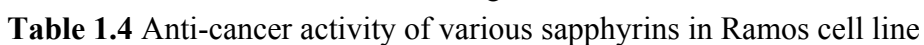
Another interesting fact is that the uptake level of sapphyrin **1.42b** is higher than other examined sapphyrins in xenograft-derived-bearing tumor (Figure 13). Specifically, drug uptake levels in several tissues were monitored using near infrared fluorescence as detected using a LI-COR odyssey scanner. Sapphyrin **1.46** and **1.47** were synthesized by Pharmacyclics, Inc. In these tumors, sapphyrin **1.42b** could be localized at concentrations (as inferred from observed fluorescence) up to 10 times greater than those displayed by

the parent dihydroxysapphyrin **1.29a**. In spleen and liver, the presence of sapphyrin **1.42b** is negligible compared to the control (5% manitol).[34]
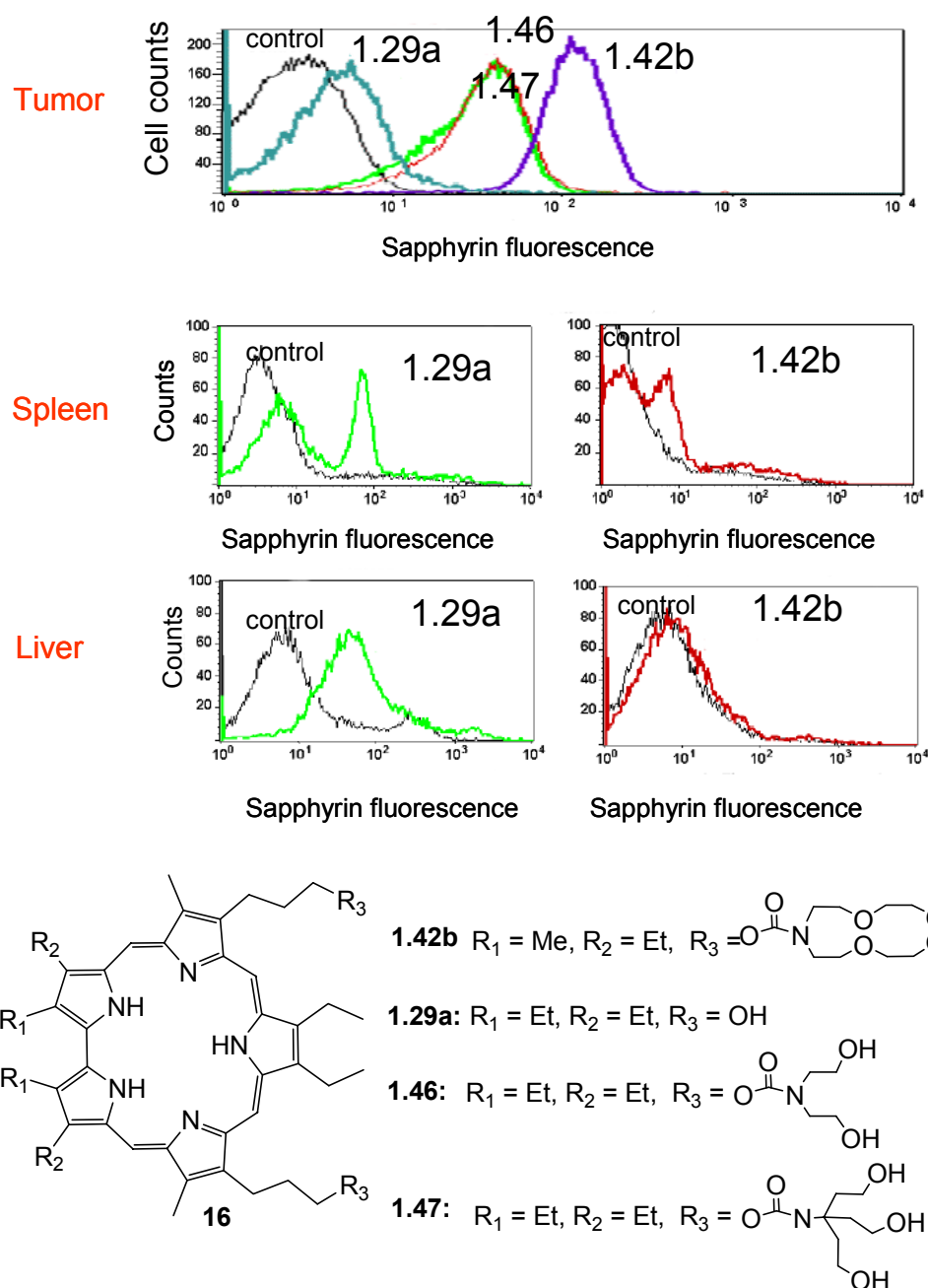
Figure 1.13 Localization studies involving various sapphyrins as inferred from fluorescent measements with xenograph Ramos murine tumor models

Tumor localization is not a particular property of sapphyrins. Many porphyrin derivatives are also known to localize in tumor.[42] The mechanisms are not simple, and there are several proposed rationales for this property that are thought to depend on molecular structure, size, charge, etc. Among these factors, it is worth mentioning two mechanisms. The first involves passive diffusion and is thought to result from the low extracellular pH present in tumors. The extracellular pH in tumor and normal tissue is about 6.5 to 7.4 and 7.5, respectively.[42] The acidic pH of tumors can shift the protonation equilibrium toward more lipophilic porphyrinoid species, impeding escape of the porphyrinoid from the cell (i.e., by slowing the rate of across-membrane transport). The second explanation involves a LDL/Protein-mediated mechanism. LDL (low-density lipoprotein) is known to have high affinity for porphyrins and related species. The resulting LDL-porphyriniod adduct binds the apolipoprotein (apo) B/E receptor. LDL is major source of cholesterol and tumor requires more cholesterol to build more membrane, which provides a rationale for why apoB/E receptors are upregulated in cancers. As a consequence, porphyrinoids are effectively delivered to tumors (Figure 1.14).
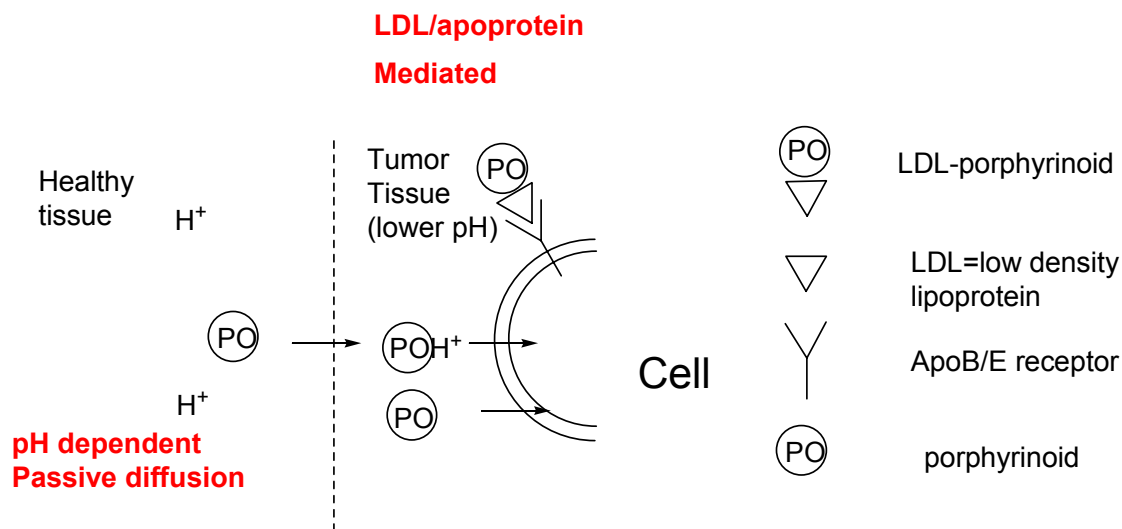
Figure1.14 Proposed mechanism of porphyrinoid localization in tumors

1.4.3. CONCLUSION

As the result of functionalizing the bipyrrole units and modifying the water solubilizing units, a lead system, sapphyrin **1.42b,** was produced. It and its analogues were evaluated *in vitro*. On this basis, sapphyrin **1.42b** is selected as the best compound among various sapphyrins tested in Ramos cell line. However, even this current lead compound (**1.42b**) is far from perfect. It displays high toxicity (general phototoxicity of sapphyrins). Therefore, at the very least, it will be necessary to reduce the phototoxicity of sapphyrins to move this project forward.

1.5 REFERENCES

(1)   Sessler, J. L.; Daniel, S. *Angew. Chem., Int. Ed. Eng.* **2003**, *42*, 5134-5175.

(2)   Rath, H.; Sankar, J.; PrabhuRaja, V.; Chandrashekar, T. K.; Nag, A.; Goswami, D. *J. Am. Chem. Soc.* **2005**, *127*, 11608-11609.

(3)   Sessler, J. L.; Callaway, W.; Dudek, S. P.; Date, R. W.; Lynch, V.; Bruce, D. W. *Chem. Comm.* **2003**, *19*, 2422-2423.

(4)   Bonnett, R. *Chem. Soc. Rev.*, **1995**, *24*, 19-33.

(5)   (a) Maiya, B. G.; Cyr, M.; Harriman, A.; Sessler, J. L. *J. Phys. Chem.* **1990**, *94*, 3597-3601. (b) Magda, D.; Wright, M.; Miller, R. A.; Sessler, J. L.; Sansom, P. I. *J. Am. Chem. Soc.* **1995**, *117*, 3629-3630. (c) Sessler, J. L.; Andrievsky, A.; Sansom, P. I.; Kral, V.; Iverson, B. L. *Bioorg. & Med. Chem. Lett.* **1997**, *7*, 1433-1436.

(6)   (a) First reported by R. B. Woodward at the Aromaticity Conference, Sheffield, U.K., **1966**. (b) Bauer, V. J.; Clive, D. R.; Dolphin, D.; Paine, J. B.,III; Harris, F. L.; King, M. M.; Lcder, J.; Wang, S.-W. C.; Woodward, R. B. *J. Am. Chem. Soc.* **1983,** *105,* 6429-6436.

(7)   (a) Broadhurst, M. J.; Grigg, R.; Johnson, A. W. *Chem. Commun.* **1969**, 23-24. (b) Broadhurst, M. J.; Grigg, R.; Johnson, A. W. *J. Chem. Soc., Perkin Trans. 1* **1972**, 2111-2116.

(8)   (b) Bauer, V. J.; Clive, D. R.; Dolphin, D.; Paine, J. B.,III**;** Harris, F. L.; King, M. M.; Lcder, J.; Wang, S.-W. C.; Woodward, R. B. *J. Am. Chem. Soc.* **1983**, *105,* 6429-6436.

(9)   Sessler, J. L.; Cyr, M. J.; Lynch, V.; McGhee, E.; Ibers, J. A. *J. Am. Chem. Soc.* **1990**, *112*, 2810-2813.

(10)   Richter, D. T.; Lash, T. D. *J. Am. Chem. Soc.* **1998**, *120*, 9965-9966.

(11)   Pushpan, S. K.; Srinivasan, A.; Anand, V. G.; Venkatraman, S.; Chandrashekar, T. K.; Joshi, B. S.; Roy, R.; Furuta, H. *J. Am. Chem. Soc.* **2001**, *123*, 5138-5139.

(12)   Panda, P. K.; Kang, Y.; Lee, C.-H. *Angew. Chem.*, *Int. Ed.* **2005**, *44*, 4053-4055.

(13)   Jeong, S.-D.; Sessler, J. L.; Lynch, V. Lee, C.-H. *J. Am. Chem. Soc.*, **2008**, 130, 390 -391.

(14)   Vogel, E. *Pure & Appl. Chem.,* **1993**, *65*, 145-152.

(15)   Shionoya, M.; Furuta, H.; Lynch, V.; Harriman, A.; Sessler, J. L. *J. Am. Chem. Soc.* **1992**, *114*, 5714-5722.

(16)   Fustner, A. *Angew. Chem., Int. Ed. Engl.* **2003**, *31*, 3582-3603.

(17)   (a) C. Yamamoto, H.; Takemoto, H.; Kuno, D.; Yamamoto, A.; Tsubura, K.; Kamata, H.; Hirata, A.; Yamamoto, H.; Kano, T.; Seki, T.; Inoue, K. *Hepatology* **1999**, *30*, 894-902. (b) D. Yamamoto,; Y. Kiyozuka, Y.; Uemura, C.; Yamamoto, H.; Takemoto, H.; Hirata, K.; Tanaka,; K. Hioki,; Tsubura, A. *J. Cancer Res. Clin. Oncol.* **2000**, *126*, 191-197.

(18)   Sessler, J. L.; Eller, L. R.; Cho, W.-S.; Nicolaou, S.; Aguilar, A.; Lee, J. T.; Lynch, V. M.; Magda, D. J. *Angew. Chem., Int. Ed. Engl.* **2005**, *44*, 5989-5992.

(19)   Stepien, M.; Latos-Grażyński, L.; Sprutta, N.; Chwalisz, P.; Szterenb, L. *Angew. Chem., Int. Ed. Engl.* **2007**, *46*, 7869-7873.

(20)   Chmielewski, P. J.; Latos-Grażyński, L.; Rachlewicz, K.; Głowiak, T. *Angew. Chem., Int. Ed. Engl.* **1994**, *33*, 779-781.

(21) Furuta, H.; Asano, T.; Ogawa, T. *J. Am. Chem. Soc.* **1994**, 116, 767-768.

(22) Srinivasan, A.; Furuta, H. *Acc. Chem. Res*. **2005**, *38*, 10-20.

(23) Wang, J.; Scott, A. I. *Tetrahedron Lett*. **1995**, *36*, 7043-7046.

(24) Sessler, J. L.; Johnson, M. R.; Lynch V. *J. Org. Chem*.; **1987**, *52*, 4394-4397.

(25) A similar incorporation of EtOH into a double N-confused macrocycle has been reported; Furuta, H.; Maeda, H.; Osuka, A. *J. Am. Chem. Soc*. **2000**, *122*, 803-807.

(26) Chmielewski, P. J.; Latos-Grażyński, L.; Rachlewicz, K. *Chem. Eur J.* **1995**, *1*, 68-73.

(26) Furuta, H.; Ishizuka, T.; Osuka, A.; Dejima, H.; Nakagawa, H.; Ishikawa, Y. *J. Am. Chem. Soc.* **2001**, 123, 6207-6208.

(27) Furuta, H.; Maeda, H.; Osuka, A. *J. Am. Chem. Soc*. **2000**, *122*, 803-807.

(28) For another example of borderline aromaticity in porphyrinoids, cf. Lash, T. D.; Chaney, S. T. *Angew. Chem., Int. Ed. Eng.* **1997**, *36*, 839-840.

(29) Gorski, A.; Lament, B.; Davis, J. M.; Sessler, J.; Waluk, J. *J. Phys. Chem. A* **2001,** *105*, 4992-4999.

(30) Krygowski, T. M.; Cyrański, M. K. *Chem. Rev.* **2001**, *101*, 1385-1419.

(31) Krygowski, T. M.; Anulewicz, R.; Kruszewski, J. *Acta Cryst., Sect. B*, **1983**, *B39*, 732-739.

(32) (a) Chen, Z.; Wannere, C. S.; Corminboeuf, C.; Puchta, R.; Schleyer, P. R. *Chem. Rev.* **2005**, *105*, 3842-3888. (b) Nakamura, Y.; Aratani, N.; Shinokubo, H.; Takagi, A.; Kawai, T.; Matsumoto, T.; Yoon, Z. S.; Kim, D. Y.; Ahn, T. K.; Kim, D.; Muranaka, A.; Kobayashi, N.; Osuka, A. *J. Am. Chem. Soc*. **2006**, *128*, 4119-4127.

(33)   Srinivasan A.; Anand, V. R. G.; Pushpan, S. K.; Chandrashekar, T. K.; Sugiura, K.; Sakata, Y. *J. Chem. Soc., Perkin Trans. 2* **2000**, 1788-1793.

(34)   (a) Wang, Zhong.; Lecane, P. S.; Thiemann, P.; Fan, Q.; Cortez, C.; Ma, X.; Tonev, D.; Miles, D.; Naumovski, L.; Miller, R. A.; Magda, D.; Cho, D.-G.; Sessler, J. L.; Pike, B. L.; Yeliger, S. M.; Karaman, M. W.; Hacia, J. G. *Molecular Cancer* **2007**, *6*, 9-20. (b) Naumovski, L.; Sirisawa, M.; Lecane, P.; Chen, J.; Ramos, J; Wang, Z.; Cortez, C.; Magda, D.; Thiemann, P.; Boswell, G.; Miles, D.; Cho, D.-G.; Sessler, J. L.; Miller, R. *Mol. Cancer Ther*. **2006**, *5*, 2798-2805. (c) Naumovski, L.; Ramos, J.; Sirisawad, M.; Chen, J.; Thiemann, P.; Lecane, P.; Magda, D.; Wang, Z.; Cortez, C.; Boswell, G.; Cho, D.-G.; Sessler. J. L.; Miller, R. *Mol. Cancer Ther*. **2005**, *4*, 968-976.

(35)   Sessler, J. L.; Hoehner, M. C.; Gebauer, A.; Andrievsky, A.; Lynch, V. *J. Org. Chem.* **1997**, *62*, 9251-9260. (b) Sessler, J. L.; Cyr, M.; Burrell, A. K. *Tetrahedron* **1992**, *48*, 9661-9672.

(36)   Nuth, G. Chem. Ber, 1887, 1332-1338.

(37)   (a) Shukla, R.; Kida, T.; Smith, B. D. *Org. Lett*. **2000**, *2*, 3099-3102. (b) Tumcharern, G.; Tuntulani, T.; Coles, S. J.; Hursthouse, M. B.; Kilburn, J. D. *Org. Lett.;***2003**; *5*; 4971-4974. (c) Camiolo, S.; Coles, S. J.; Gale, P. A.; Hursthouse, M. B.; Tizzard, G. J. *Supramol. Chem*. **2003**, *15*, 231-234.

(38)   Kral, V.; Davis, J.; Andrievsky, A.; Kralova, J.; Synytsya, A.; Pouckova, P.; Sessler, J. L. *J. Med. Chem*. **2002**, *45*,1073-1078.

(39)   (a) Sessler, J. L.; Mody, T. D.; Hemmi, G. W.; Lynch, V. *Inog. Chem.* **1993**, *32*, 3175-3187. (b) Sessler, J. L.; Hemmi, G.; Mody, T. D.; Murai, T.; Burrell, A.; Young, S. W. *Acc. Chem. Res.* **1994**, *27*, 43-50.

(40)   Selve, C.; Ravey, J. C.; Stebe, M. J.; El Moudjahid, C.; Moumni, E. M.; Delpuech, J. I. *Tetrahedron* **1991**, *47*, 411-428.

(41)   Dombi, K. L.; Griesang, N.; Richert, C. *Synthesis* **2002**, *6*, 816-834.

(42)   Osterloh, J.; Vicente, M. G. *J. Porphyr. Phthalocyan*. **2002**, *6*, 305-324.

1.6 EXPERIMENTAL SECTION

Proton and ^{13}C-NMR spectra were measured at 25 ºC using a Varian Unity Innova instrument at 500 MHz. UV-vis spectra were recorded on a BECKMAN DU 640B spectrophotometer. High resolution ESI mass spectra were obtained on a VG ZAB2-E mass spectrometer.

1.6.1 SYNTHETIC EXPERIMENTAL

7,18-Dimethyl-3,22-di(*p*-tosyl)-23-methoxy-8,12,13,17-tetraethyl-3,22-diaza-25,26-carbasapphyrin Cl (1.15) Tetramethyldiethyltripyrromethane dicarboxylic acid **1.22** (50 mg, 0.10 mmol) was stirred with TFA (2 mL) under argon at room temperature for 2 min, after which dichloromethane (200 mL) and dialdehyde **1.21** (45 mg, 0.10 mmol) were added to the solution. The solution was stirred in the dark under argon for 12 h. DDQ (22 mg, 0.096 mmol) was added and the reaction mixture was stirred for 30 min. The solvents were then removed from the solution and the residue was then directly purified by chromatography over silica gel, eluting with methanol-dichloromethane (0-4% MeOH in CH_2Cl_2). The yellowish-green fraction was collected and the solvent was removed under reduced pressure. The resulting solid was further purified by preparative thin layer chromatography (PTLC) and then washed with NH_4Cl and recrystallized from methanol-ether. This procedure consistently afforded pure inverted sapphyrin **1.15** (8 mg; 9%). ^{1}H-NMR (500 MHz, DMSO-d_6) [ppm] 1.33 (m, 12H), 2.15 (s, 3H), 2.26 (s, 3H), 2.55 (s, 3H), 2.61 (s, 3H), 3.07 (m, 4H), 3.17 (m, 4H), 3.27 (s, 3H), 3.77 (bs, 1H), 4.04 (bs, 1H), 5.99 (vbs, 1H), 6.94 (s, 1H), 7.24 (d, J = 8 Hz, 2H), 7.36 (d, J = 8.5 Hz, 2H + 1H NH)

7.56 (s, 1H), 7.63 (s, 1H), 7.75 (s, 1H), 7.89 (s, 1H), 7.92 (d, J = 8 Hz, 2H), 7.96 (d, J = 8.5 Hz, 2H), 8.06 (bs, 1H), 8.56 (s, 1H). ^{13}C-NMR (125 MHz, CDCl$_3$) [ppm] 9.74, 10.18, 14.97, 15.93, 16.39, 17.04, 17.79, 17.85, 18.12, 18.25, 20.78, 20.95, 52.16, 84.73, 93.06, 94.44, 96.82, 105.98, 117.91, 122.78,124.44, 125.76, 126.99, 127.45, 128.11, 129.51,129.78, 130.47, 134.47, 134.68, 135.53, 136.69, 138.82, 139.97, 140.78, 142.19, 144.04, 144.50, 145.17, 145.43, 146.10; HRMS (ESI): m/z 856.3569 ((M+H), calcd for C$_{49}$H$_{54}$N$_5$O$_5$S$_2$ 856.3566. UV-vis (CH$_2$Cl$_2$) max [nm] (M^{-1}•cm^{-1}) 419 (43,300), 464 (44,500), 755 (15,300), 827 (24,500). This compound was further characterized by X-ray diffraction analysis.

Diethyl 3,6-dimethylbenzofuran-2,7-dicarboxylate (1.26) Dicarboxylate **1.26** was obtained from the disubstituted pyrocatechol in 5.7% yield according to the literature procedure (Nuth, G. Chem. Ber, 1887, 1332-1338). ^{1}H-NMR (400 MHz, CDCl$_3$) [ppm] 1.44 (t, J = 7.2 Hz, 6H), 2.63 (s, 6H), 4.45 (q, J = 7.2 Hz, 4H), 7.49 (s, 2H). ^{13}C-NMR (100 MHz, CDCl$_3$) [ppm] 9.48, 14.28, 61.03, 115.92, 126.50, 129.51, 139.07, 141.29, 159.94.; HRMS (CI): m/z 331.1183 (M+H), calcd for C$_{18}$H$_{19}$O$_6$ 331.1182.

(3, 6-dimethylbenzofuran-2,7-yl)dimethanol (1.27) Diester **1.26** (140 mg, 0.423 mmol in 5mL THF) was added slowly to a suspension of LiAlH$_4$ (160 mg, 4.23 mmol in 20 mL anhydrous THF) under argon at 0 ^{o}C. After the addition was completed, the reaction was stirred for 1 h at 0 ^{o}C. The reaction was then stirred at room temperature overnight. Water was added carefully to quench the reaction. The resulting solution was filtered through a celite pad and washed with ethyl acetate. The filtrate and washings were washed with water and the organic layer was separated, dried over anhydrous Na$_2$SO$_4$ and the solvent was removed in vacuo. Analytically pure **1.27** was isolated in this way without having to

resort to column chromatography (70 mg, 70%). ^{1}H-NMR (500 MHz, DMSO-d_6) [ppm] 2.24(s, 6H), 4.57 (d, J = 6.0 Hz, 4H), 5.31 (t, J = 6.0 Hz, 2H). ^{13}C-NMR (125 MHz, DMSO-d_6) [ppm] 7.81, 53.82, 112.55, 114.65, 137.65, 152.41.; HRMS (CI): m/z 229.0864 [M-H$_2$O]$^+$, calcd for C$_{18}$H$_{19}$O$_6$ 229.0865.

Diethyl 3,6-dimethylbenzofuran-2,7-dialdehyde (1.28) MnO$_2$ (42 mg, 0.483) was added to the suspension of diol **1.27** (70 mg, 4.83 mmol in 10 mL anhydrous CH$_2$Cl$_2$) under argon at room temperature. The reaction was then stirred at room temperature overnight. The resulting solution was filtered through a celite pad and washed with CH$_2$Cl$_2$. The filtrate and washings were collected and solvent was removed in vacuo. Analytically pure solid **1.28** could be isolated in this way without the need for column chromatography (70 mg, 70%). ^{1}H-NMR (500 MHz, DMSO-d_6) [ppm] 2.66 (s, 6H), 7.80 (s, 2H), 10.04 (s, 2H). ^{13}C-NMR (125 MHz, DMSO-d_6) [ppm] 8.08, 117.79, 130.06, 139.21, 148.77, 179.98; HRMS (CI): m/z 243.0660 [M+H]$^+$, calcd for C$_{14}$H$_{11}$O$_4$ 243.0657.

Benzoxasapphyrin (1.25) Tetramethyldiethyltripyrromethane dicarboxylic acid **1.22** (18.7 mg, 0.041 mmol) was stirred with TFA (1 mL) under argon at room temperature for 2 min, after which dichloromethane (83 mL) and dialdehyde **1.28** (10 mg, 0.041 mmol) were added to the solution. The solution was stirred in the dark under argon for 12 h. DDQ (24 mg, 0.10 mmol) was added and the reaction mixture was stirred for 30 min. The solvents were then removed and the residue was then directly purified by chromatography over silica gel, eluting with methanol-dichloromethane (0-5% MeOH in CH$_2$Cl$_2$). The green fraction was collected and the solvent was removed under reduced pressure. The resulting solid was further purified by recrystallizing from ethyl acetate, a

purification procedure that consistently afforded pure benzoxasapphyrin **1.25** (9.3 mg; 40%). ^{1}H-NMR (500 MHz, CDCl$_3$ + *p*-TsOH + MeOH-*d$_4$*) [ppm] -5.29 (bs, 2H), -2.56 (1.33 (bs, 1H), 2.26 (t, J = 7.5 Hz, 12H), 4.33 (s, 6H), 4.77 (m, 8H), 4.88 (s, 6H), 4.17 (m, 8H), 4.88 (s,6H), 10.08 (s, 2H), 11.81 (s, 2H), 12.08 (s, 2H). ^{13}C-NMR (125 MHz, CDCl$_3$ + *p*-TsOH + MeOH-*d$_4$*) [ppm] 12.90, 13.20, 17.76, 18.43, 21.12, 101.32, 122.10, 124.56, 128.01, 129.23, 133.22, 136.55, 138.90, 140.88, 145.57, 146.47, 147.22. HRMS (ESI): m/z 570.3121 [M+H]$^+$, calcd for C$_{38}$H$_{40}$N$_3$O$_2$ 570.3121. UV-vis (**1.25**·2(HClO$_4$) in CH$_2$Cl$_2$) max [nm] (ε, M^{-1}•cm^{-1}) 458 (200,000), 673 (23,300), 681 (16,100). 827 (24,500). This compound was further characterized by X-ray diffraction analysis.

3,12,13,22- **Tetraethyl-8,17-bis(hydroxylethyl)-2,7,18,23-tetramethylsapphyrin (1.29b)** In a 4L three-neck round bottom flask, bipyrrole **1.34** (500 mg, 2.31 mmol) and tripyrane **1.35** (1.11 g, 2.31 mmol) were dissolved in a solution of MeOH (300 mL) and CH$_2$Cl$_2$ (3 L). Concentrated HCl (0.76 mL; about 9.2 mmol) was added. The reaction was protected from light with aluminum foil and stirred overnight. Triethylamine (250 g, 2.47 mol) was added dropwise to the solution. The resulting mixture was concentrated on a rotary evaporator to a volume of about 500 mL and then extracted three times with water (100 mL, 200 mL, and 200 mL). The organic phase was directly loaded on a neutral aluminum oxide column. The column was first eluted with 1% MeOH/CH$_2$Cl$_2$ to separate a red-colored band (ascribed to porphyrin byproduct). After the red band had eluted off the column, the polarity of the eluent was increased to 5% MeOH/CH$_2$Cl$_2$. This permitted the green band (recognized as being the sapphyrin product) to elute. The sapphyrin fraction was concentrated to give dihydroxysapphyrin **1.29b** as a shiny blue solid (730

mg, 47.8% yield). HRMS (ESI): m/z 660.4285 [M+H]$^+$, calcd for C$_{41}$H$_{51}$N$_5$O$_2$·2CF$_3$CO$_2$H, 660.4277.

3,2,13,22-Tetraethyl-8,17-bis(bis(2-(2-(2-methoxyethoxy)ethoxy)ethyl)aminocarboxylethyl)-2,7,18,23-tetramethylsapphyrin (1.42b) 25 mL two neck flask was loaded with sapphyrin **1.29b** (46 mg, 0.069 mmol), N-N-disuccinimidyl carbonate (107 mg, 0.418 mmol), and a magnetic stir bar before being dried *in vacuo* for 2h. Anhydrous CH$_2$Cl$_2$ (4 mL) and diisopropylethylamine (54 mg, 0.418 mmol) were added and the resulting mixture was stirred at rt for 2h under Ar. The bis-PEG amine **1.44** (129 mg, 0.418 mmol) was then added and the resulting solution was stirred for another 1 h. The reaction mixture was evaporated to dryness on a rotoryevaporator and purified using a neutral aluminum oxide column. The eluent used ranged from CH$_2$Cl$_2$ to 1% MeOH/CH$_2$Cl$_2$. The green band afforded the final compound, which was subsequently treated with 1N HCl to provide **1.42b** in the form of its diprotonated, bis-HCl salt (46 mg, 50% yield). ^{1}H NMR (500 MHz, CDCl$_3$) [ppm] −4.90 (2H, *NH*, s), −4.59 (1H, *NH*, s), −4.29 (2H, *NH*, s), 2.27 (6H, CH$_2$C*H$_3$*, t), 2.29 (6H, CH$_2$C*H$_3$*, t), 3.04 (4H, CH$_2$C*H$_3$*CH$_2$OH, m), 3.32 (6H, OCH$_3$, s), 3.39 (6H, O*CH$_3$*, s), 3.49-3.79 (48H, *polyether*, m), 4.12 (6H, C*H$_3$*, s), 4.23(6H, *CH$_3$*, s), 4.56 (4H, C*H$_2$*CH$_3$, m), 4.77 (12H, C*H$_2$*CH$_2$C*H$_2$*OH and CH$_2$C*H$_3$*, m), 11.62 (2H, *meso*-H, s), 11.71 (2H, *meso*-H, s); ^{13}C NMR (125 MHz, CDCl$_3$) [ppm] 12.86, 17.36, 18.56, 18.81, 20.95, 21.03, 21.86, 24.20, 29.69, 32.91, 48.00, 48.25, 52.17, 59.01, 65.21, 69.61, 69.98, 70.45, 70.57, 70.66, 71.95, 91.51, 129.08, 130.21, 132.34, 135.06,135.38, 137.34, 138.43, 141.89, 142.72, 156.49. HRMS (CI): m/z 1330.8211 [M+H]$^+$, calcd for C$_{72}$H$_{111}$N$_7$O$_{16}$·2HCl, 1330.8165.

3,12,13,22-Tetraethyl-8,17-bis(2-(2-(2-methoxyethoxy)ethoxy)ethanaminocarboxylethyl)-2,7,18,23-tetramethylsapphyrin (1.43) Following the general procedure used to prepare **1.42b**, sapphyrin **1.29a** (120 mg, 0.18 mmol) was functionalized with mono-PEG amine **1.45** (118mg, 0.72 mmol) to obtain **1.43** in the form of its diprotonated, bis-HCl salts (111 mg, 59.1% yield).

^{1}H NMR (500 MHz, CDCl$_3$): [ppm] −4.71 (2H, *NH*, s), −4.40 (1H, *NH*, s), −4.10 (2H, *NH*, s), 2.37 (6H, CH$_2$C*H*$_3$, t), 2.46 (6H, CH$_2$C*H*$_3$, t), 3.17 (4H, CH$_2$C*H*$_3$CH2OH, m), 3.45-3.81 (30H, *polyether*, m), 4.27 (6H, C*H*$_3$, s), 4.38(6H, CH$_3$, s), 4.69 (4H, C*H*$_2$CH$_3$, m), 4.90 (12H, C*H*$_2$CH$_2$C*H*$_2$OH and C*H*$_2$CH$_3$, m), 5.33(2H, CH2N*H*COOCH$_2$), 11.80 (2H, *meso*-H, s), 11.87 (2H, *meso*-H, s). ^{13}C NMR (125 MHz, CDCl$_3$) [ppm] 12.81, 15.78, 17.7,7 18.50, 20.84, 24.22, 32.56, 40.52, 58.94, 64.61, 69.84, 70.08, 70.40, 71.80, 91.56, 98.30, 126.98., 129.50, 130.03, 132.44, 134.89, 135.45, 137.24, 138.57, 141.80, 142.61, 156.71. HRMS (CI): m/z 1038.6299 [M+H]$^+$, calcd for C$_{58}$H$_{83}$N$_7$O$_{10}$·2HCl, 1038.6279.

2,3,12,13,22,23-Hexaethyl-8,17-bis(bis(2-(2-(2-methoxyethoxy)ethoxy)ethyl)amino carboxylethyl)-7,18-dimethylsapphyrin (1.42a) Following the general procedure used to prepare **1.42b**, sapphyrin **1.29a** (120 mg, 0.174 mmol) was functionalized with bis-PEG amine **1.44** (215 mg, 0.69 mmol) to obtain **1.42a** in the form of its diprotonated, bis-HCl salt (90 mg, 38% yield). ^{1}H NMR (500 MHz, CDCl$_3$) [ppm] −4.68 (2H, N*H*, s), −4.49 (1H, N*H*, s), −4.16 (2H, *NH*, s), 2.16 (6H, CH$_2$C*H*$_3$, t), 2.37 (6H, CH$_2$C*H*$_3$, t), 3.09 (4H, CH$_2$C*H*$_3$CH$_2$OH, m), 3.39 (6H, OCH$_3$, s), 3.58 (6H, OCH$_3$, s), 3.56-3.83 (48H, *polyether*, m), 4.31 (6H, C*H*$_3$, s), 4.66 (8H, C*H*$_2$CH$_3$, m), 4.81 (12H, C*H*$_2$CH$_2$C*H*$_2$OH and C*H*$_2$CH$_3$, m), 11.67 (2H, *meso*-H, s), 11.82 (2H, *meso*-H, s). ^{13}C NMR (125 MHz,

CDCl$_3$) [ppm] 12.80, 17.31, 18.52, 18.77, 20.94, 21.77, 24.11, 32.81, 47.89, 48.13, 58.91, 65.09, 69.50, 69.87, 70.33, 70.47, 70.56, 71.80, 91.39, 98.58, 128.97, 130.09, 132.24, 132.84, 134.93, 135.26, 137.28, 138.35, 141.83, 142.64, 156.38. HRMS (CI): m/z 1358.8483 [M+H]$^+$, calcd for C$_{72}$H$_{111}$N$_7$O$_{16}$·2HCl, 1358.8483.

12,13-Diethyl-8,17-bis(bis(2-(2-(2-methoxyethoxy)ethoxy)ethyl)aminocarboxylethyl)-3,7,18,22-tetramethylsapphyrin (1.42c) Following the general procedure used to prepare **1.42b**, sapphyrin **1.29c** (65 mg, 0.107 mmol) was functionalized with bis-PEG amine **1.44** (129 mg, 0.42 mmol) to obtain **1.42c** in the form of its diprotonated, bis-HCl salt (49 mg, 45% yield). ^{1}H NMR (500 MHz, CDCl$_3$) [ppm] −5.42 (2H, *NH*, s), −4.92 (1H, *NH*, s), −4.84 (2H, *NH*, s), 2.35 (6H, CH$_2$C*H*$_3$, t), 3.03 (4H, CH$_2$C*H*$_3$CH$_2$OH), 3.30 (6H, OCH$_3$, s), 3.36 (6H, OCH$_3$, s), 3.47-3.73 (48H, *polyether*, m), 4.27 (6H, C*H*$_3$, s), 4.37(6H, CH$_3$, s), 4.74 (8H, C*H*$_2$CH$_3$ and *CH$_2$*CH$_2$CH$_2$OH, m), 4.83 (4H, CH$_2$CH$_2$*CH$_2$*OH, m), 10.47 (2H, *pyrrolic*-H), 11.79 (2H, *meso*-H, s), 11.88 (2H, *meso*-H, s). ^{13}C NMR (125 MHz, CDCl$_3$) [ppm] 12.93, 14.81, 18.73, 21.07, 24.31, 32.95, 47.92, 48.18, 58.99, 65.16, 69.55, 69.91, 70.38, 70.51, 71.88, 92.25, 97.16, 121.59, 128.11, 131.57, 133.17, 134.44, 135.13, 137.06, 139.15, 139.47, 142.96, 156.44. HRMS (CI): m/z [M+H]$^+$ 1274.7516, calcd for C$_{68}$H$_{103}$N$_7$O$_{16}$·2HCl, 1274.7534.

12,13,-Diethyl-8,17-bis(bis(2-(2-(2methoxyethoxy)ethoxy)ethyl)aminocarboxylethyl)-7,18-dimethylsapphyrin (1.42d) Following the general procedure used to prepare **1.42b**, sapphyrin **1.29d** (49.7 mg, 0.086 mmol) was functionalized with bis-PEG amine **1.44** (106 mg, 0.34 mmol) to obtain **1.42d** in the form of its diprotonated, bis-HCl salt (50 mg, 45% yield). This compound was not fully characterized. HRMS (EI): m/z 1246.7210 [M+H]$^+$, calcd for C$_{66}$H$_{99}$N$_7$O$_{16}$·2HCl, 1246.7226.

1.6.2 NICS Calculations

The NICS values were calculated by our collaboration group (Prof. Dongho Kim of Yonsei University). The NICS values of the inverted sapphyrin **1.15** were calculated based on the crystal structure coordinates obtained from Dr. Vincent Lynch of The University of Texas at Austin and geometry optimization. The NICS value of sapphyrin **4b** was calculated using the procedure summarized below.

| B3LYP/3−21g geo opt | → | B3LYP/6−31g geo opt | → | B3LYP/6−31g* geo opt | → | B3LYP/6−31g* NMR |
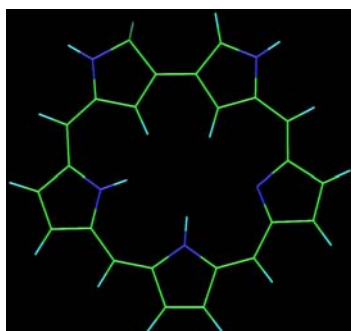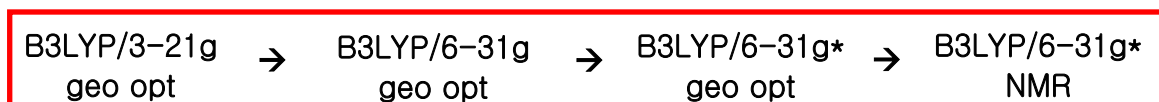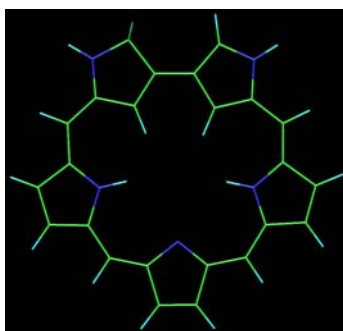
NICS(0) = -2.36 ppm   NICS(0) = -2.16 ppm   NICS(0) = -1.89 ppm
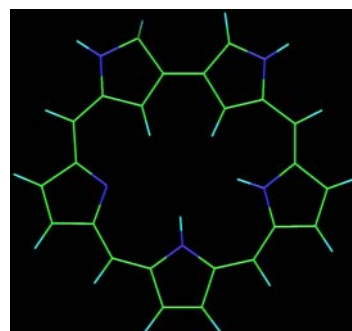
Figure 1.15 NICS(0) values of inverted sapphyrin **1.15** calculated using a process of geometry optimization
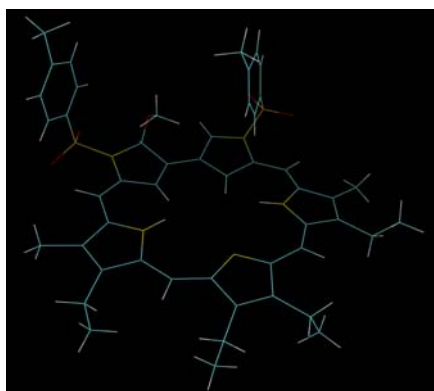
NICS(0) = -2.022 ppm

Figure 1.16 NICS(0) value of inverted sapphyrin **1.15** calculated starting from the X-ray structure coordinates
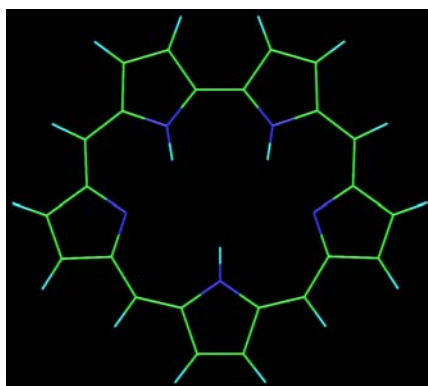
NICS(0) = -14.9 ppm

Figure 1.17 NICS(0) value of sapphyrin **4b** obtained after a process of geometry optimization

Chapter 2 Diindolylquinoxalines: Effective Indole-Based Receptors for Phosphate Anion

2.1 INTRODUCTION

Anion recognition is central to understanding the diverse roles of anions including the pivotal function of anion channels and various enzyme-catalyzed reactions. To mimic these natural systems, various anion recognition motifs have been developed. Recently, considerable effort in this area has been focused on the use of acyclic small molecule receptors,[1] including those based on amide, sulfonamide, urea, and pyrrole recognition units. While each of these motifs presents certain advantages, they are also subject to limitations. Accordingly, there is incentive to explore additional putative binding subunits that could be used to generate new receptor systems. One such motif is indole, a potential hydrogen bond donor that has yet to be exploited extensively in the area of anion sensor.
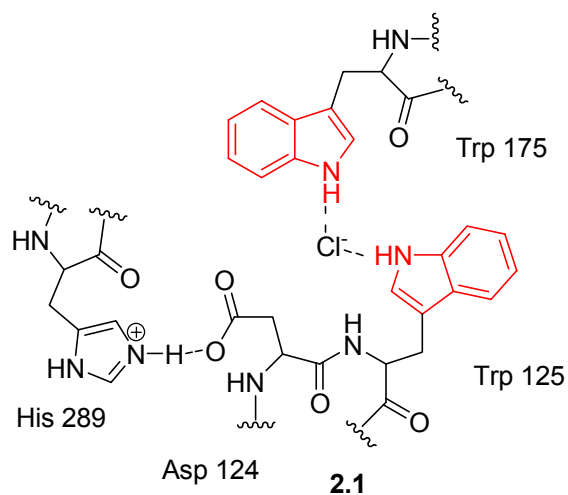
Figure 2.1 Schemetic structure of haloalkane dehydrogenase

Interestingly, nature has exploited indolic motifs for the purpose of anion binding. One containing such a motif is haloalkanedehydrogenase. The X-ray structure of haloalkane dehydrogenase was solved in 1993 and it is known to convert haloalkanes into the corresponding primary alcohol.[2] As shown in Figure 2.1, a chloride anion can be bound and activated by the indolic NHs contained in the active site. This occurs through hydrogen bonds. Therefore, indolic hydrogen bonding interactions can be useful, presumably, and can be combined with, e.g., an additional hydrogen bonding motif to produce effective synthetic receptors. Logical as this seems, when this research was started, indole-containing small molecular recepors were rare. Indeed, only indolocarbazoles **2.2**[3] and bis(indolyl)methane, **2.3**[4] had been studied for anion recognition. In the case of the latter system **2.3**, quantitative binding studies were not fully carried out.

2.2

2.3

2.4

2.5 (X=H)
2.6 (X=NO$_2$)
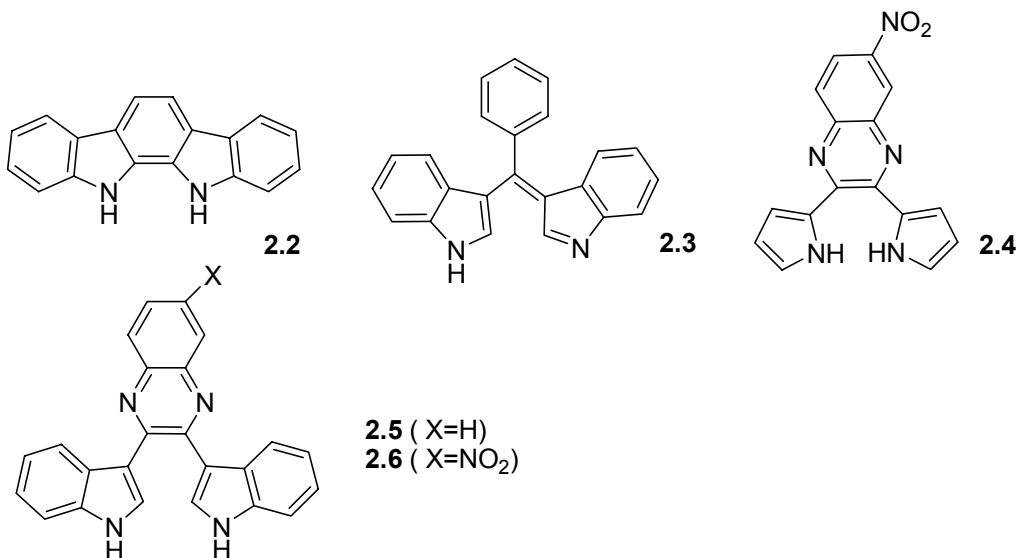
We envisioned that two indole subunits could be easily connected to produce a functionalized quinoxaline. Two such systems, **2.5** and **2.6**, were synthesized.[5] These systems containing linked pyrrole subunits, were expected to provide a more open binding cleft than 2,3–dipyrrol–2´yl quinoxalines, such as **2.4**. Therefore, it was expected that 2,3–diindol–3´yl quinoxalines **2.5** and **2.6**, would display greater affinity for larger anions than the existing system **2.4**. The pKa values of indolic NH and pyrrolic NH protons also differ (20.9 and 23.0 measured in DMSO, respectively).[6] As a result, for directly analogous system, it was expected that the indole-based receptor would function more effectively than the pyrrole analogue.

2.2 SYNTHESIS AND CHARACTERIZATION

Receptors **2.5** and **2.6** require very short syntheses. Although the synthesis of receptor **2.6** was not clearly described in the literature, the syntheses of 2,3–diindol–3´yl diketone **2.8**[7] and receptor **2.5**[8] have been published. During the synthesis of these species, we found that intermediate **2.8** could be easily prepared by the reaction of indole-Grignard reagent with indolyl chloride **2.7**. In addition, the minor product **2.9** was obtained in 8% yield. Compound **2.9** is believed to result from the radical reaction between an acyl radical and an indolic radical via a one electron transfer mechanism. In the event, the exact structure of **2.9** was revealed by an X-ray diffraction analysis. Subsequent reaction between the resulting diketone **2.8** and either *o*-phenyldiamine or its mono nitro analogue gave the final receptors **2.5** and **2.6** in unoptimized yields of 48 and 30%, respectively.
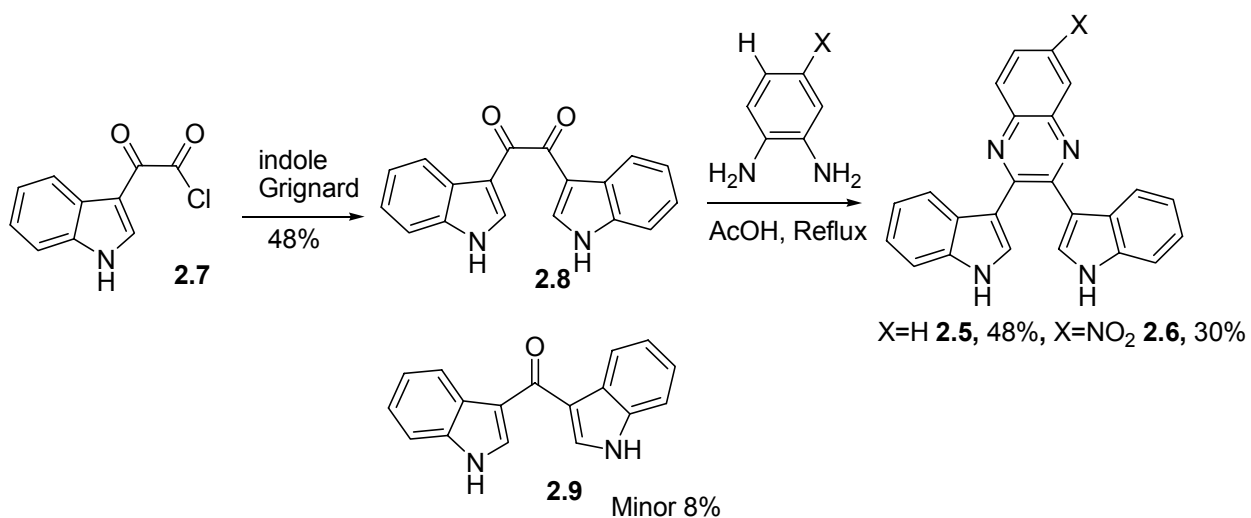
Scheme 2.1 Synthesis of receptors **2.5** and **2.6**, and minor byproduct **2.9**
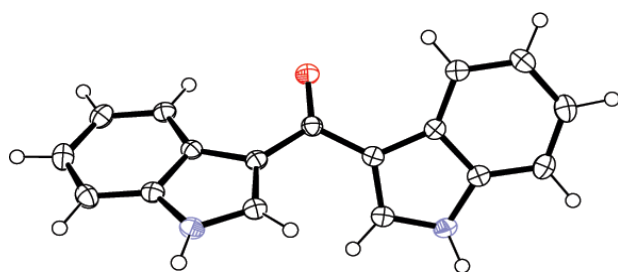
(a)   (b)
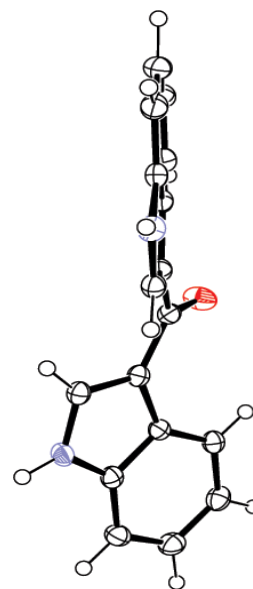
Figure 2.2 X-ray structures of **2.9**. a) Top view; b) side view. Thermal ellipsoids are scaled to the 50% probability level.

2.3 BINDING STUDY

Initial solution-phase anion binding studies were carried out in CD_2Cl_2 with a view to testing the anion recognition property of the indolic receptor **2.5**. Upon the addition of tetrabutylammonium chloride, the indolic NH signal, originally present at 8.88 ppm, was shifted to lower field. This experiment provides strong support for the notion that the indolic NHs are involved in Cl^- recognition. Assuming that this Cl^- binding is responsible for the observed shifts, association constants of $K_a = 130$ for receptor **2.5** could be obtained from this typical NMR spectroscopic analysis. The values are comparable to those obtained from UV-vis titrations (Figure 2.3 and Table 2.1). Unfortunately, other NMR titrations were not successful due to the fact that receptor **2.6** was not sufficiently soluble in CD_2Cl_2 and $H_2PO_4^-$ resulted in an unreasonable broadening of the indolic NH signals.
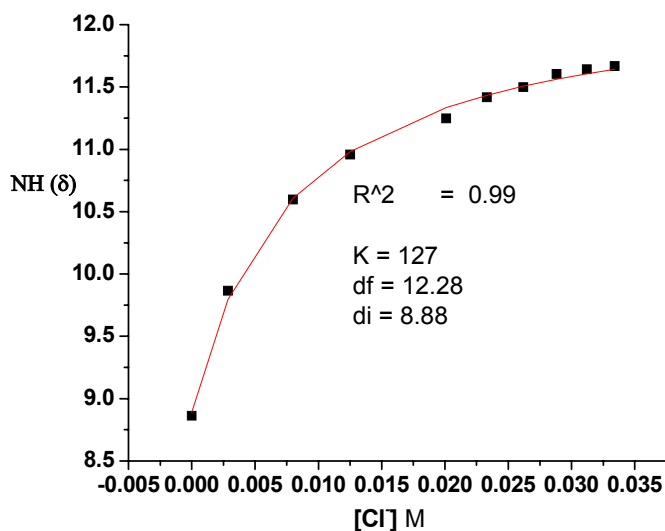
Figure 2.3 ^{1}H-NMR titration curves obtained when receptor **2.5** (0.1 mM) in CD_2Cl_2 is titrated with TBACl

Given the above limitations, standard UV-vis absorption titration was used to determine the association constants (K_a) of receptors **2.5** and **2.6** with various anions in dichloromethane. Figure 2.4 was generated by recording the observed changes in the UV-vis spectrum of receptor **2.6** in dichloromethane upon the addition of tetrabutylammonium hydrogen phosphate (TBA·H_2PO_4). During the titration, a large bathochromic shift ($\Delta\lambda_{max}$ = 40 nm) was seen. Several isosbestic points were also seen, as expected for a 1:1 binding stoichiometry for the interaction between TBA·H2PO4$^-$ and **2.6**. Similar isosbestic points were also observed during the course of titrations carried out with F$^-$, Cl$^-$, HSO_4^- and BzO$^-$ anions as well (all anions studied as the corresponding TBA salts). Further, both a single crystal X-ray analysis and a Job plot revealed a 1:1 binding stoichiometry between TBA·H2PO4$^-$ and **2.6**.

(a)   (b)
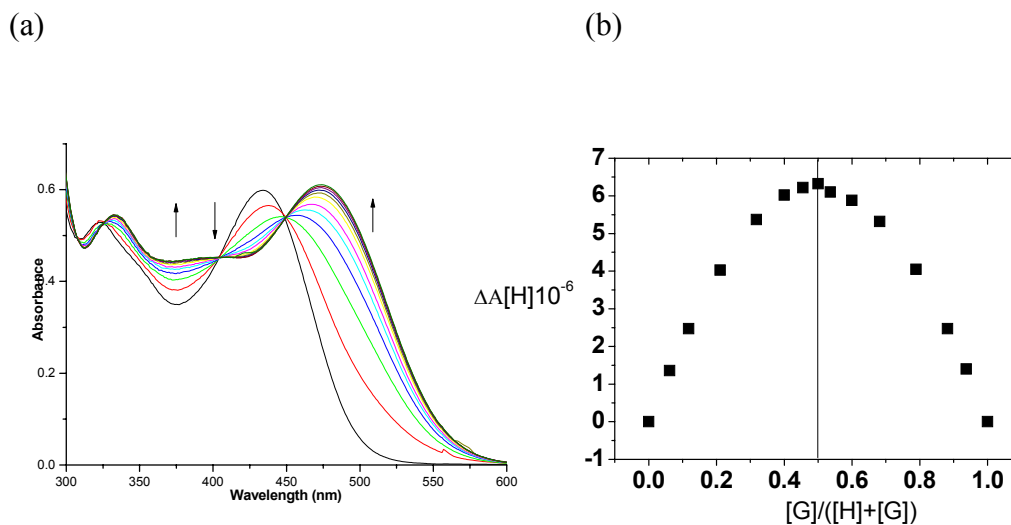
Figure 2.4 (a) Evolution of the UV-vis spectrum of receptor **2.6** (3.99 × 10^{-5} M in dichloromethane) seen during titration with tetrabutylammonium hydrogen phosphate (TBA·H_2PO_4) (0 to 10 equiv.). (b) Job plot for the interaction between receptor **2.6** and TBA·H_2PO_4.

61

Table 1. Anion Binding Constants $(K_a; \text{M}^{-1})^a$ for Receptors **2.5** and **2.6** in Dichloromethane at 22 ºC

	2.4	2.5	2.6
F^-	118000	2100	$-^b$
Cl^-	65	170	470
HSO_4^-	N.D.	80	250
BzO^-	N.D.	600	2700
$H_2PO_4^-$	80	6800	20000^c

^{a}Values were determined by UV-vis spectroscopic titrations; errors are $< \pm 10\%$. All anions were used in the form of their respective tetrabutylammonium (TBA) salts. ^{b}A reliable binding constant could not be determined due to the observation of biphasic behavior. ^{c}The association constant for the interaction of receptor **2.6** with $H_2PO_4^-$ was also examined in acetone, acetonitrile, and DMSO: the K_a values are 5,600, 2,400 and 300 M^{-1}, respectively. N.D. – not determined.

Association constants determined from these titrations are summarized in Table 1. An inspection of this table reveals that in the case of receptor **2.5** the greatest affinity is displayed for the dihydrogen phosphate anion, followed by $F^- > BzO^- > Cl^- > HSO_4^-$. This same table also confirms that, as proved true in the case of the corresponding DPQ (**2.4**) systems, the nitro-bearing receptor **2.6** shows higher affinities across the board than does the unsubstituted system **2.5**. This result is attributed to the electron withdrawing nitro group, which serves to increase the pyrrole NH acidity. Consistent with this postulate, receptor **2.7** shows biphasic behavior[9] when subject to titration with fluoride anion in

dichloromethane (Figure 2.5). Under these latter conditions, the fluoride anion presumably acts as both a general base and as an anionic substrate.
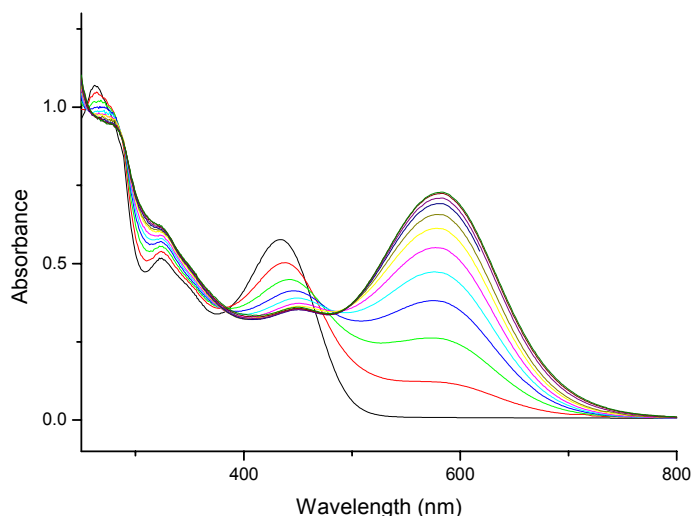
Figure 2.5 Plot of the absorption spectral changes seen when receptor **2.6** (3.99×10^{-5} M) is subject to titration with TBAF in dichloromethane.

Among the anionic substrates for which clean binding behavior is seen, receptor **2.6**, like its congener **2.5**, shows good selectivity for phosphate anion ($K_a(H_2PO_4)/K_a(Cl)$ = 42, $K_a(H_2PO_4)/K_a(BzO) = 7$ and $K_a(H_2PO_4)/K_a(HSO_4) = 80$). Such a high inherent selectivity was not seen in either the corresponding DPQ systems (K_a(rept. **2.6**)/K_a(rept. **3**) = 250 for $H_2PO_4^-$)[5] or in the indolecarbazole[3] based receptors reported recently by Beer. We ascribe this phosphate anion selectivity[10] to the presence of the β-connectivity linking the two indole motifs to the quinoxaline core; this provides a more open (and potentially less rigid) cavity that is expected to favor binding of this relatively larger anionic substrate.

(a)   (b)
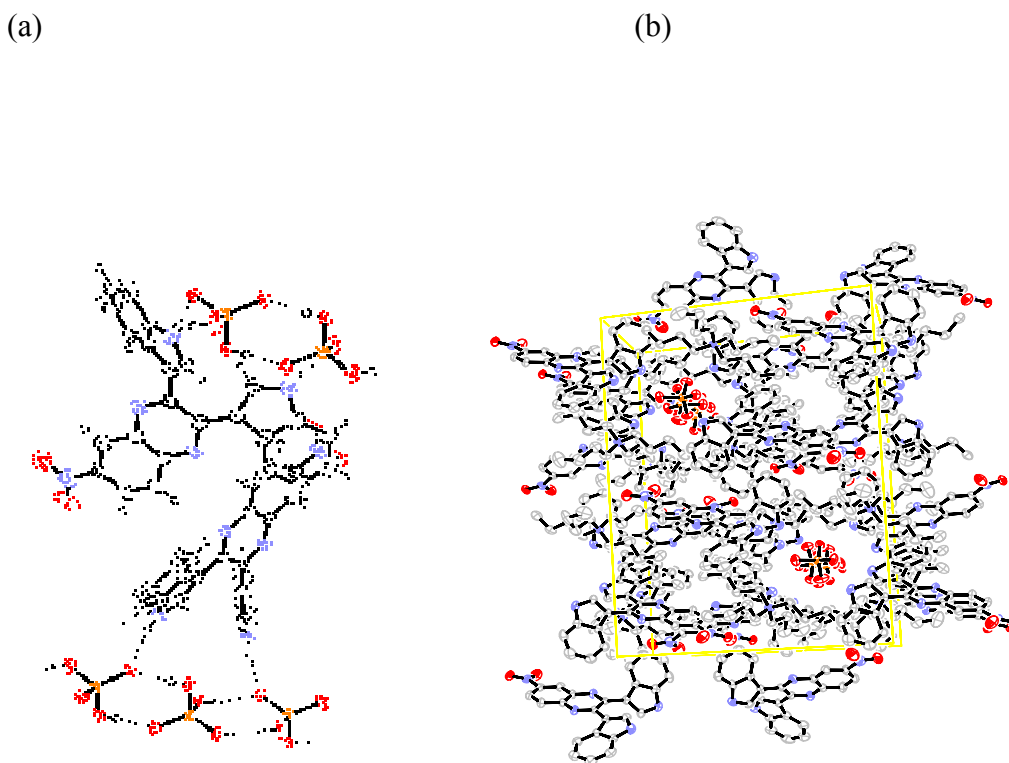
Figure 2.6 Single crystal X-ray diffraction structure of receptor **2.6**·TBA·H$_2$PO$_4$. Thermal ellipsoids are scaled to the 50% probability level. Most hydrogen atoms and the TBA cations have been omitted for clarity. (a) View illustrating the two types of phosphate-bound complexes of receptor **2.6** found in the solid state structure; (b) view of the complex (receptor **2.6**·TBA·H$_2$PO$_4$)$_8$ seen in the unit cell.

The X-ray crystal structure of the complex (**2.6** TBA·H$_2$PO$_4$) provides for the assumption that the complexed dihydrogen phosphate anion is bound to **2.6** via hydrogen bonding interactions. This structure reveals the presence of two different phosphate-receptor interactions in the solid state. In one complex, a molecule of receptor **2.6** interacts with two phosphate anions that, in turn, interact with one another via hydrogen bonds. In the other complex, receptor **2.6** binds three phosphates that exist in a self-associated network (cf. Figure 2.6a). As the result of the multiple hydrogen bonding

64

interactions in the solid state, a series of infinite phosphate channels and wires are formed, sometimes that is not common in the solid state.[11] Nonetheless, the overall anion-to-receptor binding stoichiometry is 1:1, as expected based on the the solution phase Job plot analysis presented above.

A further notable feature of receptor **2.6** is that color changes are seen upon the addition of F$^-$ and H$_2$PO$_4^-$ anions (Figure 2.7). Such color changes are considered as a useful feature of receptor **2.6** in that it allows analytes to be detected easily without use of spectrometers.[12]
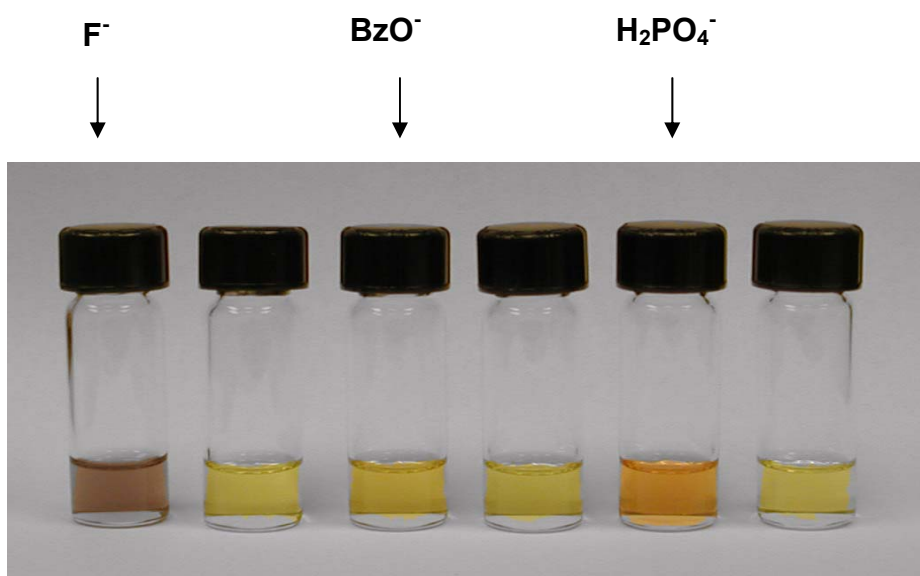
Figure 2.7 Color changes observed upon the addition of anions (10 equiv.) to otherwise identical solutions of receptor **2.6** (4.34 $\times$ 10^{-5} M in dichloromethane). From left to right; F$^-$ + **2.6**, Cl$^-$+ **2.6**, BzO$^-$ + **2.6**, HSO$_4^-$ + **2.6**, H$_2$PO$_4^-$+ **2.6**, **2.6**.

65

2.4 CONCLUSION

The new indole-based small molecular receptors **2.5** and **2.6** can effectively detect dihydrogen phosphate anion. The current system provides support for the suggestion that a range of indole derivatives could be used to design anion receptors. In the case of receptor **2.6**, the combined use of an indole motif and quinoxaline framework allows for the visual detection of $H_2PO_4^-$ via the production of a simple, anion-triggered color change. This is also true for fluoride, a species for which less clean binding behavior is seen. The interactions between $H_2PO_4^-$ and receptor **2.6** also give rise to a unique extended structure in the solid state.

2.5 FUTURE DIRECTIONS

Indole derivatives are commercially available, which leads us to propose its use in the construction of new anion receptors via imine forming DCC (Dynamic Combinatorial Chemistry). DCC can be a powerful tool for the self-assembly of new receptors, including in the present instance, with an anion template. For example, Scheme 2.2 outlines a way whereby template driven acyclic receptors could be prepared. Specifically, in what is a two-fold enhanced DCC approach, an array of amines and aldehydes could be used to obtain a template-driven receptor in the presence of a templating agent. The formed species, to the extent they are obtained, could be analyzed via liquid chromatography mass spectrometry. As appropriate, they could be resynthesized and examined for their anion binding properties.
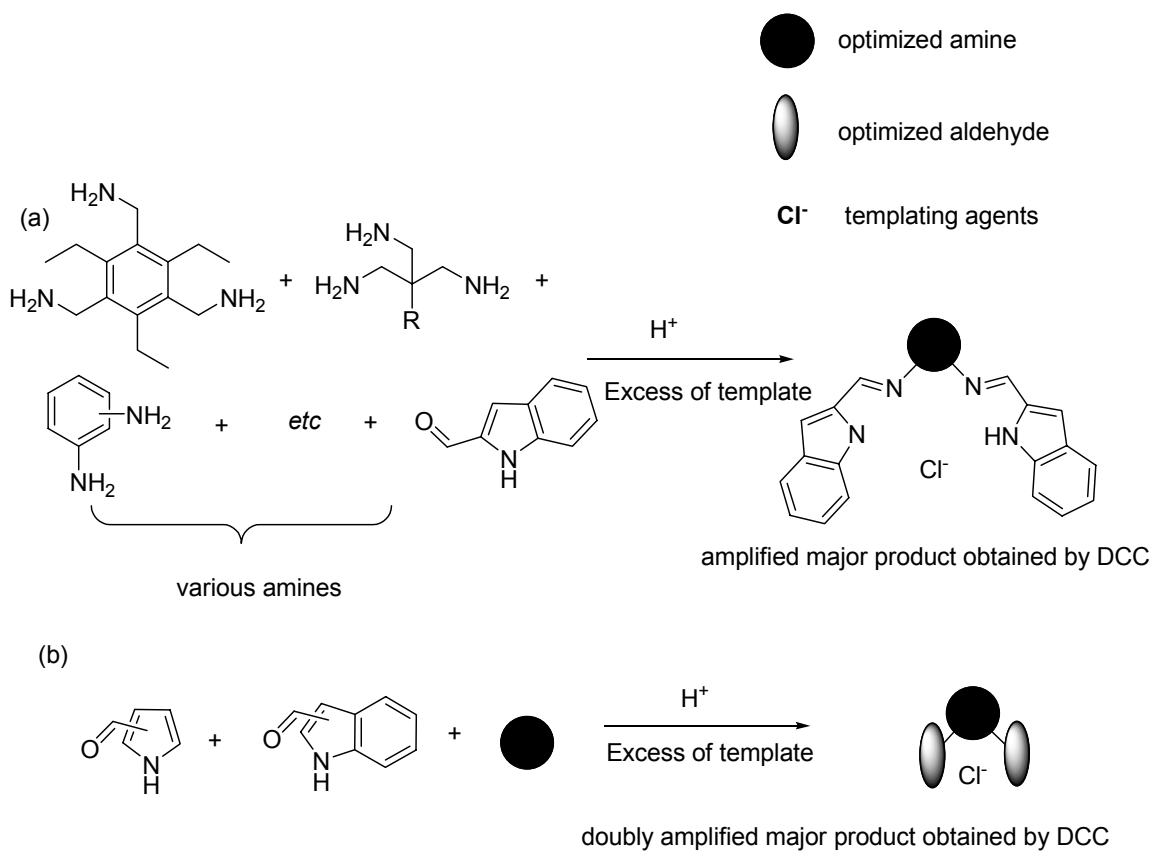
Scheme 2.2 Formation of an acyclic imine-derived receptor. (a) Optimization of an amine. (b) Optimization of an aldehyde.

2.6 REFERENCES

(1)   (a) Sessler, J.; Gale, P. A.; Cho W.-S. *Anion Receptor Chemistry*; The Royal Society of Chemistry: Cambridge, UK, 2006. (b) Beer, P. D.; Gale, P. A. *Angew. Chem., Int. Ed.*, **2001**, *41*, 486-516.

(2)   Verschueren, K. H. G.; Seljee, F.; Rozenboom, H. J.; Kalk, K. H.; Dijkstra, B. W. *Nature,* **1993***, 363*, 693-698.

(3)   Curiel, D.; Cowley, A.; Beer, P. D. *Chem. Comm.* **2005**, 236-238.

(4)   He, X.; Hu, S.; Liu, K.; Guo, Y.; Xu, J.; Shao, S. *Org. Lett*. **2006**, *8*, 333-336.

(5)   (a) Black, C. B.; Andrioletti, B.; Try, A. C.; Ruiperez, C.; Sessler, J. L. *J. Am. Chem. Soc*. **1999**, *121*, 10438-10439. (b). Sessler, J. L.; Maeda, H.; Mizuno, T.; Lynch, V. M.; Furuta, H. *J. Am. Chem. Soc*. **2002**, *124*, 13474-13479.

(6)   Bordwell, F. G.; Zhang X.; Cheng, J.-P. *J. Org. Chem.* **1991**, *56*, 3216-3219.

(7)   (a) Bergman, J.; Janoik, T.; Johnsson, A. L. *Synthesis*, **1999**, *4*, 580-582. (b) Bergman, J.; Carlsson, R.; Sjöberg, B. *J. Heterocycl. Chem*. **1977**, *14*, 1123-1134.

(8)   Lopatinskaya, K. Y.; Skorobogatova, Z. M.; Sheinkman, A. K.; Zaritovskaya, T. A. *Chem. Heterocycl. Compd.* **1985**, *21*, 675-679.

(9)   Anzenbacher, P., Jr.; Jursikova, K.; Shriver, J. A.; Miyaji, H.; Lynch, V. M.; Sessler, J. L.; Gale, P. A. *J. Org. Chem*. **2000**, *65*, 7641-7645.

(10)   (a) Kendo, S.-I.; Hiraoka, Y.; Kurumatani. N.; Yano, Y. *Chem.Comm*. **2005**, 1720-1722. (b) Seong, H. R.; Kim, D.-S., Kim, S.-G.; Choi, H.-J.; Ahn, K. H. *Tetrahedron Lett.* **2004**, *45*, 723-727. (c). Chmielewski, M. J.; Charon, M.;

Jurczak, J. *Org. Lett.* **2004**, *6*, 3501-3504. (d) Han, M. S. and Kim, D. H., *Angew. Chem., Int. Ed.*, **2002**, *41*, 3809-3811. (e) Kuo, L.-J.; Liao, J.-H.; Chen, C.-T.; Huang, C.-H.; Chen C.-S.; Fang, J.-M. *Org. Lett.* **2003**, *5*, 1821-1824. (f) Tobey S. L.; Anslyn, E. V. *Org. Lett.* **2003**, *5*, 2029-2031. (g) Anzenbacher, P., Jr.; Jursikova, K.; Sessler J. L. *J. Am. Chem. Soc.* **2000**, *122*, 9350-9351. (h) Beer, P. D.; Dickson, C. A. P.; Fletcher, N.; Goulden, A. J.; Grieve, A.; Hodacova, J.; Wear, T. *J. Chem. Soc., Chem. Commun.* **1993**, 828-830.

(11)   (a) Yin, Z.; Zhang, Y.; He, J.; Cheng, J.-P. *Terahedron.* **2006**, *62*, 765-770. (b) Amendola, V.; Boiocchi, M.; Esteban-Gómez, D.; Fabbrizzi, L.; Monzani, E. *Org. Biomol. Chem.* **2005**, *3*, 2632-2639. (c) Král, V.; Furuta, H.; Shreder, K.; Lynch, V.; Sessler, J. L. *J. Am. Chem. Soc.* **1996**, *118*, 1595-1607.

(12)   (a) Miyaji, H.; Sato, W.; Sessler, J. L. *Angew. Chem., Int. Ed.* **2000**, *39*, 1777-1780. (b) Anzenbacher, P., Jr.; Jursikova, K.; Sessler, J. L. *J. Am. Chem. Soc.* **2000**, *122*, 9350-9351.

2.7 EXEPERIMENTAL SECTION

Proton and ^{13}C-NMR spectra were measured at 25 ºC using a Varian Unity Innova instrument at 400 MHz. UV-vis spectra were recorded on a BECKMAN DU 640B spectrophotometer. High resolution CI mass spectra were obtained on a VG ZAB2-E mass spectrometer.

2.7.1 SYNTHETIC EXPERIMENTAL

2,3-di(1H-indol-3-yl)quinoxaline (2.5) Diketone **2.8** (200 mg, 6.93×10^{-4} mol) and *o*-phenyldiamine (225 mg, 2.08×10^{-3} mol) were added to one another in a 25 mL round bottom flask under argon. Acetic acid (15 mL) was added and stirred. The resulting solution was heated at reflux overnight. The residual acetic acid was then removed by vacuum distillation. The semi-solid that remained was dissolved using a mixture of dichloromethane and water. The organic layer was separated off and treated with anhydrous sodium sulfate. After filtration to remove the sulfate salts, the solution was evaporated to dryness under reduced pressure. The residue obtained in this way was purified by column chromatography over silica gel (ethyl acetate : hexane = 1:2, eluent) to afford **2.5** (120 mg, 48 %) as a yellow foamy solid. ^{1}H-NMR (400 MHz, DMSO-d_6) [ppm] 7.03 (dd, J = 7.2, 7.2 Hz, 2H), 7.14 (dd, J = 7.2, 7.2 Hz, 2H), 7.41(d, J = 8 Hz, 2H), 7.43 (s, 1H), 7.70 (dd, J = 6.4, 3.6 Hz, 2H), 7.95(d, J = 8.0 Hz, 2H), 8.01(dd, J = 6.4, 3.2 Hz, 2H), 11.40(d, J = 2.0 Hz, 2H); ^{13}C-NMR (100 MHz, CDCl$_3$) [ppm] 112.5, 114.8, 120.7, 121.8, 122.5, 126.7, 128.5, 128.8, 129.3, 136.8, 140.2, 150.4; HRMS (CI): m/z

361.1454 ((M+H), calcd for $C_{24}H_{17}N_4$ 361.1453; UV-vis (CH_2Cl_2) max [nm] ($M^{-1} \cdot cm^{-1}$) 262 (26290), 323 (12629), 434 (14310).

2,3-di(1H-indol-3-yl)-6-nitroquinoxaline (2.6) Diketone **2.8** (50 mg, 1.73×10^{-4} mol) and 4-nitro-1,2-phenyldiamine (79 mg, 5.19×10^{-4} mol) were added to one another in a 25 mL round flask under argon and subject to reaction and work-up as per **2.5**, In this case, recrystallization from hexanes afforded **2.6** as an analytical pure red solid (21 mg, 30 %). ^{1}H-NMR (400 MHz, DMSO-d_6) [ppm] 7.12 (m, 2H), 7.18(m, 2H), 7.44(dd, J = 10.0, 8.0 Hz, 1H), 7.58(d, J = 1.6Hz, 1H), 7.63(d, J = 2.4 Hz, 1H), 8.01(d, J = 8.0 Hz, 1H), 8.15(d, J = 8.0 Hz, 1H), 8.16(d, J = 9.2 Hz, 1H), 8.37(dd, J = 9.2, 2.8 Hz, 1H), 8.75(d, J = 2.4Hz, 1H), 11.59(s, 1H), 11.61(s, 1H); ^{13}C-NMR (100 MHz, CDCl$_3$) [ppm] 112.7, 112.8, 114.2, 114.3, 121.1, 121.3, 122.0, 122.4, 122.6, 122.8, 123.0, 124.6, 126.5, 126.6, 129.6, 130.1, 130.5, 136.9,137.0, 138.7, 143.3, 146.9, 152.4, 153.3; HRMS (CI): m/z 406.1304 ((M+H), calcd for $C_{24}H_{16}N_5O_2$ 406.1304; UV-vis (CH_2Cl_2) max [nm] ($M^{-1} \cdot cm^{-1}$) 259 (26190), 392 (12937). The complex of **4**·H_2PO_4·TBA was further characterized by X-ray diffraction analysis.

Chapter 3 Reaction-Based Indicator Systems

3.1 INTRODUCTION

Supramolecular chemistry has continued to develop in an even broader manner since it was recognized with the 1987 Nobel Prize for Chemistry, awarded jointly to Donald J. Cram, Jean-Marie Lehn, and Charles J. Pedersen. In theory, the principles of supramolecular chemistry may be (and often have been) embodied in synthetic host molecules that can recognize guest molecules in a very selective way using weak and generally reversible non-covalent bonds.[1] Appreciating this fact, considerable effort within the supramolecular community has been devoted to the synthesis of chemical sensor systems ("sensors") based on noncovalent interactions, including hydrogen bond, π-π, hydrophobic, or hydrophilic interactions.[2] Although considerable progress has been made, there remains a need for new approaches to chemical sensing. Indeed, a variety of strategies are currently being pursued. One approach that has received relatively little attention involves reaction-based sensory systems.

Reaction-based chemical sensors may be defined as those where the visualized response is based on an irreversible or essentially irreversible reaction. Needless to say, in the extreme, when the equilibrium is shifted (or almost shifted) to the product and the product is isolable, the underlying response chemistry involves a bonafide reaction.[3] Strictly speaking reaction-based sensors fall outside the definition of supramolecular chemistry. However, as long as the reactions are used for detecting guests, reaction-based sensory systems can be considered as falling within the general category of molecular recognition. In some respects, therefore, the concept of reaction-based sensing represents

a new twist on the venerable field of analyte-specific qualitative analysis. The main difference is that the concept of molecular specificity plays a key role in the design of modern reaction-based sensors.

conventional sensory systems

reaction-based sensory systems
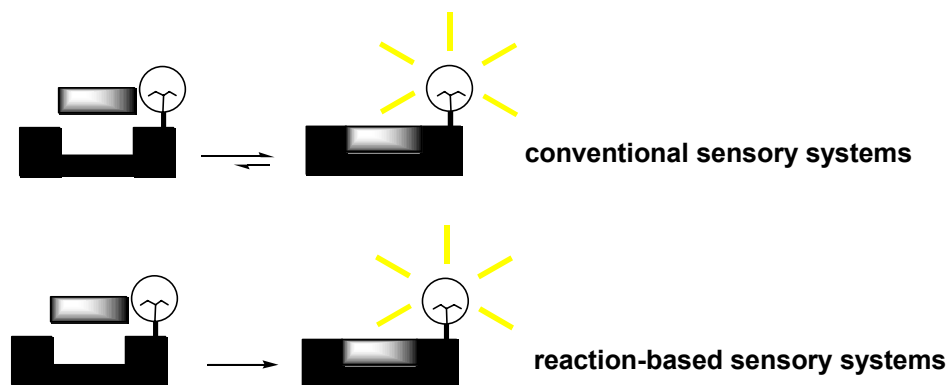
Figure 3.1 Schematic illustration of conventional sensors and reaction-based sensors

Currently, the field of reaction based sensors is still in its infancy. Nonetheless, it is already apparent that reaction based sensory systems should have two requirements, namely, i) high reaction selectivity and ii) product(s) that can be used as a marker for the analyte in question. As a result of these design considerations, reaction-based sensory systems promise near ultimate selectivity. While this promise has yet to be fully realized, this chapter describes many sensory systems that rely on complete or partial reactions and which help illustrate the concepts of reaction-based sensory systems in chemistry and related fields.

3.1 ANION RECOGNITION

One of the areas where reaction-based sensors have enjoyed greatest success is in the area of cyanide-based sensing, although several more conventional supramolecular

sensors for this species have been described recently.[4] The prevalence and toxicity of cyanide anion makes it of considerable interest in terms of new sensor development. Cyanide is widely used in gold mining, electroplating, and metallurgy among other applications and its early or facilitated detection could help mitigate environmental disasters such as that which plagued the Danube in 2001.[4] On the other hand, cyanide is relatively basic and nucleophilic. These paired attributes make it one of the better anions with which to explore the potential of reaction-based sensor chemistry.

3.1.1 CYANIDE
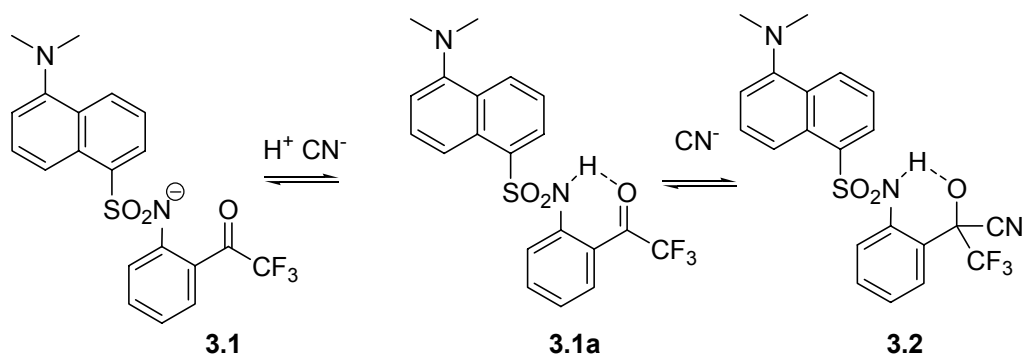
Scheme 3.1 Proposed cyanide-sensing mechanism of **3.1**

ortho-TFADA receptor **3.1**[5] is one of the first reaction-based receptors to be reported. This system, designed by the Ahn group, relies on the cyanohydrin reaction. It owes its success to the fact that the *ortho*-TFADA receptor contains both an activated ketone (cyanohydrin reaction site) and a dansyl signaling motif. Further, this receptor takes advantage of an activated fluorinated ketone and a hydrogen bonding donor to facilitate cyanide recognition and to stabilize the cyanohydrin formed from cyanide addition reaction.

74

The photophysical properties of *ortho*-TFADA correspond to those of the dansyl moiety, displaying strong absorption at 260 and 350 nm. The sensing properties were studied *via* fluorescence titration by irradiating at 350 nm in CH₃CN. The selectivity of receptor **3.1** was examined by adding 1 equiv. of various anions to a solution of the host (20 μM). Cyanide induced a 5-fold increase in the fluorescence intensity relative to unreacted **3.1**. Both OAc⁻ and F⁻ anions enhanced the fluorescence intensity by a factor of 2, whereas H₂PO₄⁻ produced very little enhancement. Anions tested (H₂SO₄⁻ ClO₄⁻, Cl⁻, Br⁻, SCN⁻) did not change the fluorescence intensity of *ortho*-TFADA. A pseudo association constant for the interaction of TFADA with the cyanide anion was obtained from the fluorescence titration ($K_a = 3 \times 10^5 \ M^{-1}$).

The position of the sulfonamide in **3.1** was pivotal to the observation of anion-induced fluorescence enhancement. For instance, *para*-TFADA displayed quenching behavior when cyanide anion was added. The authors effectively excluded that the possible acid and base derived reaction pathways by comparison studies involving *para*-TFADA. ¹H NMR and ¹⁹F NMR spectral studies of **3.1** support the proposed cyanohydrin reaction. For example, the NH proton in the ¹H NMR was shifted to lower field (Δδ = 3.6), whereas the signal for the CF₃ group in the ¹⁹F NMR was upfield shifted upon the addition of cyanide.

Scheme 3.2 Proposed cyanide-sensing mechanism of **3.3**

Receptor **3.3**[6] was developed by the Sun group. This sensor also relies on the cyanohydrin reaction to elicit a cyanide-triggered response. While the analyses carried out were mostly visual and spectroscopic, the authors did infer the presence of the product from the electrospray mass spectrometric data ($[\mathbf{3.4}+2Bu_4N+CN^-]^+$ = 948.68 m/z).

Cyanide anion selectivity was probed in H_2O/acetonitrile (1:1, v/v) by adding various anions such as CN^-, F^-, Cl^-, Br^-, I^-, AcO^-, BzO^-, NO_3^-, $H_2PO_4^-$, $HP_2O_7^{3-}$ ClO_4^- and HS^- (10 equiv) to a solution of **3.3** (18 μM). Only the cyanide anion generated a new absorption band at 454 nm. This addition served to change the solution from colorless to yellow in color. Under these conditions, the calculated association constant is reasonably high (log K_a = 9.2 M^{-2}) for a 2:1 binding process. In fact, **3.3** displays a selectivity for cyanide over fluoride in a water-containing organic solvent.
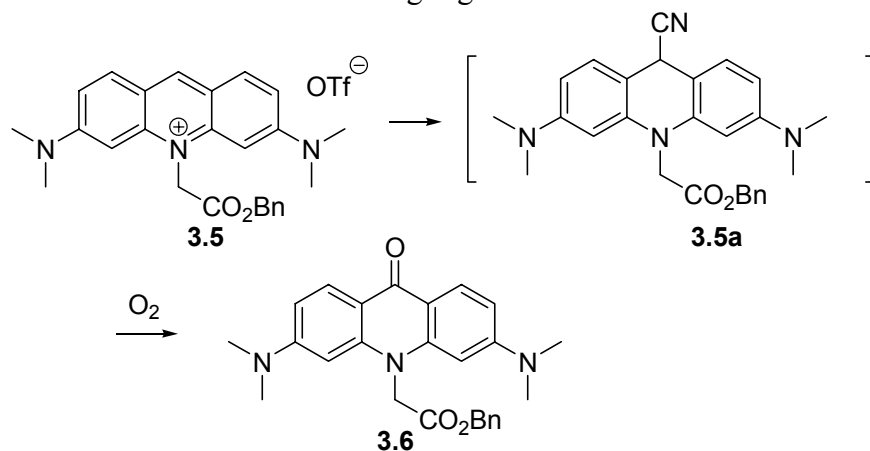
Scheme 3.3 Proposed cyanide-sensing mechanism of **3.5**

In 2006, the Tae group reported an acridinium salt **3.5** that reacts with the cyanide anion.[7] In this case, a nucleophilic addition reaction takes place at the activated 9-position of *N*-alkylated acridinium to produce intermediate **3.5a**. Subsequent oxidation produces

3.6. A similar reaction between methylated acridinium and cyanide had been published with the final product, *N*-methylacridon, being fully characterized in 1970.[8] Undoubtedly, this cyanide detection procedure is dependent on the solvent conditions, temperature, and reaction time. The indicator experiments were optimized and carried out in DMSO/water (95:5, v/v) at 50 $^\circ$C for 10 min by monitoring the observable fluorescence spectroscopic or visual changes upon the addition of cyanide. In the case of the fluorescence changes, the studies were carried out by adding various anions (1 equiv.), including CN^-, AcO^-, ClO_4^-, F^-, Br^-, Cl^-, I^-, $H_2SO_4^-$, $H_2PO_4^-$, SCN^-, BzO^-, NO_3^- CH_3S^-, and N_3^-. Among the tested anions, only cyanide produced a color change (yellow to blue), decreasing the fluorescence emission intensity ($F_o/F = 14$). Other potential nucleophiles (Et_2NH, $BuNH_2$, PhSH, NaSMe, NaOPh and $n\text{-}Bu_4NOH$) yielded no detectable change. The detection limit for cyanide proved to be below 1.9 μM as judged by visual inspection under these optimized conditions.
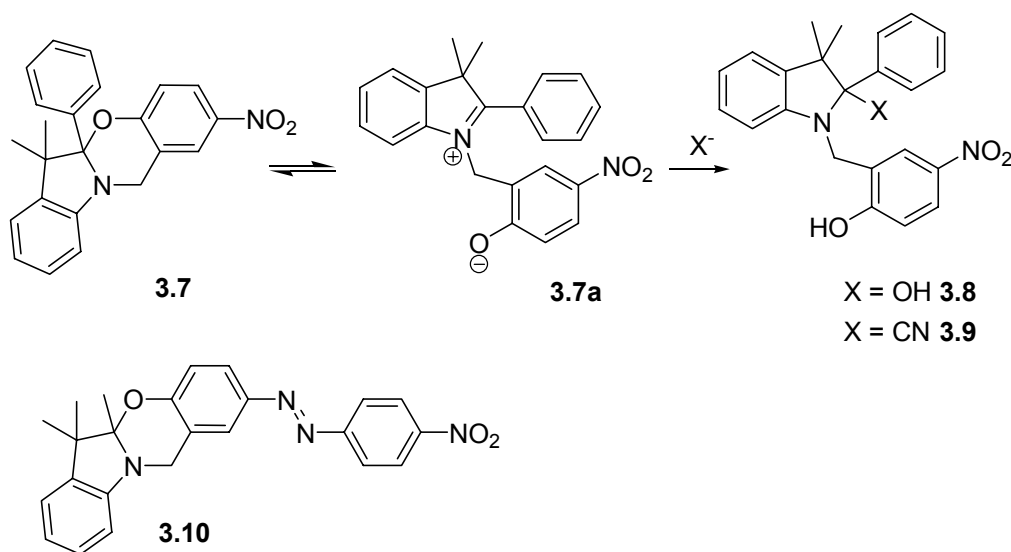
Scheme 3.4 Proposed cyanide-sensing mechanism of **3.10**

The Raymo and Sortino groups noted that the oxazine **3.7** is subjected to a ring opening equilibrium.[9] These workers also discoverd that the ring-opened species could be trapped by the addition of n-Bu$_4$N·OH. Presumably, the addition of this or other nucleophiles can suppress the ring closing reaction effectively. ^{1}H NMR studies supported the quantitative formation of hemiaminal **3.8**, and the conclusion was further supported by a single crystal structural analysis of the hemiaminal compound.[9] Based on this information, the Raymo group developed the oxazine system **3.10**[10] as a possible colorimetric indicator. It differs from the original oxazine **3.7** in that it contains an azo group, which serves to enhance the absorption intensity upon the addition of cyanide anion. The selective nature of this class of oxazine indicators was probed *via* the addition of NaF, NaCl, NaBr, NaI and NaCN. It was found that the absorption spectrum only changed appreciably when NaCN (10 mM) was added to the solution of **3.10** (0.1 mM, in acetonitrile). When the concentration of water in the medium was appreciable, a considerable amount of NaCN had to be added to induce a significant change. To overcome this problem, the cyanide addition was carried out as a two phase reaction (CH$_2$Cl$_2$/aqueous sodium phosphate buffer solution, pH = 9.0) using a phase transfer catalyst (n-Bu$_4$N·Cl). The characteristic absorbance of the phenolate chromophore was observed upon the addition of 1 μM cyanide under these bi-phasic conditions. The limit of cyanide detection was judged to be 1 μM as inferred from UV-vis titrations.
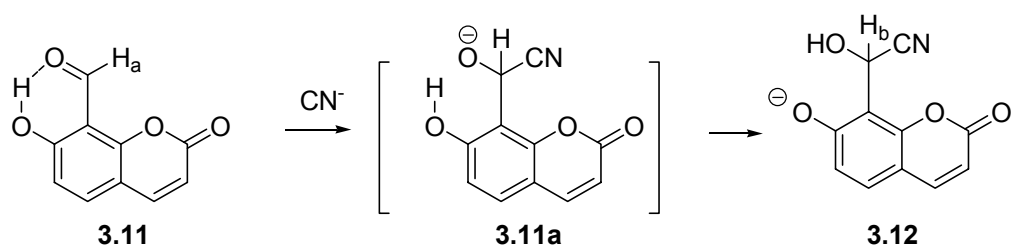
Scheme 3.5 Proposed cyanide-indicator mechanism for compound **3.11**

A coumarin indicator receptor **3.11**[11] reported by the Hong group also relies on a cyanohydrin reaction in analogy to previous systems. In this case, the cyanide sensing mechanism was supported by a study of the chemical shifts of H_a and H_b in the ^{1}H-NMR spectrum. The aldehyde proton (H_a) of coumarin **3.11** appeared at 10.1 ppm in D_2O. Upon the addition of NaCN, the aldehyde proton undergoes a dramatic shift to 6.1 ppm (H_b). The specific cyanide indicator properties were demonstrated in HEPES buffer solution (pH = 7.4) using fluorescence emission methods. Based on these studies, it was concluded that the coumarin receptor **3.11** (10 μM) is very inert to other anions including F^-, $H_2PO_4^-$, AcO^-, ClO_4^-, Br^-, Cl^-, I^-, NO_3^-, and N_3^- up to 1500 equiv. of anion. This respective specificity of this cyanohydrin-type reaction was ascribed to the presence of ancillary hydrogen bonding interaction between the aldehyde functionality and the phenolic OH in **3.1l**. System **3.11**, although not very fancy in terms of molecular design, represents an important advance in that it shows a fluorescence response to cyanide ions under aquous conditions that mimic those present in biological milieus.

3.1.2 FLUORIDE

Although fluoride anions allow some selectivity due to relatively small size of fluoride, some of fluoride selectivity may partly result from the basicity of fluoride

anions which have been highlighted in recent years.[12] Relatively speaking, reaction-based sensors for fluoride are less developed than those for cyanide.
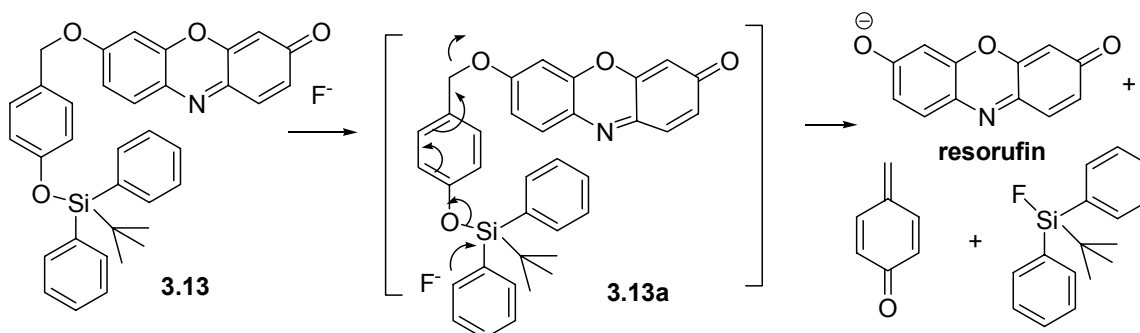
Scheme 3.6 Proposed fluoride-indicating mechanism of **3.13**

The fluoride indicator **3.13**[13] reported by the Hong group takes advantage of a silyl ether deprotection reaction,[14] a transformation that is commonly used in multistep syntheses. Indicator **3.13** reacts with TBA·F (or NaF), and the formed resorufin anion displays increased fluorescence intensity. In this case, the proposed sensing mechanism was confirmed by comparing the maximum emission wavelength of resorufin sodium salt in the presence and absence of fluoride in CH_3CN/water (50:50, v/v). The maximum emission band (λ_{max} = 591 nm) observed in these experiments is responsible for resorufin sodium salt.

The fluoride anion specificity of dosimeter **3.13** (0.5 μM in acetonitrile) was examined by testing its ability to produce a response in the presence of a variety of anions, including F^-, Cl^-, Br^-, I^-, AcO^-, $H_2PO_4^-$, HSO_4^-, NO_3^-, N_3^-. This was done by adding each anion (1400 equiv) to a solution of **3.13** in CH_3CN and monitoring the fluorescence response. The addition of F^- increases the fluorescence intensity 500-fold at 591 nm. The effect of the other anions is negligible. In addition, UV-vis absorption changes produced with different anions were monitored with dosimeter **3.13** (20 μM).

80

When 11 equiv. of F⁻ were added, the absorption peak intensity was increased by 250-fold and the response saturated at this point.

The response of indicator **3.13** (5 μM) was also tested in a water-containing medium (CH₃CN/H₂O, 50:50, v/v). Upon the addition 3000 equiv. of F⁻, the fluorescence intensity (λ_{em} = 589 nm) became saturated. A 200-fold increase was observed. The color of the solution changed from pale yellow to pink under these conditions. Other anions produced no color change. Although this system demonstrates the effectiveness of this general approach to F⁻ detection, the current detection limit of **3.13** is still too poor to make it a viable indicator.
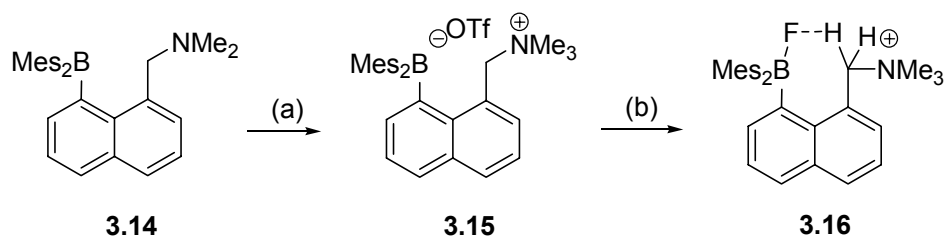
Conditions: (a) MeOTf, CH₂Cl₂, 25 °C, 88%. (c) [Me₃SIF₂][S(NMe₂)₃], CH₂Cl₂, 25 °C, 64%.

Scheme 3.7 Synthesis and proposed fluoride-indicating reaction of **3.15**

Lewis acidic borane derivatives have been considered as anion sponges for such species as hydride, fluoride and hydroxide.[15] However, most of these derivatives fail to produce an easy-to-monitor response. As such, they fall outside of our definition of reaction-based sensor systems. One important exception to this generalization comes from the Gabbaï group. These researchers designed a cationic Lewis acidic borane receptor **3.15**,[16] which contains a Lewis acidic borane and cationic tertiary amine. Interestingly, compound **3.14** yielded no measurable reaction when exposed to TBAF in

CHCl$_3$. The ^{1}H-NMR spectrum revealed only peaks ascribable to receptor **3.14**. However, the corresponding cationic derivative **3.15** quantitatively reacted with TBA·F or TAS·F (tris(dimethylamino)sulfonium difluorotrimethylsilicate). In solution, the boron chemical shift of receptor **3.15** resonated at 12.2 ppm in the ^{11}B NMR spectrum, while the fluorine chemical shift appeared at -152 ppm in the ^{19}F NMR spectrum. Both signals correspond to a triarylfluoroborate as would be expected for the proposed product **3.16**. The sensing mechanism was supported by a crystal structure of **3.16**, which revealed a C-H···F-B hydrogen bond. This bond is reflected in the fine splitting pattern seen in the ^{1}H NMR spectrum ($^1J_{H-F}$ = 9.2 Hz and $^2J_{H-H}$ = 12.9 Hz).

The ability of receptor **3.15** to act as a fluoride anion indicator was examined by monitoring the changes in the absorption spectrum of **3.15** in THF/MeOH (75:25, v/v) as a function of added TBA·F. The association constant was determined from these changes, with a K_a of 5.0 × 10^6 M^{-1} being obtained. Further studies of the interaction with fluoride were carried out by shaking a biphasic mixture of TBA·F in D$_2$O (2.7 × 10^{-1} M^{-1}, 0.5 mL) and receptor **3.15** in CDCl$_3$ (6.9 × 10^{-2} M^{-1}, 0.5 mL). In this experiment, receptor **3.15** afforded **3.16** in a yield of 82%.
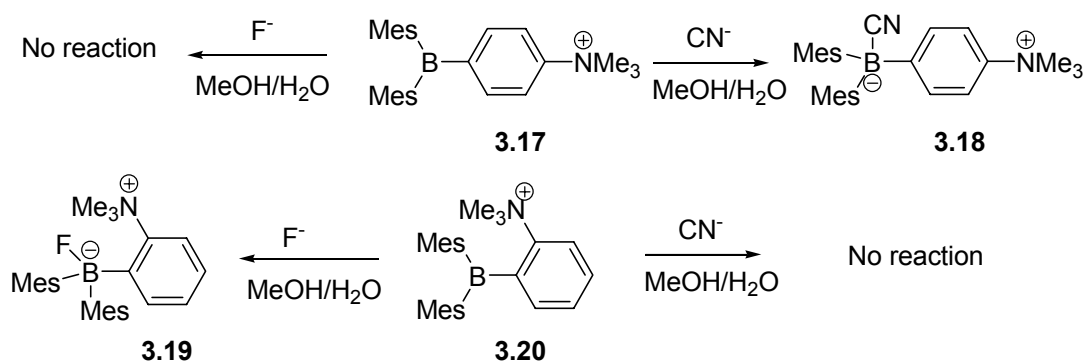
Scheme 3.8 Cyanide and flioride-sensing reactions of **3.17** and **3.20**

Building on their previous work, the Gabbaï group elaborated their Lewis acidic cationic receptor by changing the distance between the cationic amine and the Lewis acidic borane center. This produced indicators **3.17** and **3.20.** Cognizant of the fact that the [Ph$_3$BCN]$^-$ anion had been used for the preparation of cesium ion salts, these workers examined the reaction between the cyanide anion and these two new boranes (i.e., **3.17** and **3.20**).[17] It was found that **3.17** and **3.20** react with both cyanide and fluoride anions (TBA salts) in organic solvents such as chloroform. Surprisingly, in a mixture consisting of H$_2$O/DMSO (60:40, v/v), compound **3.17** reacted only with the cyanide anion, while receptor **3.20** reacted only with fluoride. In both cases, the addition of anion caused a decrease in the absorption intensity. By monitoring this decrease as a function of concentration, an effective association constant for receptors **3.17** and **3.20** could be obtained for cyanide and fluoride, respectively ($K_{a(CN)} = 3.9 \times 10^8$ M^{-1}, $K_{a(F)} = 910$ M^{-1}) in this solvent mixture. In contrast to what was seen with these receptors, Mes$_3$B does not react with cyanide. In the light of this "control," the reaction with cyanide can be ascribed to enhanced electrostatic interactions. Considering the relatively low association constant for F$^-$, the authors suggest that this favorable electrostatic interaction cannot overcome the high hydration enthalpy and relative low basicity of fluoride ($\Delta H^o{}_{hyd}$ = -504 KJ/mol, pK_a = 3.18). In both **3.17** and **3.20**, the interference from other anions such as Cl$^-$, Br$^-$, I$^-$, NO$_2^-$, HSO$_4^-$ and OAc$^-$ proved negligible under the same mixed aqueous-organic reaction. Finally, it was found that receptor **3.17** (5 µM) produces a naked eye-detectable signal with 1 equiv. of cyanide in H$_2$O/MeOH (90:10, v/v), when contained in a cuvette and illuminated with a laboratory UV lamp.

3.2 CATION RECOGNITION

Cation recognition parallels anion binding as a major interest in supramolecular chemistry. Cations such as sodium, potassium, magnesium and calcium are ubiquitous in biological systems.[2c] Some transition metal ions such as Cu, Co, Zn and Mn play important roles in metalloenzymes and other proteins.[18] Further, other metals such as Hg, Cd, and most radioactive species are very toxic. Thus the facile detection and in some cases, extraction of these cations is very important. Not surprisingly, therefore, a number of motifs, including crown ethers, cryptands, aza-crowns, polyamines and carboxylic acid derivatives, have been studied as cation complexants. The selectivity towards cations of these motifs is well appreciated to be highly dependent on structure. For instance, crown ethers can selectively bind Na^+ or K^+ depending on their size. Although specificity always remains an issue, this has inspired many structural modifications.[19] In addition to the underlying issues of selectivity, obtaining good sensors or indicators for certain cations remains a challenge. For instance, detecting palladium has proven tremendously difficult using traditional metal binding motifs. One solution involves the use of reaction-based indicator systems. A survey of such systems now follows. Excluded from our discussion are classic single element reactions, such as precipitation with H_2S, that have been used since the early days of chemistry in the context of qualitative or quantitative metal analysis.

3.2.1 MERCURY
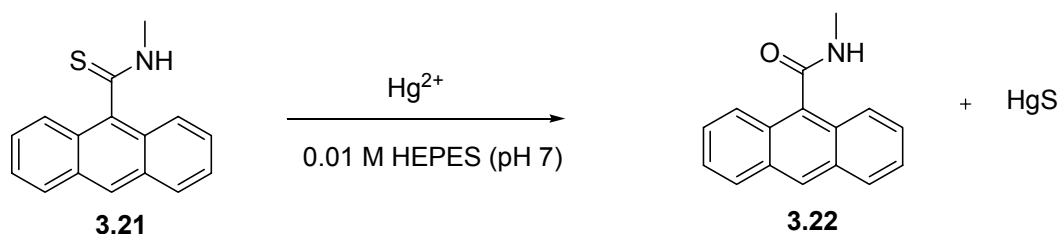
Scheme 3.9 Proposed mercury-sensing mechanism of **3.21**

Hg(II) is known to be a thiophilic metal ion. Desulfurization reactions are relatively common and well documented.[20] In fact, Hg(II) can convert many thiocarbonyl groups into the corresponding simple carbonyl. The Czarnik group used this desulfurization reaction to produce a reaction-based indicator for Hg(II). **3.21** may represent the first documented modern reaction-based sensor system for detecting metal ions.[21] What made this system noteworthy was an appreciation that the thiocarbonyl group in **3.21** would quench the anthracene fluorescence by photoinduced electron transfer (PET). By contrast, the carbonyl product **3.22** produced by desulfurization was expected to be fluorescent. In accord with such expectations, compound **3.22** proved to be 56 times more fluorescent than compound **3.21**. Test desulfurization reactions were carried out with Hg^{2+}, Ag^{+}, Al^{3+}, Ca^{2+}, Cd^{2+}, Co^{2+}, Cr^{2+}, Cu^{2+}, Fe^{3+}, In^{3+}, K^{+}, Mg^{2+}, Mn^{2+}, Na^{+}, Ni^{2+}, Sn^{4+}, Pb^{2+}, UO_2^{2+} and Zn^{2+} in aqueous buffer (HEPES buffer, pH = 7.0). Of these cations, only Hg(II) and Ag(I) reacted with receptor **3.21** as judged by the observation of an enhanced fluorescence intensity at 413.5 nm. The interactions with Hg(II) and Ag(I) proved relatively fast, proceeding to 87% and 73% completion, respectively, after 10 min. under stoichiometric conditions (23 μM) at room temperature.
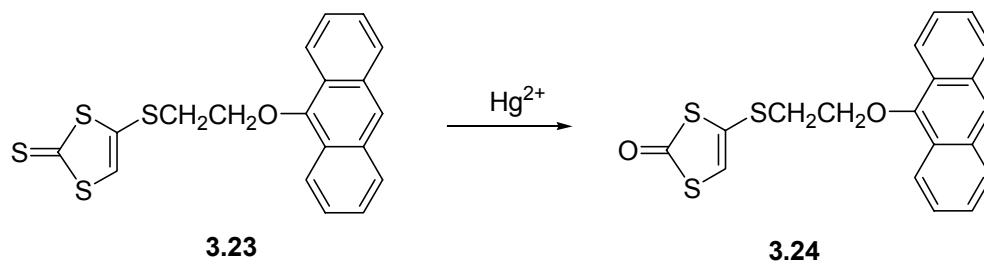
Scheme 3.10 Proposed mercury-sensing mechanism of **3.23**

The Zhang group has also reported a Hg(II) dosimeter, compound **3.23**, that is based on a desulfurization reaction.[22] As shown in Scheme 3.10, reduction with Hg(II) converts a poorly fluorescent compound, **3.23**, to a highly fluorescent compound, **3.24**. As in the case of the Czarnik system, a change in the PET properties is used as the basis for sensing. The actual experiments were conducted in THF/water (20:1, v/v) due to the low solubility of **3.23** in pure water. All reactions were carried out at 40 ^{o}C in the presence of **3.23** (10 μM) for 30 min. The fluorescence enhancement was linear in added Hg(II). Up to the point of 1 equiv., fluorescence had increased by 10-fold. Little detectable fluorescence enhancement was observed with other metal ions, including Ag^+, Ba^{2+}, Co^{2+}, Mn^{2+}, Ni^{2+}, Pb^{2+}, Zn^{2+} and Fe^{3+}. Moreover, under conditions of direct competition, the interference from these metal ions, as well as La^{3+}, Ce^{3+}, Nd^{3+}, Y^{3+} and Gd^{3+} proved negligible ([**3.25**] = 10 μM and [Hg^{2+}] = 50 μM at 40 ^{o}C). Indicator **3.23** has a better selectivity profile than **3.21** for which competition from Ag(I) was observed.

86
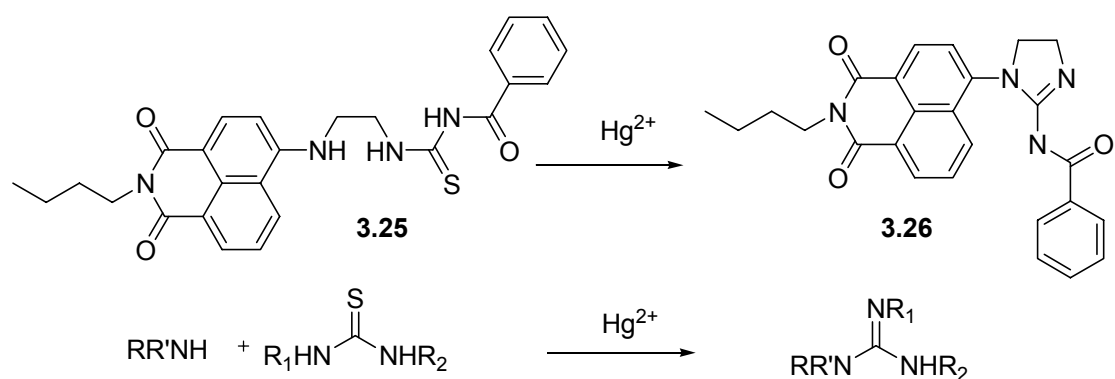
Scheme 3.11 Proposed mercury-sensing mechanism of **3.25**

The Tian group has reported what appears to be the first dual fluorescent and colorimetric reaction-based indicator for Hg(II). Their system, **3.25**, consists of a 4-amino-1,8-naphthalimide (signaling unit) and a thiourea (reaction unit), as shown in Scheme 3.11.[23] This indicator relies on the formation of guanidiums from thioureas, both of which have been widely used as motifs in supramolecular chemistry.[24] In contrast to other Hg(II) selective receptors, the guanidine motifs formed leads to a change in the π conjugation pathway, a key conversion that can be exploited to produce a change in the absorption bands in the UV-vis region of the electronic spectrum.

The sensing experiments were conducted under optimized conditions that were found to afford the best selectivity. Specifically, the Hg(II) ion (0.2 equiv.) was added to a solution of receptor **3.25** (3 μM, acetonitrile/water, 80:20, v/v) and allowed to react for 10 min. As expected, the absorption and emission maxima were shifted from 350 nm and 475 nm to 435 nm and 530 nm, respectively. No appreciable change was observed when other cations such as Ag^+, Co^{2+}, Cu^{2+}, Ni^{2+}, Pb^{2+}, and Zn^{2+}, were examined. However, for

Hg(II), the limit of detection was determined to be ca. 0.2 μM, through standard fluorescence titrations.
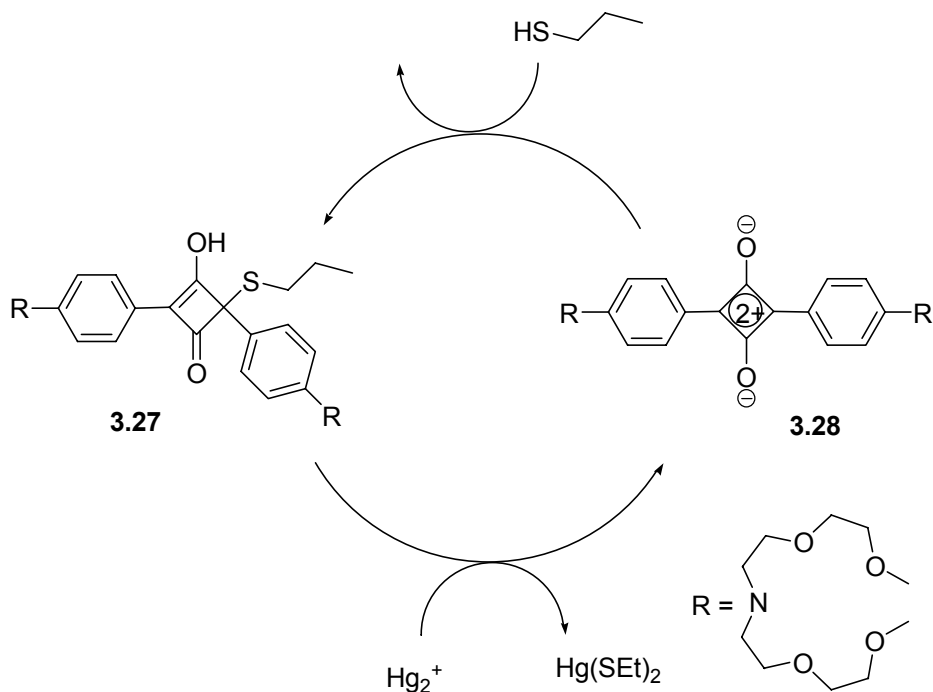
Scheme 3.12 Mercury(II)-induced reaction of **3.27** and its regeneration

Squaraine dyes have been used as a signaling unit for Ca^{2+} sensing, as well exploited extensively for other aspects of supramolecular chemistry.[25] Squaraine has an electron deficient central core that is very vulnerable to nucleophilic reactions. The squaraine-based Hg(II) indicator **3.27** exploits this reactivity pattern of squaraine-type dyes.[26] However, this system goes further in both signaling and reaction units. This allows it to act as an indicator for Hg(II). The actual sensing mechanism involves a thiol elimination step assisted by Hg(II). One interesting feature of receptor **3.27** is that can be recycled quantatively as shown in Scheme 3.12.

The conditions used for Hg(II) detection were optimized and consisted of a water/acetonitrile mixture (4:1, v/v, 0.01 M CHES buffer solution, pH = 9.6). Upon the addition of Hg(II) to a solution of **3.27** in this medium, a new absorption signal was observed at 600 nm with an emission signal appearing at 670 nm. Hg(II) selectivity was tested by adding 0.5 equiv. of metal ions to a solution of **3.27** (6 μM). Of the ions tested, which included Ni^{2+}, Zn^{2+}, Ti^+, Fe^{3+}, Hg^2, Pb^{2+}, Al^{3+}, only Hg(II) engendered a strong absorption at 650 nm. The detection limit for Hg(II) displayed by receptor **3.27** (0.1 μM) was examined by fluorescence spectroscopy and turned out to be less than 2 ppb. In addition, a prototype of a dip-stick (**3.27** was fixed on a polyethylene terephthalate film) was prepared. When the stick was placed into the preloaded Hg(II) solution, the surface changed from colorless to blue in a few seconds. This bodes well for the use of this system as a practical colorimetric sensor.
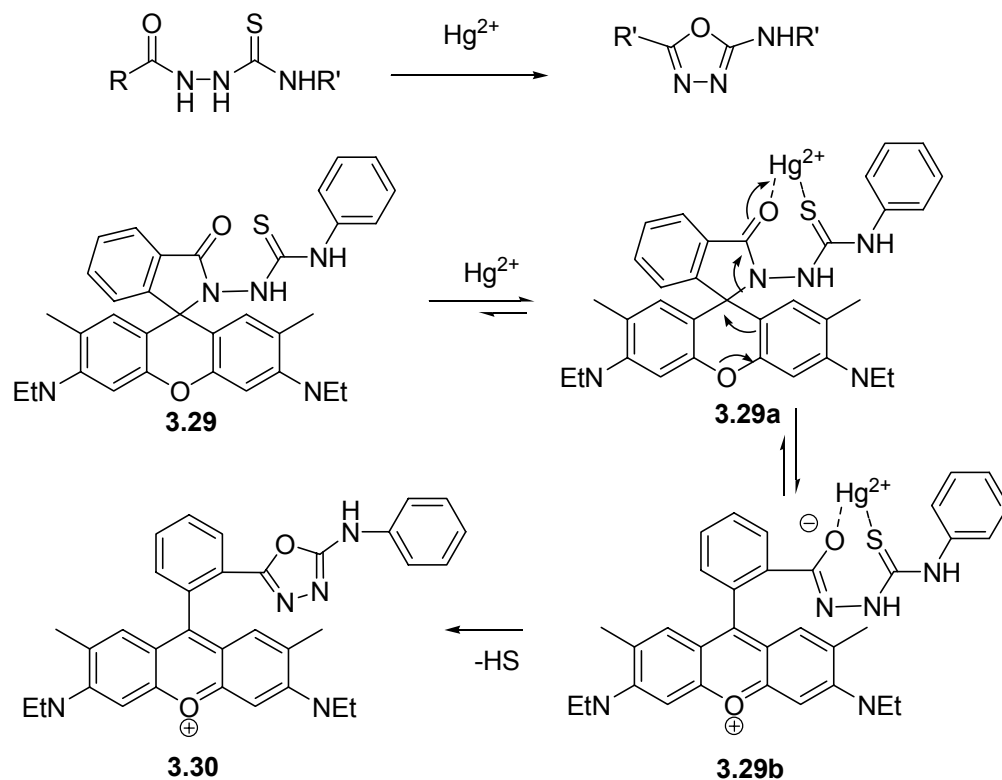
Scheme 3.13 Proposed mercury-sensing mechanism of **3.29**

The Hg (II) indicator **3.29**[27] reported by the Tae group relies on a 1,3,4-oxadiazole forming reaction.[28] In this case, the core indicating is derived from rhodamine 6G. Nonetheless, the Hg(II) detection involves a desulfurization reaction, as shown in Scheme 3.13. In this case, the sensing experiments were conducted in water/methanol (80:20, v/v). Upon addition of Hg(II) ions (1 equiv.), the fluorescence intensity of the solution **3.29** (1 μM) increased 26-fold, while the emission maximum shifted from 533 nm to 557 nm. The signal readout was relatively fast allowing for a response time of < 1 min. To test the selectivity of receptor **3.29**, 1 equiv. of various potentially competitive metal ions, such as Ag^+, Zn^{3+}, Cu^{2+}, Pb^{2+}, Cd^{2+}, Ni^{3+}, Co^{2+}, Fe^{2+}, Mn^{2+}, Mg^{3+}, Ca^{3+}, Ba^{2+}, Li^+, K^+, Na^+, Rh^{3+} and Cr^{2+} were added to **3.29** under the same conditions. Little

enhancement in the fluorescence intensity was seen for Ag(I) and Zn(II). With little

detectible change being observed for the other cations, based on the result of fluorescence

titration, the detection limit of this dosimeter is in the parts per billion range.

3.2.2 COPPER
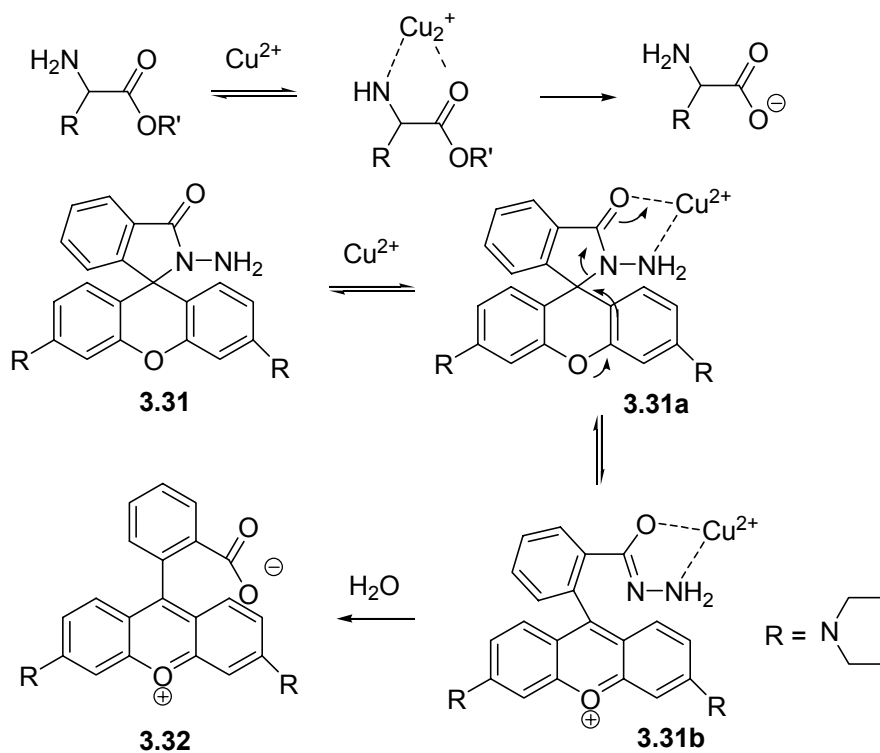
Scheme 3.14 Proposed copper(II)-based reactions relevant to an understanding of indicator **3.31**

Cu(II) is known to accelerate the hydrolysis of α-aminoacid esters.[29] This key

reactivity feature provides the basis for indicator **3.31**.[30] This system also incorporates a

rhodamine B subunit, which provides a key signaling group. The relevant chemistry is

summarized in Scheme 3.14. Cu(II) is thought to bind the hydrazide group in **3.31a**.

Cu(II) can also facilitate the equilibrium between **3.31a** and **3.31b**. Finally, water can

react with **3.31b** to generate hydrazine and rhodamine **3.32**. TLC data, electrospray mass spectrometric analyses and the absorption and emission spectra of the product were found to correspond to those of an authentic sample. Tests of **3.31** as an indicator were conducted in buffered aqueous solution (0.01 M HEPES, pH = 7.0). Specifically, 100 equiv. of various cations were added to a solution of **3.31** and monitored after 1 hour by UV-vis spectroscopy. The examined cations were Ag^+, Al^{3+}, Ca^{2+}, Cd^{2+}, Co^{2+}, Cr^{3+}, Cu^{2+}, Eu^{3+}, Fe^{3+}, Ga^{3+}, Gd^{3+}, Hg^{2+}, In^{3+}, K^+, Li^+, Mg^{2+}, Mn^{2+}, Na^+, Ni^{2+}, Pb^{2+}, Rb^+, Sn^{4+}, Sr^{2+}, U^{4+}, Yb^{3+} and Zn^{2+}. Cu(II) and Hg(II) produced a reaction. However, under optimized conditions (**3.31**; 0.5 µM, buffer/acetonitile = 80/20, v/v), the addition of Cu(II) led to complete reaction within in 1 min, whereas Hg(II) required 50 hours to produce a change. Indicator **3.31** could also detect Cu(II) concentrations less than 0.1 µM in the presence of **3.31** (10 µM) as inferred from the observed enhancement in the emission intensity.

3.2.3 PALLADIUM
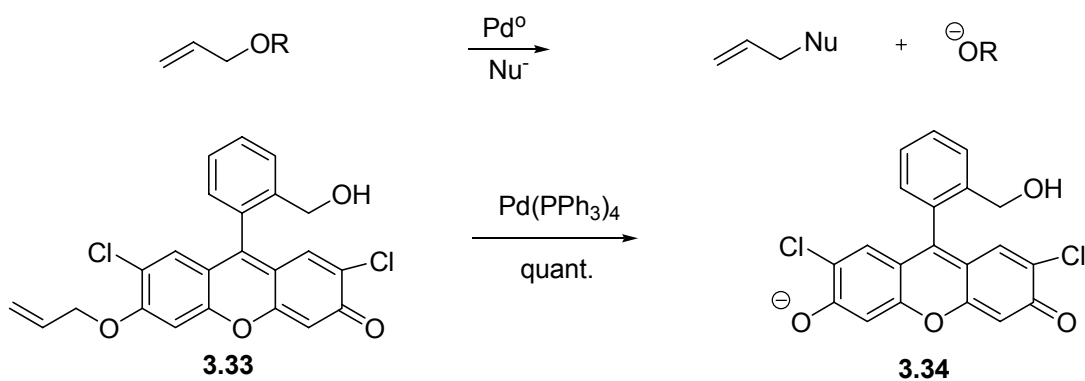
Scheme 3.15 Palladium-dependent reactions of **3.33**

Palladium catalyzed Trost-Tsuji reactions[31] have been widely used in organic synthesis and in the pharmaceutical industry. However, residual palladium contamination

is often an issue in these and other Pd catalyzed reactions, especially since the palladium residual in human-grade final products should be less than 10 ppm.[32] In spite of the resulting detection need, palladium detection has received little attention within the molecular recognition field. The Koide group has reported a Pd indicator as shown in Scheme 3.15.[33] These researchers realized that O-alkylated fluoresceins are not fluorescent, while deprotected fluoresceins are fluorescent and, indeed, have been used extensively in the biological imaging field. This disparity was paired with the Trost-Tsuji reaction to produce the O-alkylated derivative **3.33**. To test the selectivity of this putative Pd indicator, several metals, including Pd^{2+}, Pt^{2+}, Fe^{3+}, A^{2+}, Ni^{2+}, Mn^{3+}, Cd^{2+}, Au^{3+}, Rh^{+}, Cu^{3+}, Mg^{+}, K^{+}, Cr^{3+} Co^{2+}, Hg^{2+}, and Ru^{3+}, were examined in basic aqueous media (borate buffer, pH = 10) in the presence of PPh_3. Pd(II) induced an enhancement in the fluorescence signal, with Pt(II) also producing an enhancement, albeit to roughly half the level produced by Pd(II). Other metals were not effective. To quantify the presence of Pd, the indicator experiments were conducted under standard conditions involving a 10 μM concentration of **3.33** in borate buffer and a reaction time of 1 h. Linearity between the fluorescence intensity and the amount of added Pd(II) was observed over 3 to 300 nM concentrations.

Receptor **3.33** was then examined in three experiments designed to probe its potential utility under field conditions. First, a sample of aspirin containing 10 ppm Pd was tested. It was found that the observed intensity from this sample was nearly the same as that observed for a positive control (10 ppm Pd + receptor **3.33**). Second, to test what might be needed under conditions of Pd and Pt mining, where traditionally rock samples are analyzed for Pd/Pt *via* atomic absorption analysis, typical rock samples were mixed

with **3.33** (in buffer). With a laboratory UV lamp (365 nm), the authors identified two rock samples containing 36 ppm and 120 ppm of Pd/Pt sample respectively. Specifically, the two samples in question turned green when subject to such UV illumination. Third, the authors were able to detect Pd residue on a glass surface under the conditions designed to mimic the washing procedures routinely used in the organic laboratory (brushing with detergent and washing with water and acetone). Taken in concert, these three examples help illustrate the potential utility of reaction-based indicators.

3.3 NEUTRAL MOLECULE RECOGNITION

3.3.1 PHOSGENE

Phosgene was first used as a chemical weapon in World War I and its infamy for this purpose lives to this day. Even though there are now much more deadly agents known, phosgene remains one of the easiest chemical warfare agents to obtain due to its use in chemical industry.[34] Accordingly, indicators for phosgene could be potentially beneficial. However, to date, optical sensing systems for phosgene have remained rare. On the other hand, by exploiting a reaction-based approach, the late Rudkevich succeeded in developing a potential phosgene sensor. This system, which takes advantage of the urea forming reaction between **3.35** and **3.36** (coumarin 343 derivative) and fluorescence resonance energy transfer (FRET) is illustrated in Scheme 3.16.[38] In this case, FRET is observed within **3.37,** which is produced as a result of the phosgene induced coupling.
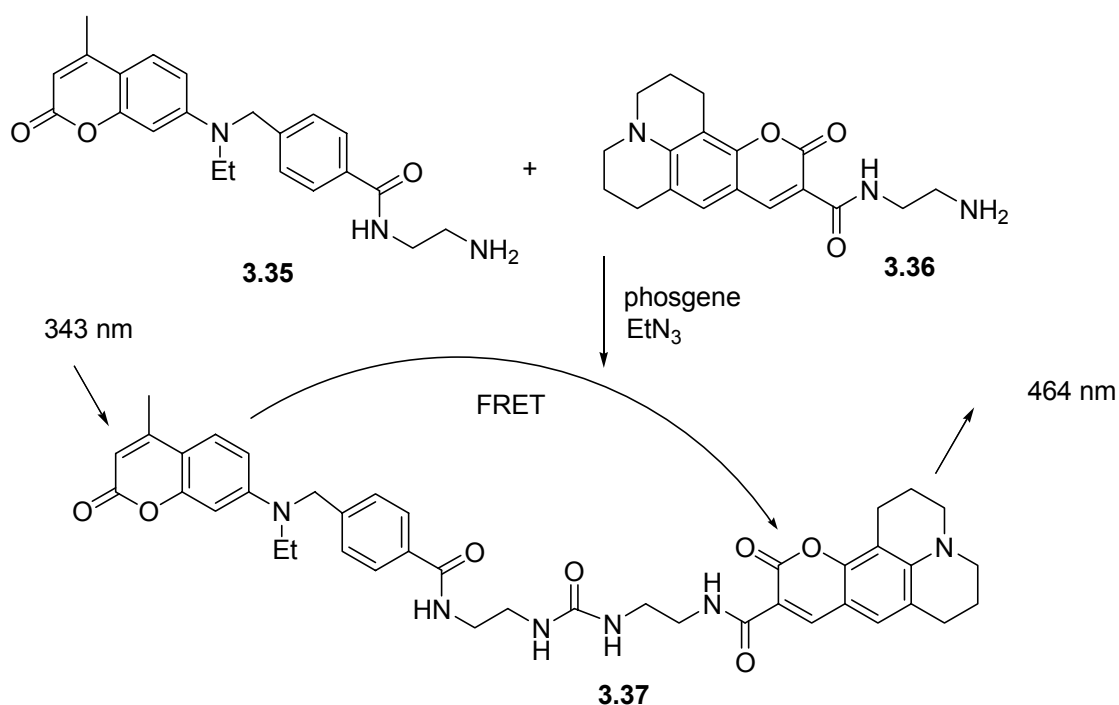
Scheme 3.16 Phosgene-sensing reaction between **3.35** and **3.36**

Tests of phosgene sensing were conducted at concentrations of 5×10^{-4} to 10^{-2} M^{-1}. In these tests, an equimolar mixture of the two starting compounds (**3.35** and **3.36**) was mixed in CHCl$_3$ in the presence of TEA (10 equiv.). Phosgene was then added to the solution. The solution was diluted to 10^{-6} M via the addition of CHCl$_3$ and monitored by irradiating at 343 nm. The dilution step proved necessary; otherwise, the reaction was very slow at a concentration range of 10^{-5} M. During the titration, it was observed that the fluorescence intensity at 464 nm increases, which corresponds to the emission of courmarin 343. In addition, the system was observed to undergo naked eye detectable changes in color when irradiated with a laboratory UV lamp. While this indicator system

is limited by a propensity of the components to undergo self coupling, the useful detection limit for phosgene was about 5×10^{-5} M.

3.3.2 HYDROGEN PEROXIDE

A variety of reactive oxygen species (ROS) are implicated in human biology. One of these is hydrogen peroxide H_2O_2/HO_2^-. H_2O_2 and other ROS have been implicated in a range of human diseases including Alzheimer's disease, neurodegerative disease, cardiovascular disorders, and cancer.[36] The need to sense H_2O_2 is thus well-appreciated. Indeed, several receptors have been developed using ROS-cleavable protecting groups.[37]
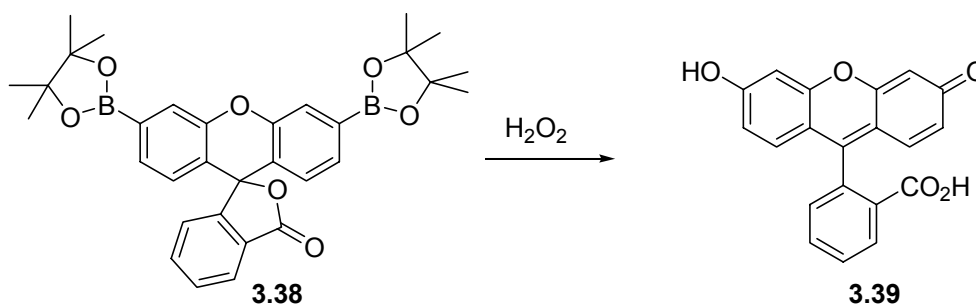
Scheme 3.17 Hydrogen peroxide-sensing reaction of **3.38**

Recent progress in the area of H_2O_2 indicators has been more focused on pure chemical reactions, which do not require enzymatic transformations. In this context, receptor **3.38**[38] developed by the Chang group is noteworthy. It is a process that responds to ROS and takes advantage of simple fluorescein chemistry. The starting material, **3.38**, is not fluorescent, whereas the product produced upon reaction with H_2O_2, **3.39**, is fluorescent. Selectivity towards H_2O_2 was demonstrated under simulated biological conditions (20 mM HEPES buffer, pH 7). Indicator **3.38** (5 uM) responds to H_2O_2,

undergoing a fluorescence increase to a level that is over 500 greater than originally seen. Similar effects were observed upon exposure to ROS, such as *tert*-butyl hydroperoxide (TBHP), O_2^-, NO, or ^-OCl. When it comes to the highly reactive radical species, $\cdot OH$ was one third of that produced by H_2O_2. Likewise, the increase produced by the O^tBu radical was one fifteenth of H_2O_2. The identity of the final product **3.39** was confirmed by comparing the absorption, emission, and electrospray ionization mass data of **3.39** produced from the reaction and an authentic sample. Finally, Chang and his group were able to observe a fluorescence enhancement in HEK cells *via* confocal microscopy. Here, the cells were incubated with 5 μM receptor **3.39** for 5 min at 25 °C after which H_2O_2 (10-100 μM) was administered.
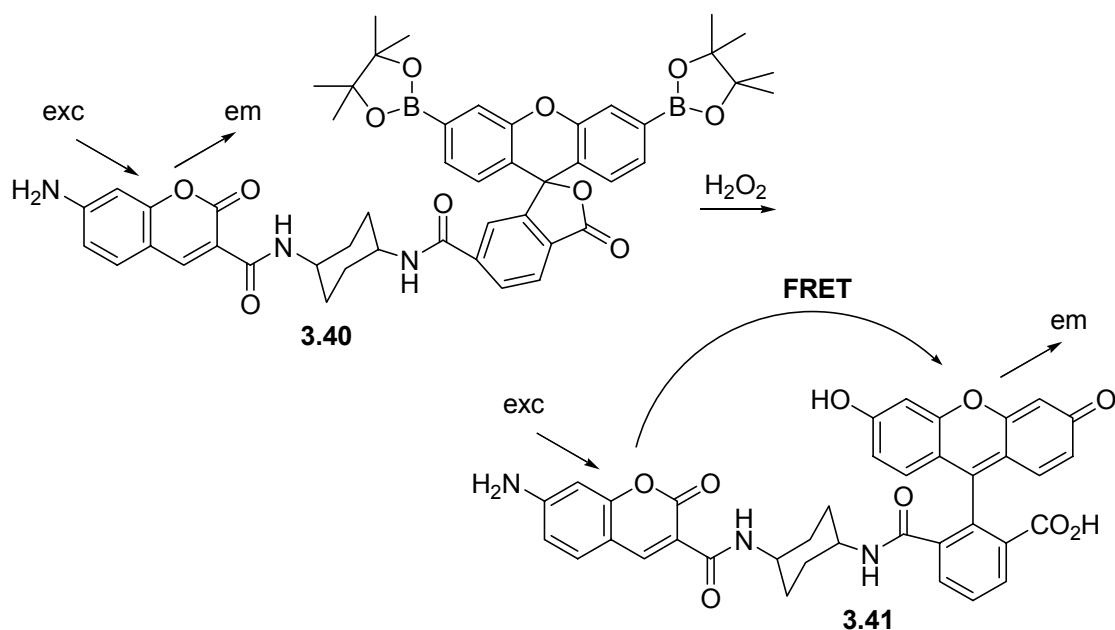
Scheme 3.18 Hydrogen peroxide-sensing reaction f **3.40** and FRET in **3.41**

Another interesting H_2O_2 probe, compound **3.40**, was developed by the Chang group as an improvement over indicator **3.38**. This new probe exploits fluorescence

resonance energy transfer (FRET) as a means of enhancing sensitivity. In this case, reaction with H_2O_2 serves to unmask a FRET cassette **3.41**[39] that contains a coumarin donor, a fluorescein derivative, and an amide linker.

Upon reaction with H_2O_2 receptor **3.40** produces one major band at 517 nm with a minor band at 461 nm when irradiated at 420 nm under simulated biological conditions (DPBS buffer, 15 FBS, pH = 7.4). Conversely, prior to the reaction, emission at 464 nm is observed, thus, the ratio $\lambda_{517}/\lambda_{464}$ could be monitored as an indicator of ROS concentration. This ratio was seen to increase from 0.45 to 3.7 over the cause of 1 hour, after 200 mM H_2O_2 was added to a solution of **3.40** at pH 7.4. Other ROS, such as $TBHP^-$, O_2^-, NO, NO^+, OH radical, TBHP radical, OCl^-, O_3 or O_2 induced little or no change in this ratio. The observed kinetics for this reaction were found to be pseudo-first-order (k_{obs} = 2.7×10^{-4} S^{-1}) under the reaction conditions (1 μM **3.40**, 1 mM H_2O_2). They also showed that probe **3.40** can be used to quantify the H_2O_2 produced by viable mitochondria stimulated with antimycin A.

3.4 CONCLUSION AND PROSPECTIVES

Reaction-based receptors have been used with increasing success over the last decade. Undoubtedly, compared to more classic supramolecular systems, reaction-based indicators can provide superior selectivity as the result of exploiting specific reactions that are less dependent than traditional receptor systems on the shape of host and guest. While clearly having antecedents in time-honored qualitative analysis, the idea of using design principles to produce reaction-based indicators represents a paradigm shift in supramolecular chemistry.

In terms of successes recorded to date, reaction-based indicators for cyanide and Hg are currently well-developed. However, other ions and toxic neutral guests are still challenging targets for reaction-based detection. In this respect, developing new reactions that respond to guests specifically may be necessary. On the other hand, a range of applicable reactions may exist in the literature and simply be awaiting our attention. On a different level, there appears to be tremendous opportunities associated with increasing the detection limit of existing reactions by introducing better signal transmitting groups or developing better readout systems that can amplify the signal. Such approaches to improving sensitivity have been used a great deal in the area of supramolecular sensor chemistry, and some first examples of this strategy are contained in this chapter.

This chapter, while not comprehensive in terms of detailing every possible reaction-based sensor systems, is nonetheless intended to illustrate the basic concepts of reaction-based indicator development. In this context, we have been pleased to contribute to the further development of the field *via* the introduction of a new class of cyanide triggered receptors. The details of this work are provided in Chapter 4.

3.5 REFERENCES

(1)   Ariga, K.; Kunitake, T. *Supramolecular Chemistry: Fundamentals and Applications*; Springer: Heidelberg, **2006**.

(2)   A consider body of literature exists that deals with this topic. For instance, see: (a) Sessler, J. L.; Gale, P. A.; Cho W.-S. *Anion Receptor Chemistry*; The Royal Society of Chemistry: Cambridge, UK, **2006**. (b) Beer, P. D.; Gale, P. A. *Angew. Chem., Int. Ed.*, **2001**, *41*, 486-516. (c) Valeur, B.; Leray. I. *Cord. Chem. Rev.* **2000**, *205*, 3-40.

(3)   Cyanohydrin reaction-based indicators differ from most other like system in that they are for the most part based on reactions that are reversible.

(4)   Koenig, R. *Science*. **2000**, *287*, 1737-1738.

(5)   Chung, Y. M.; Raman, B.; Kim, D.-S.; Ahn, K. H. *Chem. Commun*. **2006**, 186-188.

(6)   Chen, C.-L.; Chen, Y.-H.; Chen, C.-Y.; Sun, S.-S. *Org. Lett.* **2006**, *8,* 5053-5056.

(7)   Yang, Y.-K.; Tae, J. *Org. Lett.* **2006**, *8*; 5721-5723.

(8)   Happ, J. W.; Janzen, E. G.; Rudy, B. C. *J. Org. Chem.* **1970**, *35*, 3382-3389.

(9)   Tomasulo, M.; Sortino, S.; White, A. J. P.; Raymo, F. M. *J. Org. Chem.* **2005**, *70*, 8180-8189.

(10)   (a) Tomasulo, M.; Raymo, F. M. *Org. Lett.* **2005**, *7*, 4633-4636. (b) Tomasulo, M.; Sortino, S.; White, A. J. P.; Raymo, F. M. *J. Org. Chem.* **2006**, *71*, 744-753.

(11)   Lee, K.-S.; Kim, H.-J.; Kim, G.-H.; Shin, I.; Hong, J.-I. *Org. Lett.* **2008**, *10*, 49-51.

(12)   Crystallographic evidence; see: Evans, L.S.; Gale, P.A.; Light, M. K.; Quesada, R. *Chem. Commun*., **2006**, 965-967.

(13)   Kim, S. K.; Hong, J.-I. *Org. Lett.* **2007**, *9*, 3109-3112.

(14)   Greene, T. W.; Wuts, P. G. M. *Protective Groups in Organic Synthesis*, 3rd ed.; Wiley: New York, **1999**, pp 113-148.

(15)   (a) Shriver, D. F.; Biallas, M. J. *J. Am. Chem. Soc.* **1967**, *89*, 1078-1081. (b). Katz, H. E *J. Am. Chem. Soc.* **1985**, *107*, 1420-1421. (c) Katz, H. E. *J. Org. Chem.* **1985**, *50*, 5027-5032. (d) Sole, S.; Gabbai, F. P. *Chem. Commun.* **2004**, 1284-1285.

(16)   Chin, C.-W.; Gabbaï, F. P. *J. Am. Chem. Soc.* **2006**, *128*, 14248-14249.

(17)   Hudnall, T. W.; Gabbaï, F. P. *J. Am. Chem. Soc.* **2007**, *129*, 11978-11986.

(18)   Christianson, D. W.; Cox, J. D. *Annu. Rev. Biochem*. **1999**.*68*, 33-57.

(19)   Yamada, K.; Nomura, Y.;Citterio, D.; Iwasawa, N.; Suzuki, K. *J. Am. Chem. Soc.* **2005**, *127*, 6956-6957.

(20)   Antonino, C.; Venerando, P. *Tetrahedron*, **1998**, *54*, 15027-15062.

(21)   Chae, M.-Y.; Czarnik, A. W. *J. Am. Chem. Soc*. **1992**, *114*, 9704-9705.

(22)   Zhang, G.; Zhang, D.; Yin, S.; Yang, X.; Shuai, Z.; Zhu, D. *Chem. Commun.* **2005**, 2161-2163.

(23)   Liu, B.; Tian, H. *Chem. Commun.* **2005**, 3156-3158.

(24)   (a) Manimala, J.; Anslyn, E. *Eur. J. Org. Chem.*, 2002, 3909-3922.(b) Dahmen, S.; Bräse, S. *Org. Lett.*, **2000**, *2*, 3563-3565.

(25)   Arunkumar,E.; Ajayaghosh, A.; Daub, J. *J. Am. Chem. Soc.* **2005**, *127*, 3156 - 3164.

(26)   Ros-Lis, J.; Marcos, M. D.; Martínez-Máñez, R.; Rurack, K.; Soto, J. *Angew. Chem., Int. Ed.* **2005**, *44*, 4405-4407.

(27)   Yang, Y.-K.; Yook, K.-K.; Tae, J. *J. Am. Chem. Soc*. **2005**, *127*, 16760-16761.

(28)   (a) Wang, X.; Li, Z.; Wei, B.; Yang, J. *Synth. Commun.* **2002**, *32*, 1097-1103. (b) Zou, X.; Jin, G. *J. Heterocycl. Chem*. **2001**, *38*, 993-996.

(29)   (a) Kroll, H. *J. Am. Chem. Soc*. **1952**, *74*, 2034-2036. (b) Kroll, H. *J. Am. Chem. Soc*. **1952**, *74*, 2036-2039. (c) Bender, M. L.; Turnquist, B. W. *J. Am. Chem. Soc.* **1957**, *79*, 1889-1893.

(30)   Dujols, V.; Ford, F.; Czarnik, A. W. *J. Am. Chem. Soc*. **1997**, *119*, 7386-7387.

(31)   Kurti, L.; Czako, B. *Strategic Applications of Named Reactions in Organic Synthesis*; Elsevier Academic Press: London, **2005**.

(32)   Garrett, C. E.; Prasad, K. *Adv. Synth. Catal.* **2004**, *346*, 889-900.

(33)   Song, F.; Garner, A. L.; Koide, K. *J. Am. Chem. Soc.* **2007**, *129*, 12354 -12355.

(34)   Cotarca, L. *Phosgenation: A Handbook*; Wiley-VCH: Cambridge, UK, **2004**.

(35)   Zhang, H.; Rudkevich, D. M. *Chem. Commun.* **2007**, 1238-1239.

(36)   (a) Barnham, K. J.; Masters, C. L.; Bush, A. I. *Nat. Rev. Drug Discovery* **2004**, *3*, 205-214. (b) Shah, A. M.; Channon, K. M. *Heart* **2004**, *90,* 486-487. (c) Ohshima, H.; Tatemichi, M.; Sawa, T. *Arch. Biochem. Biophys.* **2003**, *417*, 3-11.

(37)   (a) Setsukinai, K.; Urano, Y.; Kakinuma, K.; Majima, H. J.; Nagano, T. *J. Biol. Chem.* **2003**, *278*, 3170-3175. (b) Lo, L.-C.; Chu, C.-Y. *Chem. Commun.* **2003**, 2728-2729. (c) Maeda, H.; Fukuyasu, Y.; Yoshida, S.; Fukuda, M.; Saeki, K.; Matsuno, H.; Yamauchi, Y.; Yoshida, K.; Hirata, K.; Miyamoto, K. *Angew. Chem., Int. Ed.* **2004**, *43*, 2389-2391.

(38)   Chang, M. C. Y.; Pralle, A.; Isacoff, E. Y.; Chang, C. J. *J. Am. Chem. Soc.* **2004**, *126,* 15392-15393.

(39)   Albers, A. E.; Okreglak, V. S.; Chang, C. J. *J. Am. Chem. Soc.* **2006**, *128*, 9640-
         9641.

Chapter 4 The Benzil Rearrangement Reaction: Trapping of a Hitherto Minor Product and Its Application to the Development of a Selective Cyanide Anion Indicator

4.1 INTRODUCTION

Cyanide is known to be very toxic. Much of its toxicity results from the fact that it binds to the ferric ion in cytochrome-c thus stabilizing this form and inhibiting the mitochondrial electron-transport chain.[1] In fact, even small amounts of the cyanide anion are extremely toxic to most living creatures. However, cyanide salts are widely used in gold mining, electroplating, and metallurgy.[2] Given the conflict between toxicity and industrial utility, it is not surprising that accidental releases of cyanide occur on occasion and that these can result in serious environmental damage. One case in point is the large cyanide spill that took place in Romania in 2000, which was considered as "Europe's biggest environmental disaster" since the explosion of the Chornobyl nuclear power plant in 1986.[3] To reduce the biological impact of a potential cyanide release, there is a cognent need for cyanide-selective receptors and sensors. However, many of the cyanide anion receptors reported to date have relied on hydrogen bonding motifs[4] and, as a consequence, have generally displayed poor selectivities relative to other anions.[5] To overcome this limitation, reaction-based cyanide indicators have been developed recently. These include oxazine **4.1**,[6] acridinium salt **4.2**[7] dipyrrole carboxamide **4.3**,[8] and cationic borane **4.4**,[9] approaches that were reviewed in Chapter 3. Unfortunately, none of these indicators is ideal. For instance, the oxazine-based system requires biphasic conditions, and acridinium salts need an elevated reaction temperature to function as

cyanide indicators. Another interesting cyanide anion indicator, dipyrrole carboxamide, also takes advantage of a putative nucleophilic reaction due to the very basic nature of cyanide and acidic protons. However, in none of these cases were the proposed addition products isolated, making it difficult to verify the suggested mechanism of action. In the case of cationic borane system **4.4**, there is of a great interest since the electron deficient borane reacts with cyanide in water containing solvent. However, this system does not produce a visual color change and is not a colorimetric sensor. Given this uncertainty, we felt it would be advantageous to develop a cyanide-driven reaction which could be used to sense cyanide. As we saw it, the desired reaction should operate at room temperature, possess a clear mechanistic signature, and act as an off-the-shelf indicator[10] for this toxic agent.
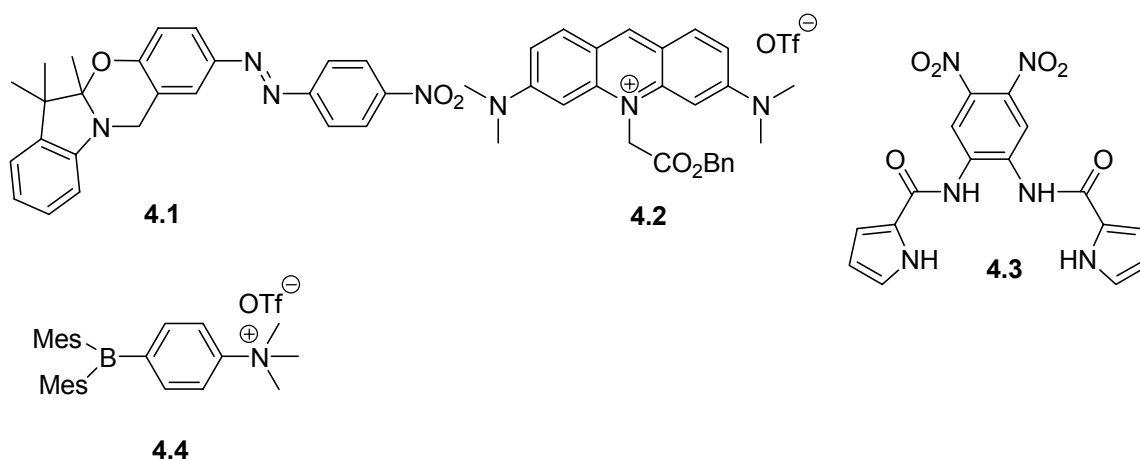
4.2 BENZIL CYANDE REACTION AND BENZIL REARRANGEMENT REACTION.

Given the above objectives, we explored various activated commercially available aldehyde compounds, as well as a number that had been previously synthesized in the

Sessler group. It is expected that the cyanide-based reaction might give such an outcome. Cyanide-related reactions have a time-honored place in organic chemistry. Such reactions include the Stetter, Franchimond, Strecker synthesis, benzil-cyanide reaction as well as the benzoin condensation. Among them, the benzil-cyanide reaction is known to undergo a certain rearrangement shown in Scheme 4.1. Specifically, benzil-cyanide related reactions are believed to proceed through intermediate **C**.[11] Intermediate **C** has long been considered to be unstable under typical benzil-cyanide reaction conditions. In fact, in alcoholic solvents, intermediate **C** undergoes scission to produce benzaldehyde and the alcohol-derived benzoate ester, whereas in DMSO the stilbenediol benzoate diester **4.6** is formed.[12] While this intermediate represents a species whose existence is widely accepted, the corresponding protonated mandelonitrile benzoate product **4.5a** has yet to be isolated as a major product from benzil.[13] In a previous publication, the putative intermediate **4.5a** was isolated in 18% yield, while unreacted benzil was recovered in 60% yield.
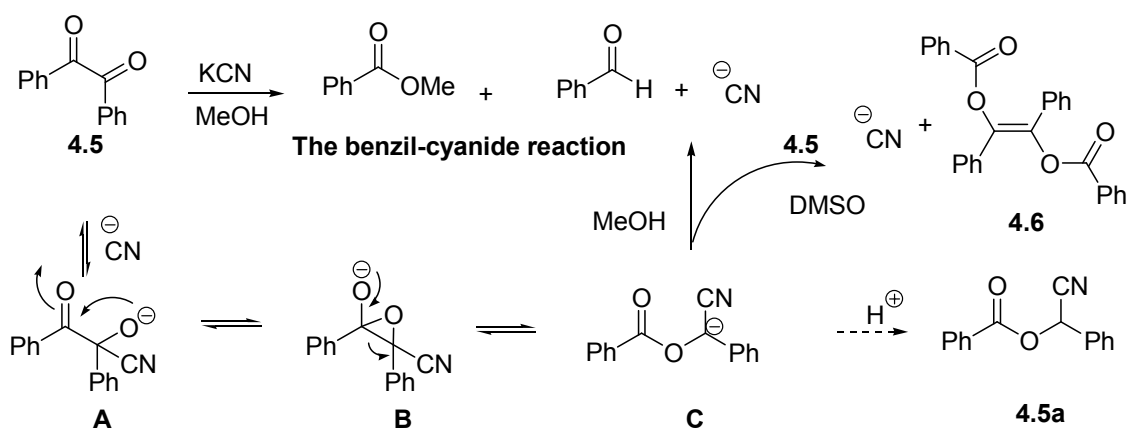
Scheme 4.1 Proposed mechanistic transformations relevant to the benzil-cyanide reaction

106

4.3 THE DEVELOPMENT OF A SELECTIVE CYANIDE ANION INDICATOR

The simple benzil compound **4.5** was first examined as a potential cyanide indicator prototype. Upon the addition of tetrabutylammonium cyanide (TBA·CN), the maximum absorption of benzil **4.5** was blueshifted from 260 nm to 233 nm in UV-vis spectrum (5.09×10^{-5} M in dichloromethane). Surprisingly, the isolated product was neither the corresponding benzoate ester derivatives nor the stilbenediol benzoate **4.6**. Rather, the isolated product proved to be cyanobenzyl benzoate **4.5a**. Encouraged by this result, efforts were made to optimize the reaction. The use of aprotic solvents (i.e., actetonitrile, CHCl₃, and EtOAc), as well as a more organic soluble cyanide source, TBA·CN, allows the protonated form of intermediate **C** to be isolated. Under these optimized condition, cyanobenzyl benzoate **4.5** was isolated in 83% yield.
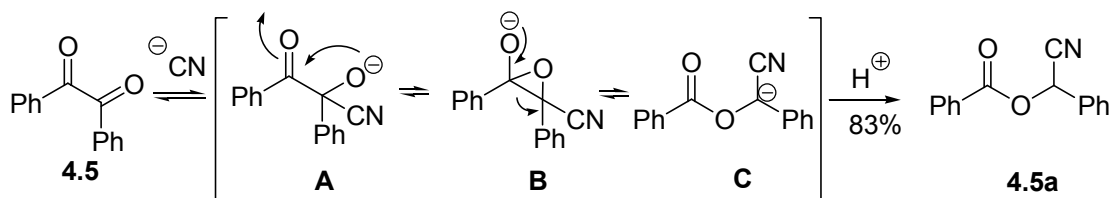
Scheme 4.2 Proposed mechanistic transformations relevant to the benzil rearrangement reaction

An interesting feature of the rearrangement of **4.5** to **4.5a** is that it serves to sever the conjugation pathway between the two aryl carbonyl groups originally present in benzil **4.5**. It is imagined that this rearrangement could be used to produce a specific,

cyanide-mediated color change, provided a suitably colored benzil derivative could be prepared. To test this hypothesis, π-extended systems, benzil analogues, were prepared from dibromobenzil **4.6** From this intermediate, the diphenyl derivative **4.7** was synthesized using a Suzuki reaction as shown in Scheme 4.3. As expected, the attachment of this functionalized phenyl served to extend the λ_{max} (maximum absorption) from 271 nm to 308 nm. However, simple π-extension only induced a 50 nm blueshift relative to benzil **4.5**. Moreover, the π-extended derivative **4.7** proved less soluble than benzil **4.5**.
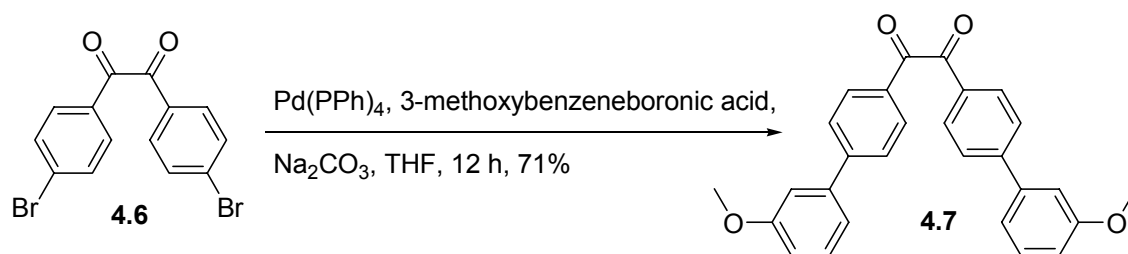
Scheme 4.3 Synthesis of receptor **4.7**
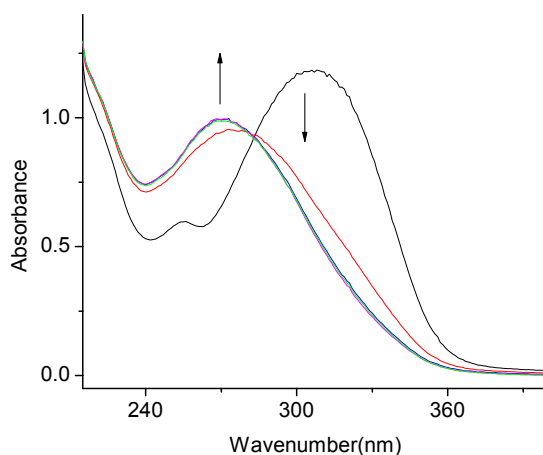
Figure 4.1 Evolution of the UV-vis spectrum of receptor **4.7** (3.20×10^{-5} M in acetonitrle) recorded every 5 minutes upon the addition of tetrabutylammonium cyanide (TBA·CN, 2 equiv.)

To address these issues, an electron pull and push system was envisioned. This is an approach that has been successfully applied to modify the absorption and emission of other compounds.[14] Thus, the electron rich diethylaminobenzene moiety was introduced. Accordingly, receptor **4.10** was prepared via a Sonogashira coupling reaction between dibromobenzil **4.6** and *N,N*-diethyl-4-ethynylbenzenamine **4.9** in 70% yield. *N,N*-diethyl-4-ethynylbenzenamine **4.9** was synthesized using a literature procedure.[15] The Sonogashira coupling reaction afforded the TMS protected acetylene compound **4.8**. Deprotection of the TMS group was effected in 82% yield.
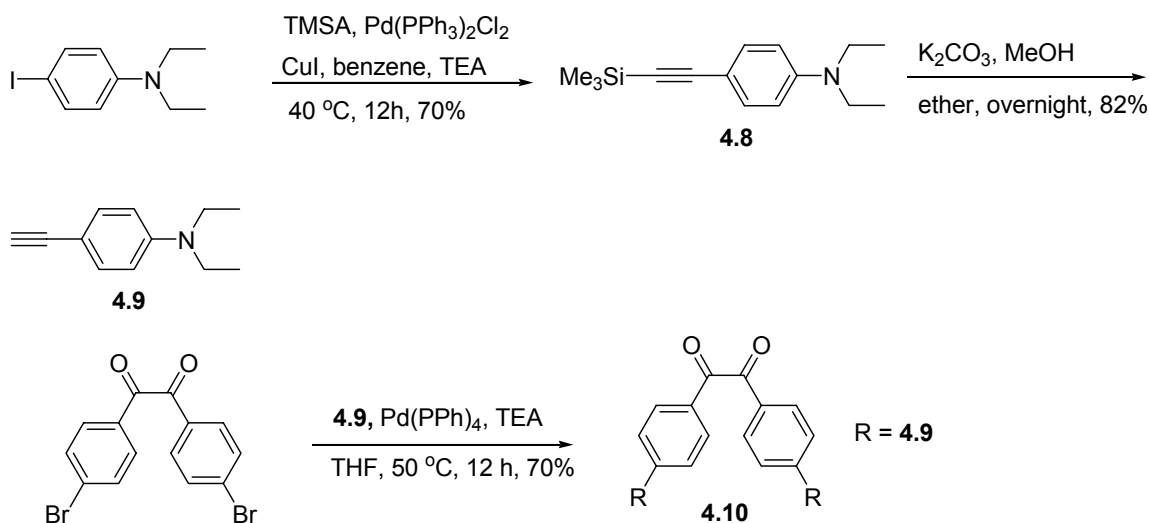
Scheme 4.4 Synthesis of receptor **4.10**

The benzil rearrangement reaction of **4.10** was monitored by UV-vis spectroscopy, as shown in Figure 4.2. In the absence of an added anion, the absorption maximum of **4.10** appears at 412 nm (in ethyl acetate). After the addition of 3 equiv of tetrabutylammonium cyanide, a large bathochromic shift was observed ($\Delta\lambda_{max}$ = 56 nm), with all spectral changes being complete within 1 min (Figure 4.2a). This blue shift is

reflected in a change in the color of the solution from yellow to colorless (Figure 4.2b), allowing for facile qualitative analysis.[16] Compound **4.10a** proved very fluorescent when visualized on a TLC plate. This observation allowed us to study the cyanide-mediated conversion using a laboratory UV lamp (Figure 4.2c), with the limit of detection (LoD) being ca. 20 μM in organic solution in ethyl acetate.

To evaluate the selectivity of receptor **4.10**, 3 equiv. of various potentially competing anions (studied as the corresponding tetrabutylammonium salts), including OH^-, F^- (as the trihydrate), N_3^-, AcO^-, Cl^-, HSO_4^-, and $H_2PO_4^-$, were added to the ethyl acetate solutions of **4.10**. In no case was a change in color observed. This stands in marked contrast to what was seen when 3 equiv. of CN^- were added (cf. Figure 4.3). Compound **4.10** thus appears to be exceptionally selective for cyanide. In particular, it is worth mentioning that great selectivity relative to basic anions is observed. This is something that is not usually seen in the case of hydrogen bonding-based receptors and sensors.

(a)

(b)

(c)
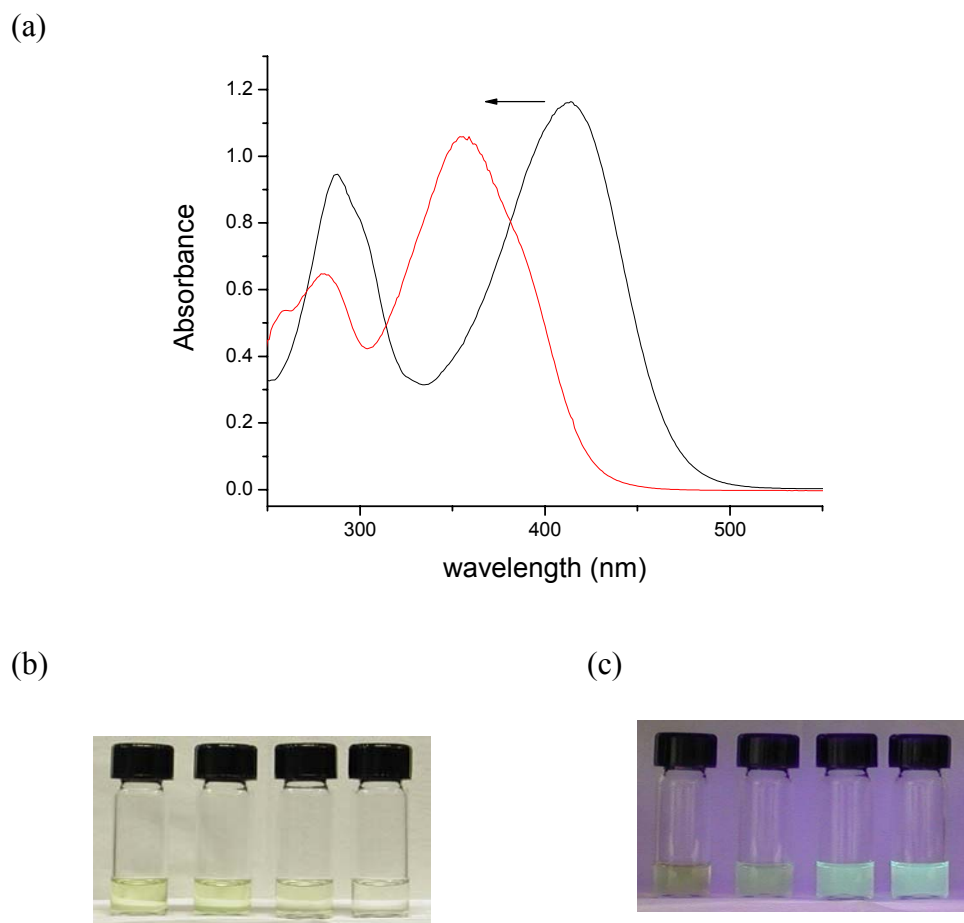
Figure 4.2 (a) UV-vis spectra of receptor **4.10** (2.13 × 10^{-5} M in ethyl acetate) recorded before and 1 minute after the addition of tetrabutylammonium cyanide (TBA·CN, 3 equiv in acetonitrile). (b) Color changes observed upon the addition of varying quantities of TBA·CN (as a 4.65 × 10^{-3} M stock solution in acetonitrile) to solutions of receptor **4.10** (2.13 × 10^{-5} M in ethyl acetate). From left to right: 0, 1, 2, and 3 equiv. (c) Fluorescence changes observed at 365 nm with a laboratory UV lamp upon the addition of varying quantities of TBA·CN (as a 4.65 × 10^{-3} M stock solution in acetonitrile) to solutions of receptor **4.10** (2.13 × 10^{-5} M in ethyl acetate). From left to right: 0, 1, 2, and 3 equiv.

(a)

(b)
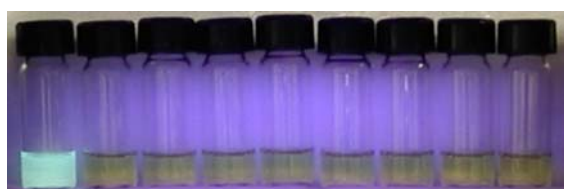
Figure 4.3 (a) Color changes observed upon the addition of various anions (3 equiv in ethyl acetate) to solutions of receptor **4.10** (2.13×10^{-5} M in ethyl acetate). From left to right; CN^-, OH^-, F^-, N_3^-, AcO^-, Cl^-, HSO_4^-, $H_2PO_4^-$, and no added anion. (b) Fluorescence change observed upon excitation at 365 nm with a laboratory UV lamp after the addition of various anions (3 equiv in ethyl acetate) to solutions of receptor **4.10** (2.13×10^{-5} M in ethyl acetate). From left to right; CN^-, OH^-, F^-, N_3^-, AcO^-, Cl^-, HSO_4^-, $H_2PO_4^-$, and no added anion. All anions were used in the form of their respective tetrabutylammonium (TBA) salts. Some of insoluble anions (*viz.* CN^-, OH^-, HSO_4^- and $H_2PO_4^-$) were dissolved in acetonitrile prior to the addition.

To see the reactive pattern of benzil derivatives, different substrates were examined in the context of this study was found that the fused benzil **4.11** afforded a different product. This finding was rationalized in terms of the alkoxide formed being precluded from attacking the adjacent Lumo of the carbonyl group due to the restriction imposed by the ring. Instead, the cyanide anion deprotonates chloroform with the resulting chlorofom anion reacting with one of the carbonyl groups.
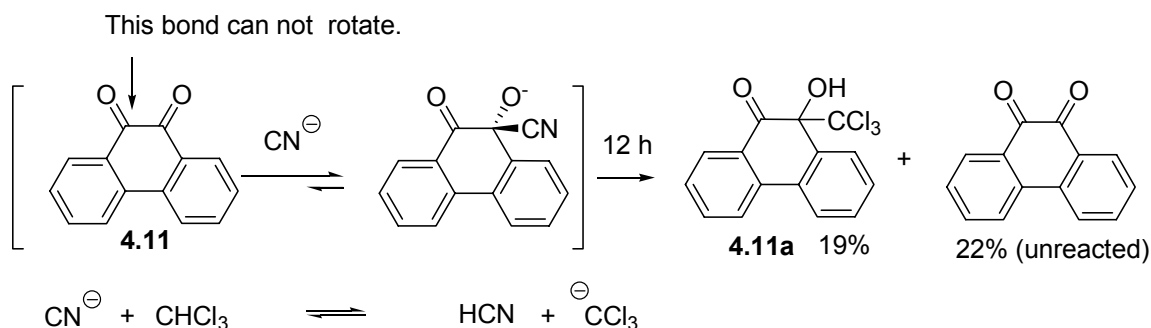
Scheme 4.5 The reactivity pattern of phenanthrene-9,10-dione (**4.11**) observed upon exposure to cyanide anion in CHCl$_3$

The reactions of cyanide anion with the protected diindoldicarbonyl compound **4.12** were also tested. In this case, little reactivity was observed, as confirmed by NMR spectroscopic experiments (Figure 4.5). Specifically, no reaction was seen for 30 min. However, a false positive signal was produce by the unprotected diindolyldiketone **4.13**. In this case, a binding-like isotherm was seen (Figure 4.5.b) that in fact reflected an acid/base equilibrium and NH deprotection. This latter conclusion was fully supported by an X-ray crystal structure of **4.13**·TBA$^+$, for which the crystal was grown from a solution of **4.13** and TBA·CN (Figure 4.5a). The overall reactivity patterns and yield of those reactions are summarized in Table 4.1.
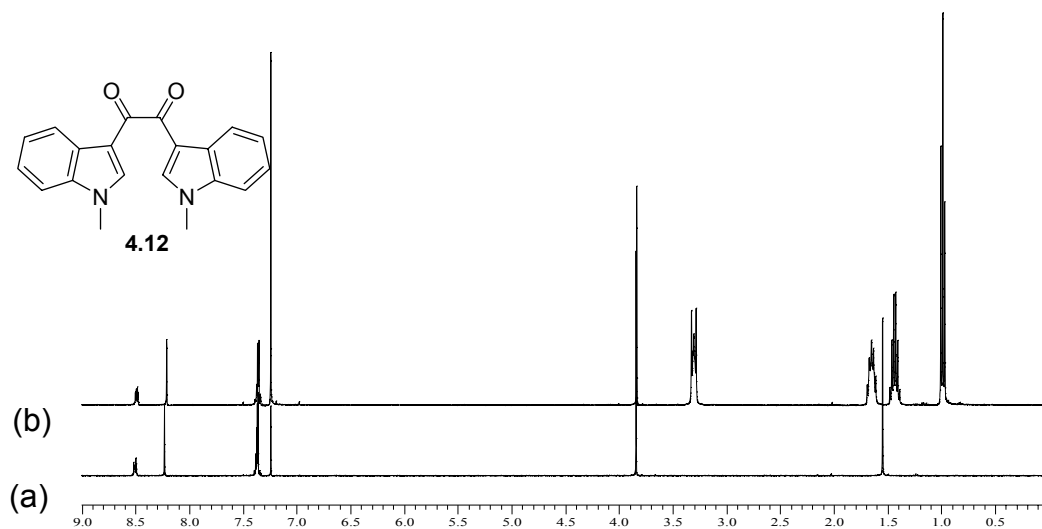
Figure 4.4 The lack of a benzil rearrangement reaction being observed in the case of **4.12** was monitored by ^{1}H NMR spectroscopy in CDCl$_3$.: (a) **4.12** only (b) **4.12** and tetrabutylammonium cyanide (2 eq) after 30 min.
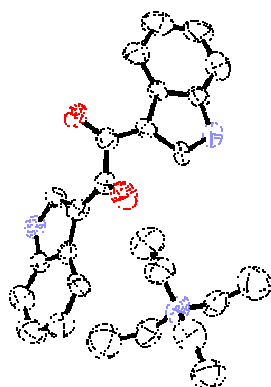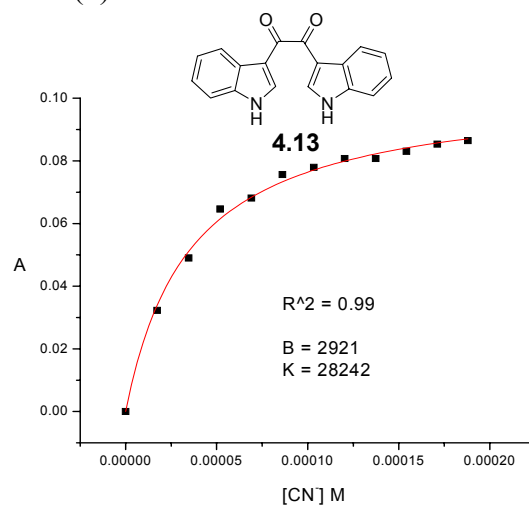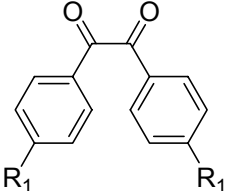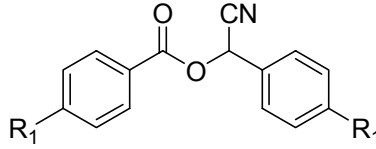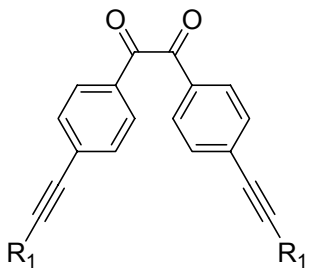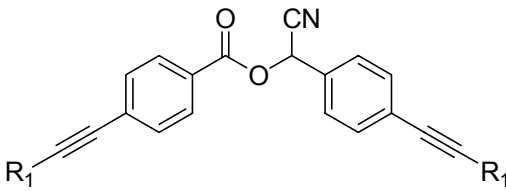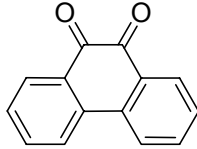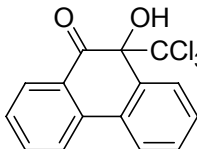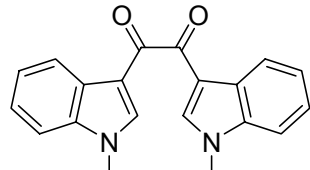
Figure 4.5 (a) X-ray crystal structure of **4.13**[-]·TBA[+] grown from a solution of **4.13** and TBA·CN. Displacement ellipsoids are scaled to the 50% probability level. Hydrogen atoms have been removed for clarity. (b) The titration of **4.13** was carried out by addition of TBA·CN to a solution of **4.13** in CH_2Cl_2 and monitoring the change by UV-vis spectroscopy.

Table 4.1 Products from the Benzil-Rearrangement.[a]

Entry	Substrate	Product	Yield (%)

| 1 | R_1 = H **4.5** | R_1 = H **4.5a** | 83 |
| 2 | R_1 = 3-methoxyphenyl **4.7** | R_1 = 3-methoxyphenyl **4.7a** | 80 |

| 3 | R_1 = 4-diethylaminobenzene **4.10** | R_1 = 4-diethylaminobenzene **4.10a** | 67 |

| 4 | **4.11** | **4.11a** | 19 |

| 5 | **4.12** | No Reaction | |

[a]All reactions were run in chloroform on a 20 mg scale (diketone substrate). Tetrabutylammonium cyanide (1.2 – 2 equiv) was added to a solution of the substrate in question (6 mL dissolved in CHCl$_3$) at 25 ^{o}C. The reaction products, if any, were then determined after 20 min.

116

4.4 CONCLUSION AND FUTURE DIRECTIONS

Compound **4.10** is not a conventional receptor in that it relies on an irreversible benzil rearrangement reaction to signal the presence or absence of cyanide. Because of this, cyanide selectivity of receptor **4.10** is exceptional and the presence of cyanide can be easily detected in organic media, either by eye or via the use of a laboratory UV lamp. Considering the effectiveness of the benzil rearrangement reaction, extension to other applications can be contemplated.

The indicator reactions of **4.10** were conducted in organic solvent. Unfortunately, compound **4.10** is not effectively soluble in MeOH or in water-containing media. The future effort should be focused on preparing water soluble benzil derivatives (**4.13**, **4.14,** and **4.15**) shown in Figure 4.6. These indicators could be useful to explore the benzil-cyanide reaction (Scheme 4.1).
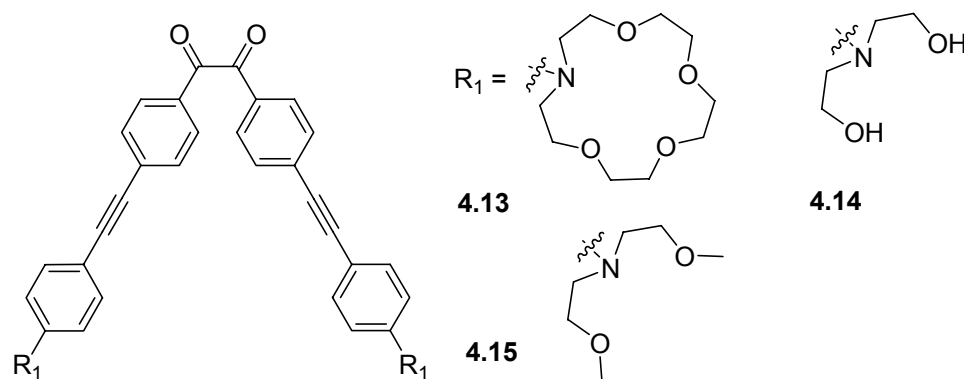
Figure 4.6 Proposed water soluble indicators

4.5 REFERENCES

(1)   Young, C.; Tidwell, L.; Anderson, C. *Cyanide: Social, Industrial, and Economic Aspects*; Minerals, Metals, and Materials Society: Warrendale, **2001**.

(2)   Bhattacharya, P. K. *Metal Ions in Biochemistry*; Alpha Science International Ltd.: Harrow, U.K., **2005**.

(3)   Koenig, R. *Science*. **2000**, *287*, 1737-1738.

(4)   (a) Kim, Y.-H.; Hong, J.-I. *Chem. Commun*. **2002**, 512-513. (b) Ros-Lis, J. V.; Martínez-Máñez, R.; Soto, J. *Chem. Commun*. **2002**, 2248-2249. (c) García, F.; García, J. M.; García-Acosta, B.; Martínez-Máñez, R.; Sancenón, F.; Soto, J. *Chem. Commun*. **2005**, 2790-2792. (d). Badugu, R.; Lakowicz, J. R.; Geddes, C. D. *J. Am. Chem. Soc*. **2005**, *127*, 3635-3641.

(5)   The basicity of the anions in question (including cyanide) could be contributing to the observed sensing and competition effects. See: (a) Anzenbacher, P., Jr.; Tyson, D. S.; Jursíková, K.; Castellano, F. N. *J. Am. Chem. Soc*. **2002**, *124*, 6232-6233. (b) Chung, Y. M.; Raman, B.; Kim, D.-S.; Ahn, K. H. *Chem. Commun*. **2006**, 186-188.

(6)   (a) Tomasulo, M.; Raymo, F. M. *Org. Lett*. **2005**, *7*, 4633-4636. (b) Tomasulo, M.; Sortino, S.; White, A. J. P.; Raymo, F. M. *J. Org. Chem*. **2006**, *71*, 744-753.

(7)   Yang, Y.-K.; Tae, J. *Org. Lett*. 2006, *8*; 5721-5723.

(8)   Chen, C.-L.; Chen, Y.-H.; Chen, C.-Y.; Sun, S.-S. *Org. Lett*. **2006**, *8,* 5053-5056.

(9)   Hudnall, T. W.; Gabbai, F. P. *J. Am. Chem. Soc*. **2007**, *129*, 11978-11986.

(10)   Miyaji, H.; Sessler, J. L. *Angew. Chem., Int. Ed*. **2001**, *40*, 154-157.

(11)   (a) Kwart, H.; Baewky, M. *J. Am. Chem. Soc.* **1958**, *80*, 580-588. (b) Kuebrich, A. W.; Schowen, R. L. *J. Am. Chem. Soc.* **1971**, *93*, 1220-1223. (c) Bwgstahler, A. W.; Walker, D. E., Jr.; Kuebrich, J. P.; Schowen, R. L. *J. Org. Chem.* **1972**, *37*, 1272-1273. (d) Okimoto, M.; Itoh, T.; Chiba, T. *J. Org. Chem.* **1996**, *61*, 4835-4837.

(12)   Trisler, J. C.; Frye, J. L. *J. Org. Chem.* **1965**, *30*, 306-307.

(13)   Clerici, A.; Porta, O. *J. Org. Chem.* **1994**, *59*, 1591-1592.

(14)   Yamaguchi, Y.; Ochi, T.; Wakamiya, T.; Matsubara, Y.; Yoshida, Z.-I. *Org. Lett.,* **2006**, *8*, 717 -720.

(15)   *N,N*-Dimethyl-4-ethynylbenzenamine is commercially available. *N,N*-Diethyl-4-ethynylbenzenamine was synthesized according to literature procedure: Miki Y.; Momotake, A.; Arai, T. *Org. Biomol. Chem.* **2003**, *1*, 2655-2660.

(16)   (a) Miyaji, H.; Sato, W.; Sessler, J. L. *Angew. Chem., Int. Ed.* **2000**, *39*, 1777-1780. (b) Anzenbacher, P., Jr.; Jursikova, K.; Sessler, J. L. *J. Am. Chem. Soc.* **2000**, *122*, 9350-9351. (c) Sessler, J. L.; Cho, D.-G.; Lynch, V. *J. Am. Chem. Soc.* **2006**, *128*, 16518-16519.

4.6 EXPERIMENTAL SECTION

Proton and ^{13}C-NMR spectra were measured at 25 ºC using Varian Unity Innova instruments (400 or 500 MHz). UV-vis spectra were recorded on a Beckman DU 640B spectrophotometer. High resolution CI mass spectra were obtained on a VG ZAB2-E mass spectrometer. HPLC analyses were done using a LC-6AD Shimadzu system equipped with a SPD-M20A detector and an Eclipse XDB-C18 column.

4.6.1 SYNTHETIC EXPERIMENTAL

Bis(4-(3-methoxyphenyl)phenyl)ethanedione (4.7) Dibromobenzil **4.6** (300 mg, 8.15×10^{-4} mol) and 3-methoxybenzeneboronic acid (272 mg, 1.79×10^{-3} mol) were added to one another in a 100 mL round bottom flask under argon. To the mixture, benzene (32 mL), ethanol (8 mL), water (16 mL), and Na_2CO_3 (0.345 g, 3.26×10^{-3} mol) were added. After N_2 gas was bubbled for 10 min, tetrakis(triphenylphosphine)palladium(0) (56 mg, 4.89×10^{-4} mol, 6 mol%) was added and the resulting mixture was stirred at 80 °C under an argon atmosphere overnight. At this point, the reaction mixture was poured into water and extracted with dichloromethane. The organic layer was washed with brine, dried over anhydrous sodium sulfate, and evaporated to dryness under reduced pressure. The residue obtained was purified by column chromatography over silica gel (ethyl acetate : hexane = 1:4, eluent) to afford **4.7** (244 mg, 71%) as a yellow solid. ^{1}H-NMR (400 MHz, CDCl$_3$) [ppm]: 3.87 (s, 6H), 6.95 (m, 2H), 7.15 (s, 2H), 7.21 (d, J = 8.0 Hz, 2H), 7.39 (dd, J = 8.0, 8.0 Hz, 2H), 7.23 (d, J = 8 Hz, 2H), 8.06 (d, J = 8 Hz, 2H); ^{13}C-NMR (100 MHz, CDCl$_3$) [ppm]: 55.36, 113.14, 113.90, 119.81, 127.72, 130.07, 130.49, 131.81, 140.97, 147.47, 160.05, 194.09. HRMS (CI): m/z 423.1593 ((M+H), calcd for $C_{28}H_{23}O_4$ 423.1596.

Cyano(4-(3-methoxyphenyl)phenyl)methyl 4-(3-methoxyphenyl)benzoate (4.7a)
Diketone **4.7** (20 mg, 4.73×10^{-5} mol) was added to a 25 mL round bottom flask and dissolved in 6 mL of $CHCl_3$. Tetrabutylammonium cyanide (25 mg, 9.46×10^{-5} mol dissolved in 1 mL $CHCl_3$) was added and the reaction mixture was stirred for 20 min at room temperature. The resulting solution was evaporated to dryness under reduced pressure. The residue obtained in this way was directly purified by column chromatography over silica gel (ethyl acetate : hexane = 1:4, eluent) to afford **4.7a** (17 mg, 80%). ^{1}H-NMR (400 MHz, $CDCl_3$) [ppm]: 3.87 (s, 6H), 6.74 (s, 1H), 6.95 (m, 2H), 7.13 (m, 2H), 7.19 (m, 2H), 7.39 (ddd, J = 8.0, 8.0, 2.4 Hz, 1H), 7.68 (m, 6H), 8.14 (d, J = 8.8 Hz, 2H); ^{13}C-NMR (100 MHz, $CDCl_3$) [ppm]: 55.61, 63.41, 113.28, 113.37, 113.53, 113.95, 116.45, 119.93, 120.01, 127.11, 127.62, 128.30, 128.62, 130.23, 130.29, 130.87, 131.11, 141.33, 141.63, 143.59, 146.99, 160.26, 160.29, 164.77. HRMS (CI): m/z 450.1704 (M+H), calcd for $C_{29}H_{24}NO_4$ 450.1705.

Bis(4-((4-(diethylamino)phenyl)ethynyl)phenyl)ethanedione (4.10) A mixture of dibromobenzil **4.6** (100 mg, 2.70×10^{-4} mol), *N,N*-diethyl-4-ethynylbenzenamine **4.9** (94 mg, 5.40×10^{-4} mol), tetrakis(triphenylphosphine)palladium(0) (18 mg, 8.10×10^{-6} mol), CuI (6 mg, 1.62×10^{-5} mol), TEA (3 mL) and THF (40 mL) was degassed by bubbling N_2 for 10 min. The solution was stirred at 50 °C under an argon atmosphere overnight. The resulting mixture was evaporated to dryness and redissolved in ethyl acetate and washed with water. The organic layer was separated off, dried over anhydrous sodium sulfate, and evaporated to dryness under reduced pressure. The residue obtained in this way was purified by column chromatography over silica gel (ethyl acetate : hexane = 1:4, eluent) to afford **4.10** (104 mg, 70%) as a red solid. ^{1}H-NMR (400 MHz, $CDCl_3$) [ppm]:

1.18 (t, J = 7.2 Hz, 12H), 3.37 (q, J = 7.2 Hz, 4H), 6.61 (d, J = 4.0 Hz, 4H), 7.39 (d, J = 4.0 Hz, 4H), 7.57 (d, J = 8.4 Hz, 4H), 7.92 (d, J = 8.4 Hz, 4H). ^{13}C-NMR (100 MHz, CDCl$_3$) [ppm]: 12.53, 44.35, 87.11, 96.71, 107.21, 111.06, 129.81, 130.98, 131.38, 131.44, 133.40, 148.08, 193.57. HRMS (CI): m/z 553.2853 (M+H), calcd for C$_{38}$H$_{37}$N$_2$O$_2$ 553.2855.

Cyano(4-((4-(diethylamino)phenyl)ethynyl)phenyl)methyl   4-((4-(diethylamino) phenyl)ethynyl)benzoate (4.10a) Diketone **4.10** (20 mg, 3.61 × 10^{-5} mol) was added to a 25 mL round bottom flask and dissolved in 6 mL of CHCl$_3$. Tetrabutylammonium cyanide (11.6 mg, 4.32 × 10^{-5} mol dissolved in 1 mL CHCl$_3$) was added and the resulting mixture was stirred at room temperature for 20 min. The resulting solution was evaporated to dryness under reduced pressure. The residue obtained in this way was directly purified by column chromatography over silica gel (ethyl acetate : hexane = 1:4, eluent) to afford **4.10a** (14 mg, 67%). ^{1}H-NMR(400 MHz, CDCl$_3$) [ppm]: 1.18 (t, J = 6.8 Hz, 12H), 3.38 (q, J = 6.8 Hz, 8H), 6.62 (d, J = 4.8 Hz, 4H), 6.65 (s, 1H), 7.38 (d, J = 4.8 Hz, 4H), 7.56 (m, 6H), 8.00 (d, J = 4.8 Hz, 2H). ^{13}C-NMR (100 MHz, CDCl$_3$) [ppm]: 12.53, 44.33, 63.10, 86.20, 86.75, 93.17, 95.66, 107.78, 108.10, 111.09, 111.12, 116.02, 126.02, 126.87, 127.83, 129.95, 130.57, 131.12, 131.85, 133.12, 133.30, 147.79, 147.99, 164.26. HRMS (CI): m/z 580.2969 (M+H), calcd for C$_{39}$H$_{38}$N$_3$O$_2$ 580.2964. Anal. Calcd for C$_{39}$H$_{37}$N$_3$O$_2$: C, 80.80; H, 6.43; N, 7.25; Found C, 80.60; H; 6.39; N, 7.26.

Sample Information

Acquired by   : Admin
Sample Name   : dgc3
Sample ID   : dgc3
Tray#   : 1
Vail#   : 44
Injection Volume   : 20 uL
Data Filename   : dgc308.lcd
Method Filename   : ACN 20 pct 1 ml min Base Method no frc 081107.lcm
Batch Filename   :
Report Filename   : Default.lcr
Date Acquired   : 10/6/2007 4:03:19 PM
Data Processed   : 10/6/2007 4:28:21 PM

Chromatogram
dgc3 C:\Documents and Settings\User\Desktop\Group Files\DongGyu\dgc308.lcd
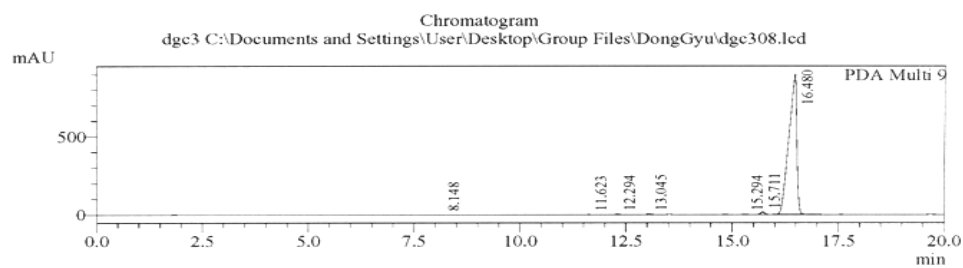
1 PDA Multi 9 / 380nm 4nm

PeakTable

PDA Ch9 380nm 4nm

Peak#	Ret. Time	Area	Area %
1	8.148	9734	0.082
2	11.623	6384	0.054
3	12.294	23449	0.198
4	13.045	32495	0.274
5	15.294	17886	0.151
6	15.711	101298	0.854
7	16.480	11663956	98.387
Total		11855201	100.000

Method

<<Comment>>
<<LC Program>>

Time	Unit	Command	Value
2.00	Pumps	B.Conc	20
5.00	Pumps	B.Conc	70
7.00	Pumps	B.Conc	70
10.00	Pumps	B.Conc	90
17.99	Pumps	B.Conc	99
18.00	Pumps	B.Conc	10
25.00	Controller	Stop	

Figure 4.7 HPLC analysis of **4.10** using an eluent (0.1 % TFA in water and acetinitrile)

123

Sample Information

Acquired by   : Admin
Sample Name   : dgc3a
Sample ID   : dgc3a
Tray#   : 1
Vail#   : 42
Injection Volume   : 20 uL
Data Filename   : dgc3a2.lcd
Method Filename   : ACN 20 pct 1 ml min Base Method no frc 081107.lcm
Batch Filename   :
Report Filename   : Default.lcr
Date Acquired   : 10/6/2007 3:29:52 PM
Data Processed   : 10/6/2007 3:54:54 PM

Chromatogram
dgc3a C:\Documents and Settings\User\Desktop\Group Files\DongGyu\dgc3a2.lcd

1   PDA Multi 9 / 380nm 4nm

PeakTable

PDA Ch9 380nm 4nm

Peak#	Ret. Time	Area	Area %
1	12.863	3491	0.077
2	13.359	4381905	97.219
3	13.823	6145	0.136
4	14.208	7101	0.158
5	16.078	17344	0.385
6	16.544	91245	2.024
Total		4507230	100.000

Method

<<Comment>>
<<LC Program>>

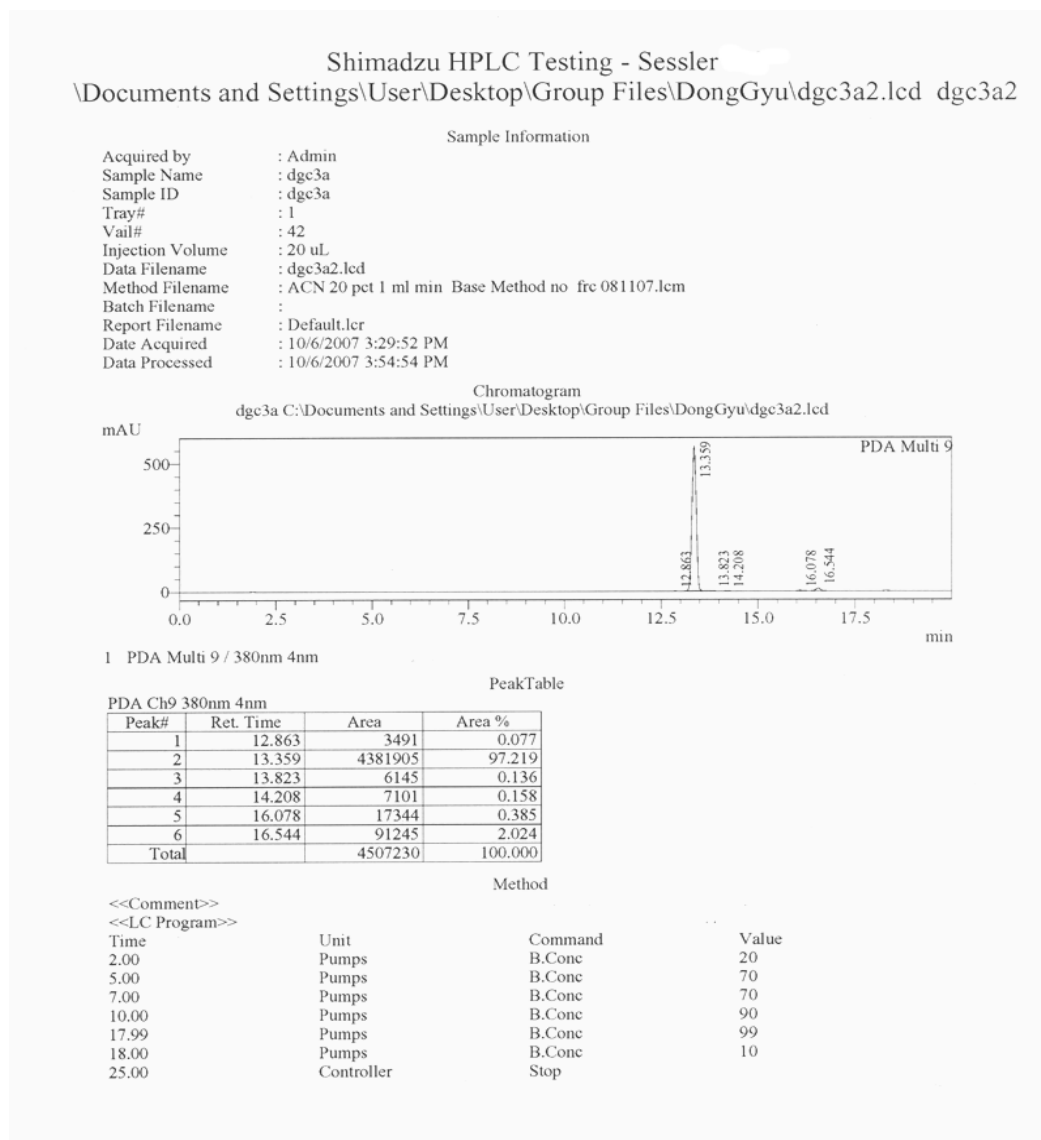| Time	Unit	Command	Value
2.00	Pumps	B.Conc	20
5.00	Pumps	B.Conc	70
7.00	Pumps	B.Conc	70
10.00	Pumps	B.Conc	90
17.99	Pumps	B.Conc	99
18.00	Pumps	B.Conc	10
25.00	Controller	Stop	

Figure 4.8 HPLC analysis of **4.10a** using an eluent (0.1 % TFA in water and acetinitrile)

Appendix: X-ray Experimental and Crystallographic Data

All crystals for X-ray crystallographic analyses described in this appendix were grown by the author. All their X-ray diffraction structures were solved Dr. Vince Lynch of the X-ray Diffraction Laboratory, Department of Chemistry and Biochemistry, University of Texas at Austin. This Appendix describes the experimental method used by Dr. Lynch in obtaining each of these structures, along with relevant data tables for each structure now follows.

X-ray Experimental for $[C_{49}H_{54}N_5O_5S_2]^{1+}$ Cl^{1-} - ½ C_5H_{12}, **1.15:** Crystals grew as black prisms by slow evaporation from heptane and CH_2Cl_2. The data crystal was prism that had approximate dimensions; 0.31 x 0.22 x 0.18 mm. The data were collected on a Nonius Kappa CCD diffractometer using a graphite monochromator with MoKα radiation (λ = 0.71073Å). A total of 648 frames of data were collected using ω-scans with a scan range of 0.7° and a counting time of 115 seconds per frame. The data were collected at 153 K using an Oxford Cryostream low temperature device. Details of crystal data, data collection and structure refinement are listed in Table A1. Data reduction were performed using DENZO-SMN.[1] The structure was solved by direct methods using SIR97[2] and refined by full-matrix least-squares on F^2 with anisotropic displacement parameters for the non-H atoms using SHELXL-97.[3] The hydrogen atoms were calculated in ideal positions with isotropic displacement parameters set to 1.2xUeq of the attached atom (1.5xUeq for methyl hydrogen atoms).

One of the phenyl rings on a tosylate group was disordered by rotation about the S-C bond. The disorder was modeled by idealizing the geometry of the two groups and assigning the variable x to the site occupancy factor of one orientation and (1-x) to the site occupancy factor of the second orientation of the ring. Additionally, a common

isotropic displacement parameter was refined for these atoms. The site occupancy refined to 60(2)% for the major component consisting of atoms, C43, C44, C45, C46, C47, C48 and C49. In subsequent refinement, the geometry of these groups was restrained to be equal. The carbon atoms of both groups were refined anisotropically while restraining their displacement parameters to be approximately isotropic.

A solvent molecule was found to be disordered near a crystallographic inversion center at 0,0,0. The solvent could not be adequately modeled. Therefore, the contribution to the scattering by this disordered molecule was removed by the use of the utility SQUEEZE in Platon98.[4] Platon98 was used as incorporated in WinGX.[5]

The function, $\Sigma w(|F_o|^2 - |F_c|^2)^2$, was minimized, where $w = 1/[(\sigma(F_o))^2 + (0.064*P)^2]$ and $P = (|F_o|^2 + 2|F_c|^2)/3$. $R_W(F^2)$ refined to 0.177, with R(F) equal to 0.0783 and a goodness of fit, S, = 1.19. Definitions used for calculating R(F), $R_W(F^2)$ and the goodness of fit, S, are given below.[6] The data were checked for secondary extinction effects but no correction was necessary. Neutral atom scattering factors and values used to calculate the linear absorption coefficient are from the International Tables for X-ray Crystallography (1992).[7] All figures were generated using SHELXTL/PC.[8]

Experimental References

1)   DENZO-SMN. (1997). Z. Otwinowski and W. Minor, Methods in Enzymology, **276**: Macromolecular Crystallography, part A, 307 – 326, C. W. Carter, Jr. and R. M. Sweets, Editors, Academic Press.

2)   SIR97. (1999). A program for crystal structure solution. Altomare, A., Burla, M. C., Camalli, M., Cascarano, G. L., Giacovazzo, C., Guagliardi, A., Moliterni, A. G. G., Polidori, G. and Spagna, R. J. Appl. Cryst. 32, 115-119.

3)   Sheldrick, G. M. (1994). SHELXL97. Program for the Refinement of Crystal Structures. University of Gottingen, Germany.

4)   Spek, A. L. (1998). PLATON, A Multipurpose Crystallographic Tool. Utrecht University, The Netherlands.

5)   WinGX 1.64. (1999). An Integrated System of Windows Programs for the Solution, Refinement and Analysis of Single Crystal X-ray Diffraction Data.   Farrugia, L. J.   J. Appl. Cryst. 32. 837-838.

6) $R_w(F^2) = \{\Sigma w(|F_o|^2 - |F_c|^2)^2/\Sigma w(|F_o|)^4\}^{1/2}$ where w is the weight given each reflection.
        $R(F) = \Sigma(|F_o| - |F_c|)/\Sigma|F_o|\}$ for reflections with $F_o > 4(\sigma(F_o))$.
        $S = [\Sigma w(|F_o|^2 - |F_c|^2)^2/(n - p)]^{1/2}$, where n is the number of reflections and p is the number of refined parameters.

7)   International Tables for X-ray Crystallography (1992). Vol. C, Tables 4.2.6.8 and 6.1.1.4, A. J. C. Wilson, editor, Boston: Kluwer Academic Press.

8)   Sheldrick, G. M. (1994). SHELXTL/PC (Version 5.03). Siemens Analytical X-ray Instruments, Inc., Madison, Wisconsin, USA.

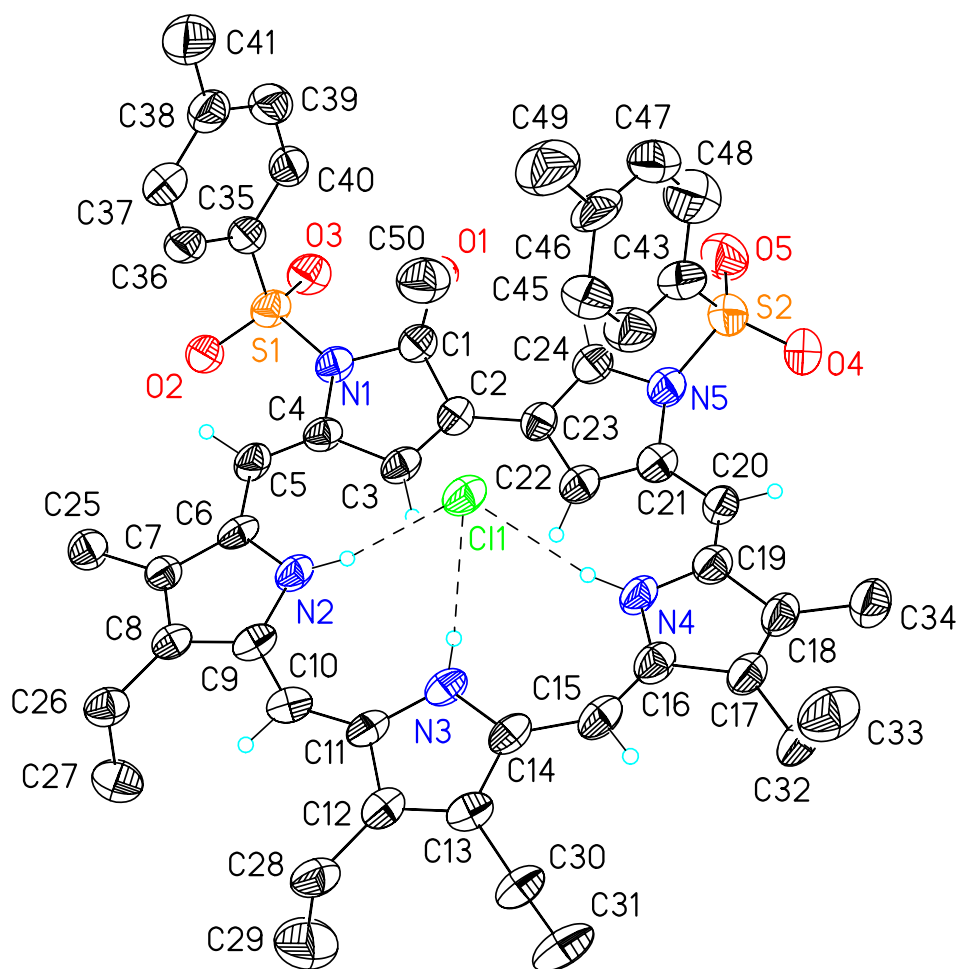**Figure A1** View of **1.15** showing the atom labeling scheme. Displacement ellipsoids are scaled to the 50% probability level. Most hydrogen atoms have been removed for clarity. The lower occupancy methyl phenyl group bound to S2 has been removed for clarity. Dashed lines are indicative of H-bonding interactions.
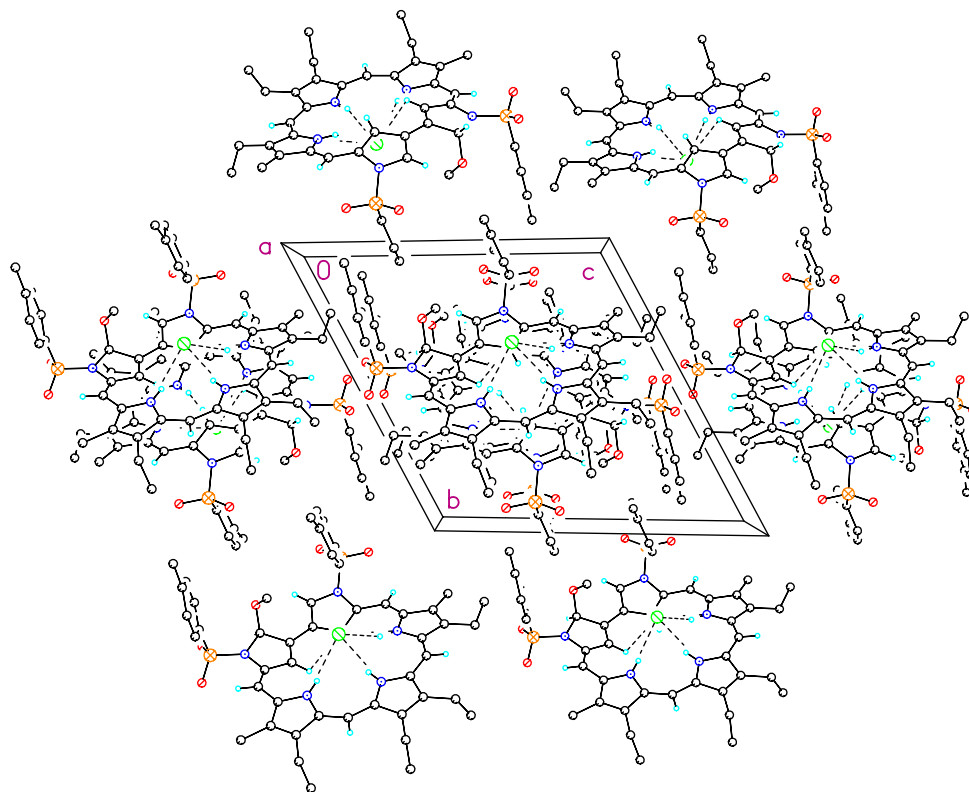
Figure A2 Unit cell packing diagram for **1.15**. The view is approximately down the **a** axis.

Table A1 Crystal data and structure refinement for **1.15**

Identification code	dg1
Empirical formula	C48 H54 Cl N5 O5 S2 – ½ C5 H12
Formula weight	928.61
Temperature	153(2) K
Wavelength	0.71073 Å
Crystal system	Triclinic
Space group	P-1
Unit cell dimensions	a = 11.6570(7) Å α = 62.647(3)°.
	b = 15.466(1) Å β = 76.458(3)°.
	c = 15.860(1) Å γ = 89.571(3)°.
Volume	2452.4(3) Å^3
Z	2
Density (calculated)	1.258 Mg/m^3
Absorption coefficient	0.215 mm^{-1}
F(000)	986
Crystal size	0.31 x 0.22 x 0.18 mm
Theta range for data collection	2.99 to 25.00°.
Index ranges	-13<=h<=13, -18<=k<=16, -18<=l<=16
Reflections collected	14293
Independent reflections	8440 [R(int) = 0.0583]
Completeness to theta = 25.00°	97.7 %
Absorption correction	None
Refinement method	Full-matrix least-squares on F^2
Data / restraints / parameters	8440 / 193 / 622
Goodness-of-fit on F^2	1.151
Final R indices [I>2sigma(I)]	R1 = 0.0783, wR2 = 0.1572
R indices (all data)	R1 = 0.1719, wR2 = 0.1770
Largest diff. peak and hole	0.341 and -0.284 e.Å^{-3}

X-ray Experimental for $(C_{38}H_{41}N_3O_2)^{2+}$ $2(C_7H_7SO_3)^{1-}$ $(C_7H_8SO_3)$ - H_2O – $CHCl_3$ - CH_2Cl_2, **1.25**: Crystals grew as very dark blue plates by slow vapor diffusion of hexane in a solution of $CHCl_3$, CH_2Cl_2, MeOH, *p*-TsOH. The data crystal was plate that had approximate dimensions; 0.22 x 0.18 x 0.06 mm. The data were collected on a Nonius Kappa CCD diffractometer using a graphite monochromator with MoKα radiation (λ = 0.71073Å). A total of 282 frames of data were collected using ω-scans with a scan range of 2° and a counting time of 266 seconds per frame. The data were collected at 153 K using an Oxford Cryostream low temperature device. Details of crystal data, data collection and structure refinement are listed in Table A2.
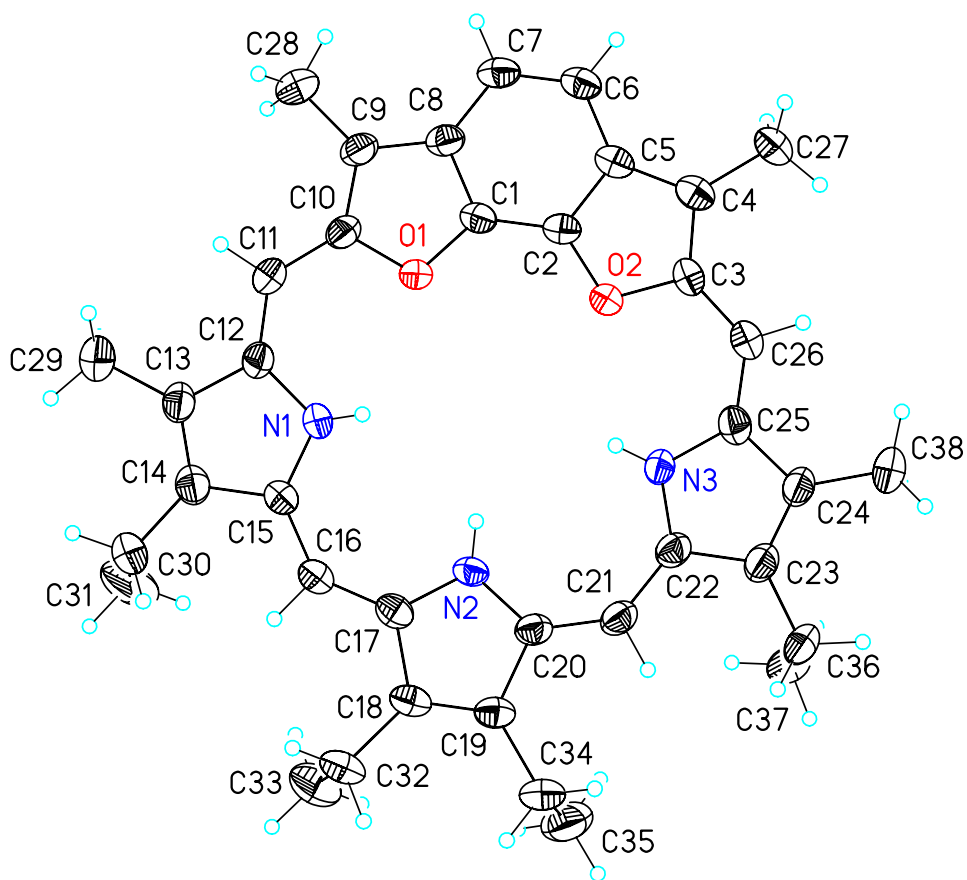
Figure A3 View of the macrocycle in **1.25** showing the atom labeling scheme. Displacement ellipsoids are scaled to the 50% probability level.
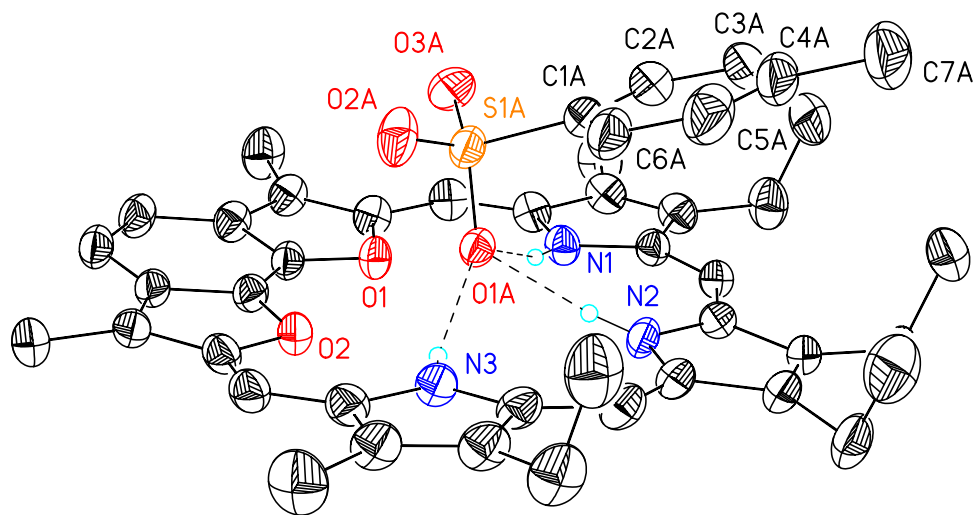
Figure A4 View illustrating the H-bonding interaction between one tosylate ion and the macrocycle in **1.25**. Displacement ellipsoids are scaled to the 50% probability level. Most hydrogen atoms have been removed for clarity. Dashed lines are indicative of H-bonding interactions
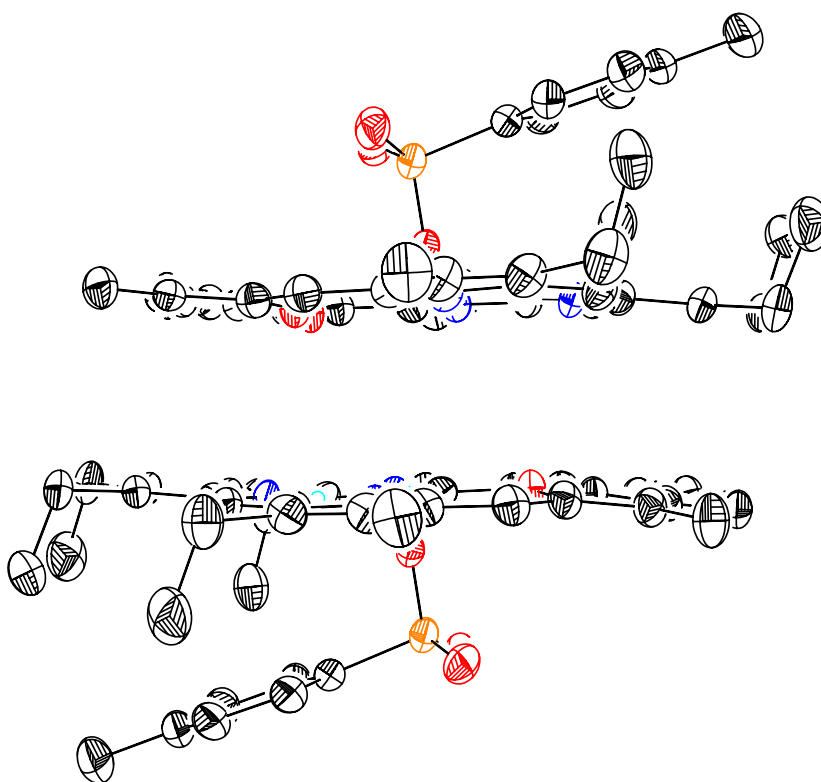
Figure A5 View illustrating the close packing interaction between adjacent macrocycles in **1.25**. Displacement ellipsoids are scaled to the 50% probability level. The two macrocycles are related by a crystallographic inversion center at ½, ½, ½. Plane to plane separation is 3.412Å.
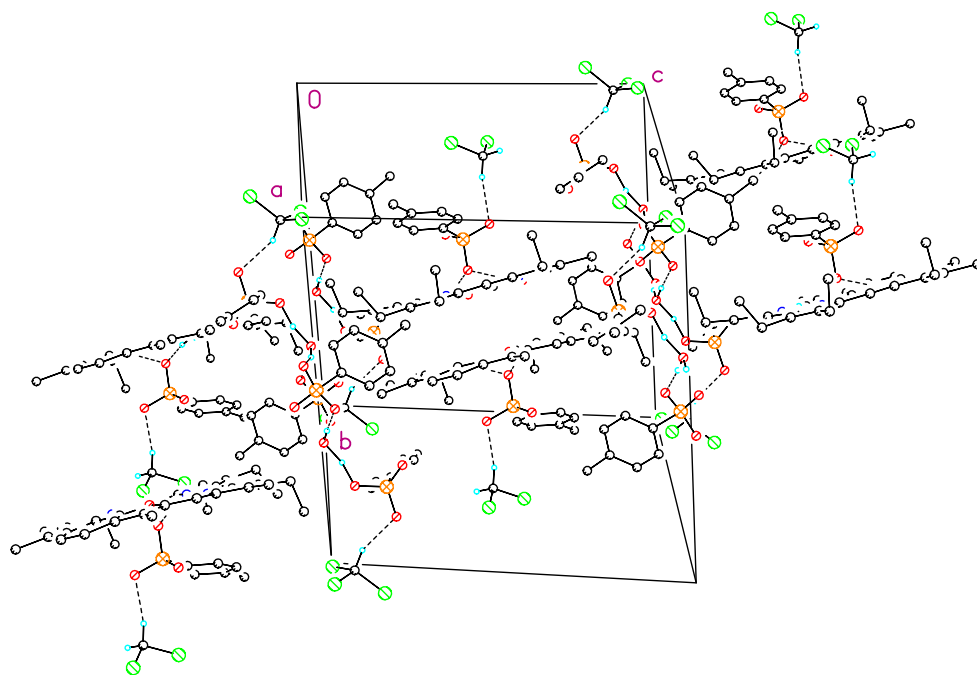
Figure A6 Unit cell packing diagram for **1.25**

Table A2 Crystal data and structure refinement for **1.25**

Empirical formula	C61 H68 Cl5 N3 O12 S3
Formula weight	1308.61
Temperature	153(2) K
Wavelength	0.71073 Å
Crystal system	Triclinic
Space group	P-1

Unit cell dimensions	a = 12.1159(2) Å	$\alpha = 89.461(1)°$.
	b = 16.7643(3) Å	$\beta = 72.917(1)°$.
	c = 17.1620(4) Å	$\gamma = 71.945(1)°$.

Volume	3155.18(11) $Å^3$
Z	2
Density (calculated)	1.377 Mg/m^3
Absorption coefficient	0.392 mm^{-1}
F(000)	1368
Crystal size	0.22 x 0.18 x 0.06 mm
Theta range for data collection	1.87 to 27.40°.
Index ranges	-15<=h<=15, -21<=k<=19, -22<=l<=20
Reflections collected	23069
Independent reflections	14287 [R(int) = 0.0473]
Completeness to theta = 27.40°	99.5 %
Absorption correction	None
Refinement method	Full-matrix least-squares on F^2
Data / restraints / parameters	14287 / 0 / 781
Goodness-of-fit on F^2	1.034
Final R indices [I>2sigma(I)]	R1 = 0.0773, wR2 = 0.1503
R indices (all data)	R1 = 0.1761, wR2 = 0.1890
Largest diff. peak and hole	0.639 and -0.676 e.$Å^{-3}$

X-ray Experimental for [($C_{28}H_{44}N_4O_4$)($C_{28}H_{44}N$)$^{1+}$(H_2PO_4)$^{1-}$], **2.6**: Crystals grew as red laths by slow vapor diffusion of hexane in a solution of EtOAc. The data crystal was cut from a long lath and had approximate dimensions; 0.33 x 0.09 x 0.04 mm. The data were collected on a Nonius Kappa CCD diffractometer using a graphite monochromator with MoKα radiation (λ = 0.71073Å). A total of 311 frames of data were collected using ω-scans with a scan range of 1° and a counting time of 244 seconds per frame. The data were collected at 153 K using an Oxford Cryostream low temperature device. Details of crystal data, data collection and structure refinement are listed in Table A3.
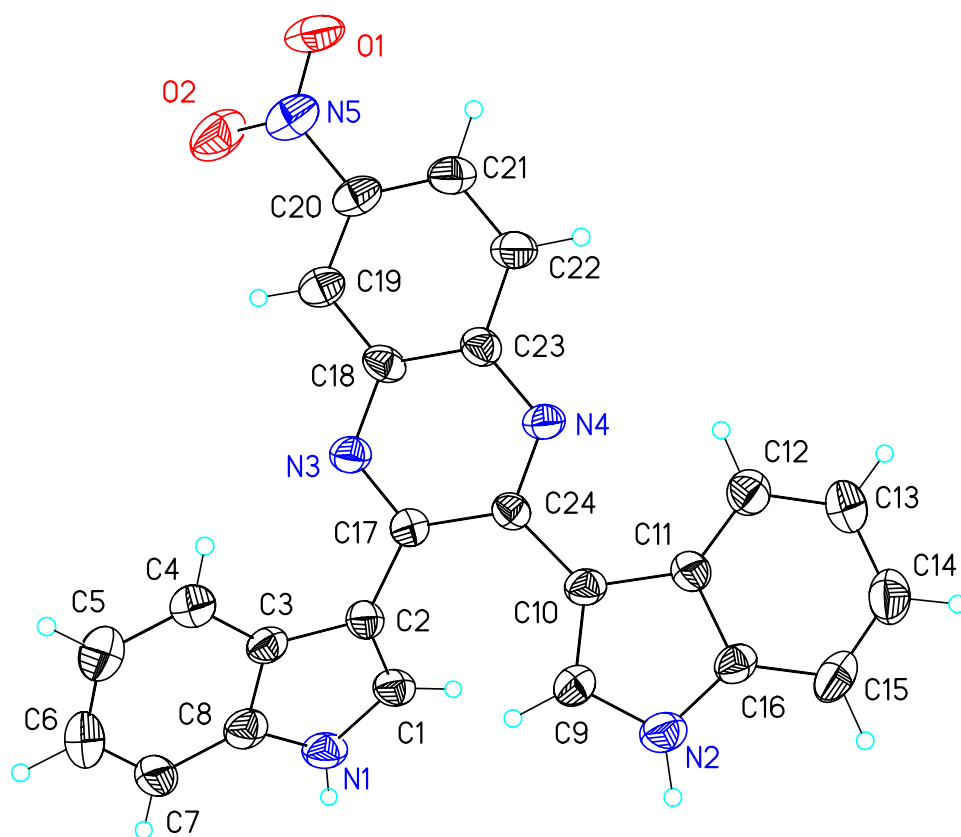
Figure A7 View of one of the bis-indole moieties found in **2.6** showing the atom labeling scheme.   Displacement ellipsoids are scaled to the 50% probability level.
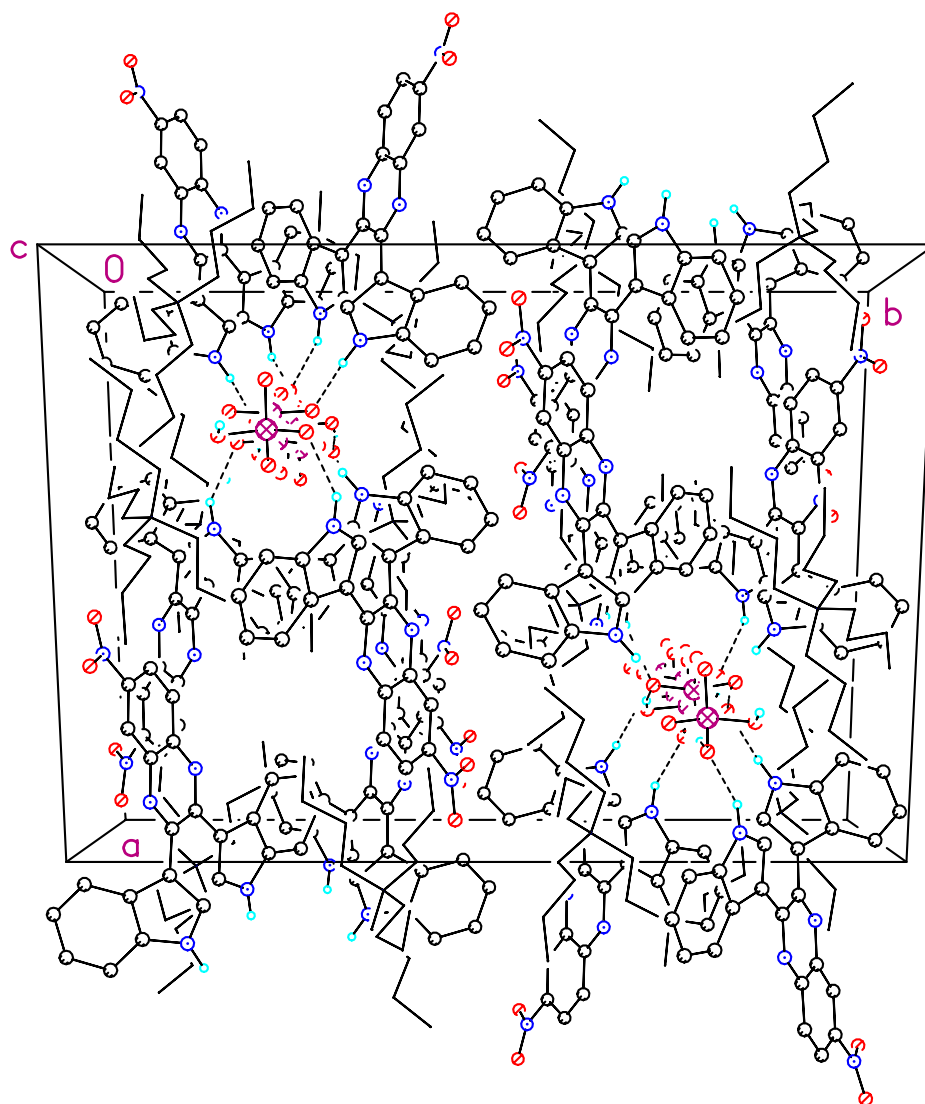
Figure A8 Unit cell packing figure for **2.6**. The view is approximately down the **c** axis. Dashed lines are indicative of H-bonding interactions.

Table A3 Crystal data and structure refinement for **2.6**

Empirical formula	C40 H53 N6 O6 P
Formula weight	744.85
Temperature	153(2) K
Wavelength	0.71073 Å
Crystal system	Monoclinic
Space group	P21/c
Unit cell dimensions	a = 19.3678(5) Å $\quad$ $\alpha = 90°$.
	b = 25.6110(7) Å $\quad$ $\beta = 110.106(3)°$.
	c = 16.8824(4) Å $\quad$ $\gamma = 90°$.
Volume	7863.8(3) Å^3
Z	8
Density (calculated)	1.258 Mg/m^3
Absorption coefficient	0.124 mm^{-1}
F(000)	3184
Crystal size	0.33 x 0.09 x 0.04 mm
Theta range for data collection	2.04 to 25.00°.
Index ranges	-23<=h<=23, -30<=k<=24, -20<=l<=20
Reflections collected	22171
Independent reflections	13603 [R(int) = 0.0962]
Completeness to theta = 25.00°	98.2 %
Absorption correction	None
Refinement method	Full-matrix-block least-squares on F^2
Data / restraints / parameters	13603 / 1 / 964
Goodness-of-fit on F^2	1.057
Final R indices [I>2sigma(I)]	R1 = 0.0843, wR2 = 0.1522
R indices (all data)	R1 = 0.2211, wR2 = 0.1987
Extinction coefficient	$1.19(16) \times 10^{-6}$
Largest diff. peak and hole	0.728 and -0.428 e.Å^{-3}

Vita

Donggyu was born in Samcheonpo, South Korea on January 27, 1970, the first son of Jongman Cho and Sungem Kim. After graduating from Myungshin High School, Jinju, South Korea in 1988, he pursued his Bachelor's degree at Sungkyunkwan University majoring in chemistry. Upon earning a B.S. degree in chemistry, he continued to study at Sungkyunkwan University towards a Master's degree in organic chemistry under the direction of Prof. Suk-Ku Kang. In 1994, he earned his M.S. degree upon writing his thesis entitled "The Synthesis of Optical Active Synthetic Intermediates and Natural Product." He was interested in medicinal chemistry and started his industry experience at Hanhyo Institute and Technology in 1994 and then moved to LG Life Science Ltd. in 1999. In August of 2003, he moved in the United States to start his Ph.D. program in organic chemistry under the direction of Professor Jonathan L. Sessler at the University of Texas at Austin. In 2006, a Professional Development Award was awarded. He is going to work as a postdoctoral fellow under the direction of Professor M.G. Finn at The Scripps Research Institute in June of 2008.

Permanent address: Hungan dulmal apt 101-1201, Pyunggudong, Jinju,

    Kyungsangnamdo, Republic of Korea

This dissertation was typed by the author.